The Society originated in the year 1821 as the Philosophical Society of Australasia. Its main function is the promotion of Science by: publishing results of scientific investigations in its *Journal and Proceedings*; conducting monthly meetings; awarding prizes and medals; and by liason with other scientific societies. Special meetings are held for: the *Pollock Memorial Lecture* in Physics and Mathematics, the *Liversidge Research Lecture* in Chemistry, the *Clarke Memorial Lecture* in Geology, Zoology and Botany, and the *Poggendorf Lecture* in Agricultural Science.

Membership is open to any person whose application is acceptable to the Society. Subscriptions for the Journal are also accepted. The Society welcomes, from members and non-members, manuscripts of research and review articles in all branches of science, art, literature and philosophy for publication in the *Journal and Proceedings*.

Unusual Baryte-bearing Hybrid Basalt, Bourke-Byrock Area, Northern New South Wales

F.L. SUTHERLAND*, B.J. BARRON†, D.M. COLCHESTER*, A.R. MCKINNON*

Abstract: Drilling near Mount Oxley and Mullagalah in the Bourke-Byrock area, NSW, intersected basaltic breccia pipes. The Mount Oxley basalt is an unusual hybrid rock involving intimate veining and intermingling between a slightly evolved basanite and a strongly evolved, late-stage, baryte-bearing trachyte. The basanite consists of abundant phenocrysts of altered olivine and diopside-augite, and rarer phenocrysts of nepheline, anorthoclase and Ti-rich magnetite, in a groundmass of plagioclase laths and Ti-rich magnetite grains. The trachytic component is dominated by alkali feldspar, largely sanidine, with calcic amphibole (Ti-Mg-rich hastingsite), baryte (with up to 2% Sr in coarser crystals) and secondary carbonates. Olivine-microgabbro and microsyenite xenoliths in the basalt suggest that the cumulates were formed from both the basanitic and trachytic magmas prior to emplacement. Xenoliths of, and xenocrysts from, high pressure ultramafic metamorphic assemblages (spinel harzburgite and spinel websterite) indicate a mantle source for the basanitic magma. Two-pyroxene temperatures based on Wells thermometry suggest these ultramafic assemblages were re-equilibrated under an ambient paleogeotherm between 990–1035°C. Similar basalt appears in the Mullagalah breccia pipe, but lacks the phenocrystic nepheline and the hybrid baryte-bearing trachyitic component found in the Mount Oxley basalt. Xenoliths in the Mullagalah breccia include a cumulate-like olivine-bearing diopside-amphibole (K-Ti-rich ferroan pargasite) assemblage. The Mount Oxley and Mullagalah intrusions are not well dated, but were probably formed during Late Mesozoic-Late Cenozoic intraplate basaltic activity that occurred in eastern Australia, from magmas generated at mantle depths exceeding 38 km.

Keywords: Breccia pipe, baryte, basalt, trachyte, xenocrysts, xenoliths

INTRODUCTION

Cenozoic to Mesozoic intraplate basaltic eruptives are a feature in eastern Australia (Johnson 1989, Sutherland 2003). In New South Wales, the most westerly Cenozoic basalts give way to Miocene potassic, leucite-bearing lavas and minor trachytes, which form a linear, apparently age-progressive trail extending from Byrock, NSW, in the north to Cosgrove, Victoria, in the south (Cundari 1973, Byrnes 1993, Zhang and O'Reilly 1997, Paul et al. 2005, McQueen et al. 2007). Mesozoic intraplate basalts and silicic derivatives also outcrop among the western Cenozoic basalts and are plentiful in the Gunnedah and Dubbo areas (Tadros 1993, Meakin and Morgan 1999). This paper describes an unusual hybrid basaltic intrusion found in this western zone, which was encountered in drill cores near Mount Oxley, east of Bourke (Byrnes 1993). Although this intrusion received petrographic examination, neither nepheline nor baryte were reported. The

significance of these minerals is discussed in this study. Another basaltic diatreme drilled nearby at Mullagalah is also described and is compared with the Mount Oxley intrusion.

The geological setting in the Bourke-Byrock area (Figure 1) forms part of the Palaeozoic Lachlan Orogen, with exposures of folded Ordovician to Devonian sedimentary and volcanic rocks, emplacements of serpentinite and a range of mineralisation (Byrnes 1993). Late Cenozoic leucititic bodies outcrop at Byrock were dated at ∼17 Ma (K-Ar dating, Sutherland 1985). Leucititic lavas of similar age outcrop farther south at El Capitan, near Cobar (Ar-Ar dating, McQueen et al. 2007). Minor fresh tholeiitic basalt was also drilled 25 km west of Byrock, but is so far undated (Byrnes 1993). Surficial Cenozoic sedimentary beds, wind blown sands and alluvium from the present Darling, Bogan and Warrego drainages partly obscure bedrock, particularly along the boundary of the Palaeozoic basement rocks and the Mesozoic Surat Basin beds to the north (Figure 1).
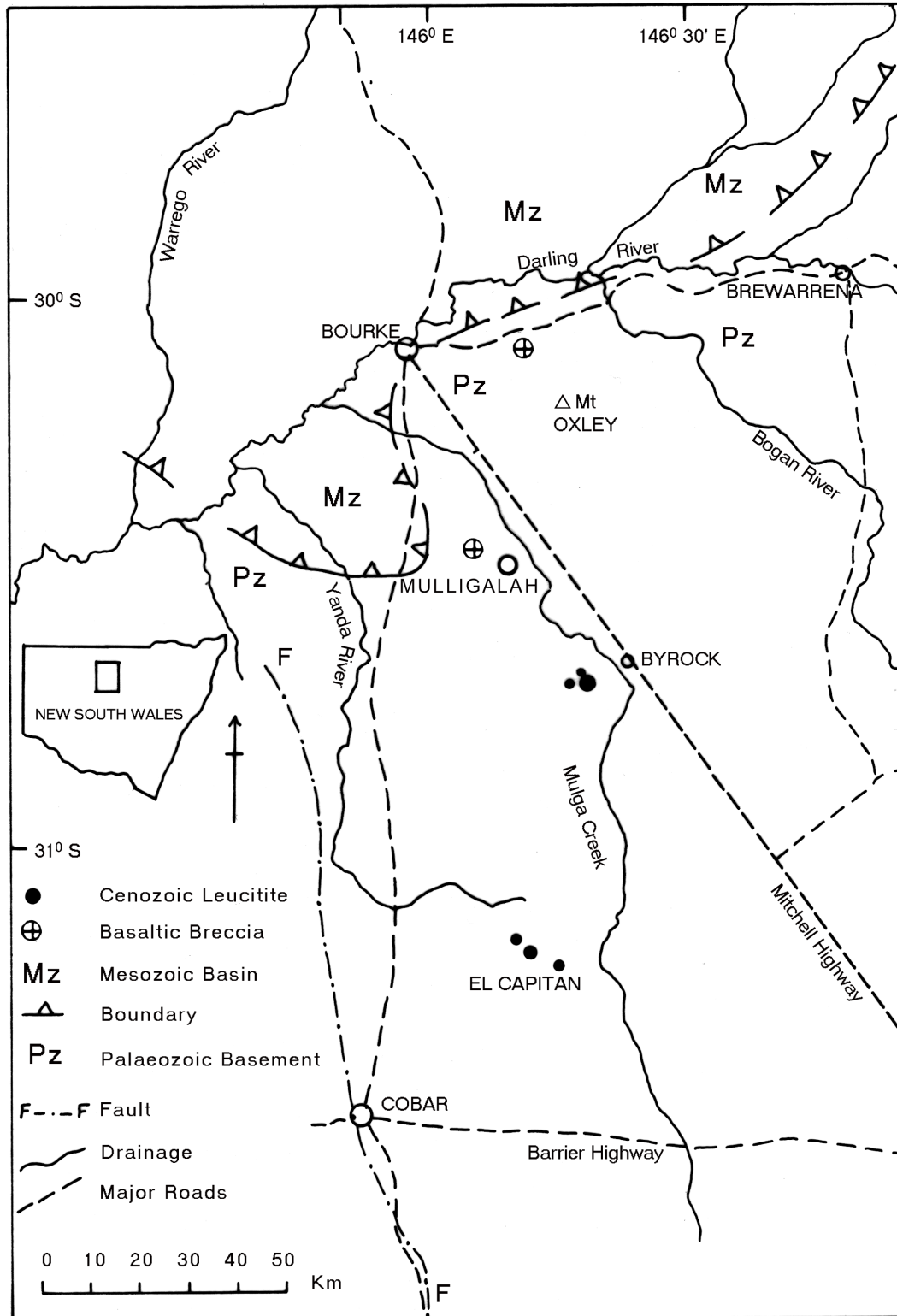
Figure 1. Locality map Bourke-Byrock area, New South Wales, showing locations of the Mt Oxley and Mullagalah basaltic diatremes (drill cores) in relation to the Paleozoic basement rocks, Mesozoic basin boundary, outcrops of Cenozoic leucitites and the main drainages and major roads. Inset shows area within New South Wales.

Samples of the Mount Oxley and Mullagalah basalts and associated intrusive breccias were made available to the authors as fragments, thin sections and polished sections, together with some initial petrographic reports and electron microprobe (EMP) analyses of mineral phases. These materials were donated to the Australian Museum, Sydney, for further study by Dr Ian Plimer, then at North Broken Hill Ltd, and Ian Matthais, CRA Cobar office, in 1983. The Mount Oxley samples (~ 419500 mE, 6671100 mN) came from a hole (T16) drilled by North Broken Hill-Preussag Australia while investigating geochemical prospects and aeromagnetic anomalies at $\sim 146.16°$E and $30.08°$S (Preussag Australia Pty Ltd & North Broken Hill Ltd 1981a,b, North Broken Hill & Preussag Australia Pty Ltd 1982).

The Mullagalah drill core sample (MUI 647) came from a drilling depth of 647 feet within a magnetic anomaly formed by an inclined diatreme west of Mullagalah, at $\sim 146.17°$E and $30.44°$S (North Broken Hill Ltd 1971 a,b). Initial mineral analyses for these company investigations were undertaken by the Geology Department of the University of Melbourne.

Further microscopic studies and mineral analyses were made on the donated samples using facilities at the School of Earth Sciences, Macquarie University and CSIRO Division of Exploration Geoscience, North Ryde, in 1989, and at the School of Natural Sciences, University of Western Sydney, Parramatta, in 2006 to complete the study. Both the Mount Oxley and Mullagalah intrusive basalt breccias contain numerous xenoliths and xenocrysts of the local country rocks and deeper crustal and mantle lithologies which are also described here. The breccias lie southwest of the Bundabulla-Bokhara basalt fields which includes buried alkaline intrusives and rare outcrops (Madden 1999, Jaques 2006 and pers. comm. 2007).

MATERIALS

Mount Oxley

Thin sections cut from the Mount Oxley core are basalt and basalt-intruded breccias (T16, 1-3; S89; 4C3/5). In the breccias, fragments of quartzite and arkose commonly reach up to 9 mm across. The quartz grains in these rocks are highly strained, partly recrystallised and show sutured grain boundaries. Some quartzite fragments show the effects of partial melting where altered brown glassy material is interspersed through the matrix, possibly as minimum melts of K-feldspar. The contact between the breccia and invading basalt is commonly marked by a coarser crystallised feldspathic selvage. The fine grained basalt is porphyritic, and contains rare sub-euhedral nepheline phenocrysts up to 3 mm long (Figure 2). Abundant phenocrysts and glomerocrysts of altered olivine and fresh clinopyroxene, up to 2 mm across, occur with sporadic microphenocrysts of opaque iron oxide and alkali feldspar (Figure 3.1). The olivine is replaced by carbonate and clay. Euhedral clinopyroxenes are sometimes partially resorbed along their margins and exhibit strong core to rim and sector growth zoning. The basalt groundmass ranges from chilled glassy material near its outer contacts with the breccia and grades into a fine grained matrix containing small plagioclase laths and opaque iron oxide grains.
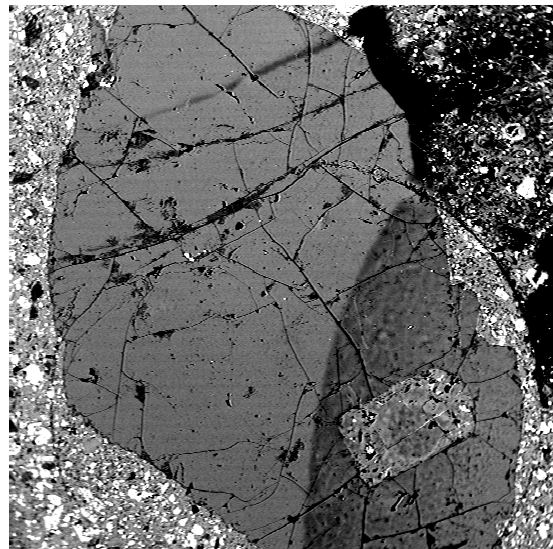

Figure 2. Nepheline 'phenocryst' (2.8 mm long, 1.7 mm wide) in basanite, with squarish inclusion of anorthoclase, with reacted margins, within the phenocryst bottom right. Back scattered SEM image. Note bright crystals in the basanite host represent opaque Fe-oxides (Ti-rich magnetite). Photomicrograph: Adam McKinnon.

Trachytic pools, veins and segregations inter-finger with the basalt and represent a late phase of crystallisation (Figure 3.2). Some veins form mosaics of alkali feldspar and in places have broken up and become incorporated into the host basalt. These trachytic veins can reach several centmetres in length and up to a centimetre in width. They grade into amphibole-baryte-carbonate-bearing trachyte that occu-pies pockets throughout the host basalt, and sometimes invades xenoliths within the host rock. This produces baryte-replacement of pyroxenes in pyroxenites (Figure 4), with baryte surrounding small cores of secondary quartz in some replacements. The last formed veins cut across all other structures in the rocks and represent fracture fillings containing secondary carbonates, clays and iron hydroxides.
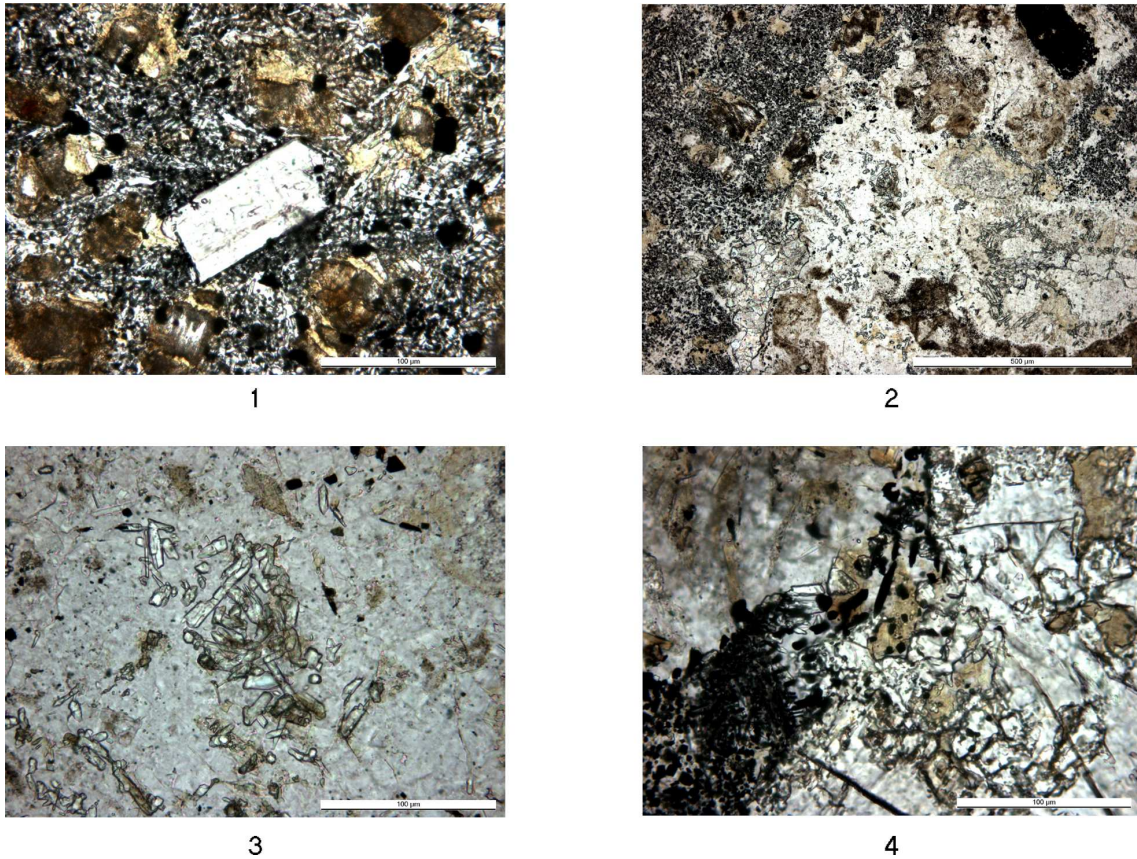
Figure 3. Mount Oxley intrusion petrology (T16). 3.1: Anorthoclase microphenocryst (centre) in basanite. Note altered olivine, rare clinopyroxene grains amid plagioclase laths and opaque Fe-oxide grains; 3.2: Pool of baryte-bearing trachyte (lighter coloured, coarser material, centre-right) interacting with basanite host (darker, finer-grained material, left); 3.3: Close up of trachyte pod, showing clinopyroxene prisms (strong relief), scattered amphibole (irregular grayish grains) and rare opaque iron oxide grains in an abundant alkali feldspar-baryte-bearing matrix; 3.4: Reaction zone between baryte-bearing trachyte (lighter material, centre-right) and microgabbro xenolith (grayish material, top left), marked by bladed ilmenite (opaque crystals). Amphibole forms scattered irregular intergrowths. Photomicrographs (PPL): Ian Graham.

Medium to coarse grained xenoliths up to 3 cm across and associated disaggregated xenocrysts are scattered liberally throughout the host basalt. In addition to local crustal materials, there are olivine microgabbro (Figure 5.1) and microsyenite assemblages. These textures suggest that they represent cumulates related to the phenocrystic basalt and its late-stage trachytic component. The microgabbro xenoliths show reaction margins against the trachytic component, which partly replaces olivine (Figure 5.2). Ultramafic metamorphic assemblages among the xenoliths are spinel meta-harzburgite (Figure 5.3), in which olivine is altered to mesh-textured carbonates, talc and clays (Figure 5.4), and spinel meta-websterite. The xenocrysts and composites (derived from the xenolith assemblages) typically show reactions with the host magmas, such as incipient melting and initial crystallisation of secondary minerals (Figure 6.1), feldspathic segregation mantles (Figure 6.2), opaque Fe-oxide reaction rims (Figure 6.3), and strong resorption (Figure 6.4).

Mullagalah

The Mullagalah drill core sample (MU1 647) from a depth of 647 ft (190 m) is an unsorted volcanic breccia (Figure 7.1). It contains volcanic lithic fragments of diverse, but related, basalts that show various degrees of crystallinity and degradation due to oxidation, as well as abundant xenoliths and xenocrysts of crustal and probable mantle origin. Fragments up to 2 cm across make up 55% of the rock embedded in a pale yellow smectite clay matrix. Basalt forms about 60% of the fragments. The largest of these contains 15% of subhedral altered olivine (up to 1.5 mm across) and sporadic clinopyroxene microphenocrysts (up to 0.2 mm across), some showing hour glass and core to rim zoning (Figure 7.2). The groundmass shows flow banding and strongly chilled broken margins containing up to 40% of flow-aligned prismatic clinopyroxene microlites (Figure 7.3), set in a clay-degraded, in part carbonated and once vesicular volcanic glass. The matrix is charged with minute opaque oxide grains (< 0.02 mm). Olivine phenocrysts are altered to patchy carbonate, talc, and a yellow to brown smectite clay, which also pervades the glassy matrix. Some basaltic fragments contain prominent, euhedral diopside crystals, with simple and knee-shaped twins and partly resorbed margins and interiors. Sparse, altered olivine euhedra reach 1.5 mm. The groundmass contains flow-aligned, wispy plagioclase microlites up to 0.05 mm long, and some cases sections or fragments contain abundant vesicular remnants up to 0.04 mm in yellow brown iron-stained glass.
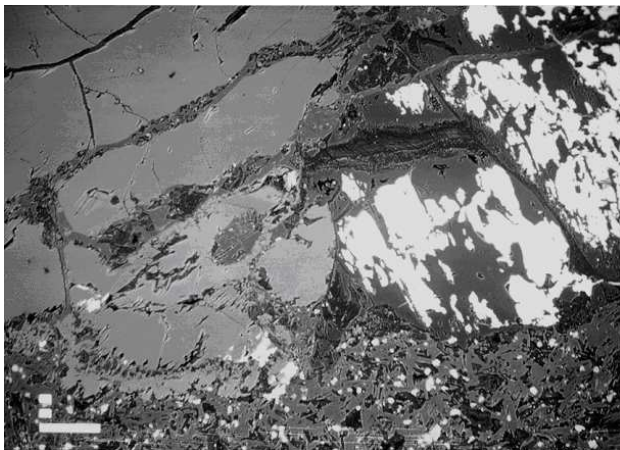

Figure 4. Enstatite-rich meta-websterite, showing invasion of Ba-rich trachyte melt into xenolith. Note replacement of pyroxenes with baryte (bright white patches). The less intense white grains in the host basanite represent Ti-rich magnetite-ulvospinel grains in the groundmass. Large scale bar = 100 μm. Back scattered SEM image: K. Kinealy.

The breccia contains a range of xenocrysts (20%) mostly less than 1.5 mm in size. These are cleavage fragments of diopside, pale yellow to orange brown, pleochroic amphibole, yellow-brown Cr-bearing spinel, green spinel; rare opaque Fe-oxides, carbonate-altered olivine, quartz, rare degraded plagioclase and oxidised biotite flakes up to 1 mm long. Some quartz exhibits reactions rims of prismatic diopside. A diopside-amphibole composite 2.5 mm across encloses a small altered olivine grain and may represent a cognate source for xeno-crystal material (Figure 7.4). Subrounded crustal xenoliths include partly recrystallised microsyenite, foliated feldspathic microbreccia, foliated sandy and silty claystone, deformed and finely recrystallised mircoporphyritic felsic volcanic material, and recrystallised quartzite or vein quartz. The Mullagalah basalts differ from that at Mount Oxley in lacking significant groundmass plagioclase, phenocrystic nepheline or a late-stage baryte-bearing trachytic phase.
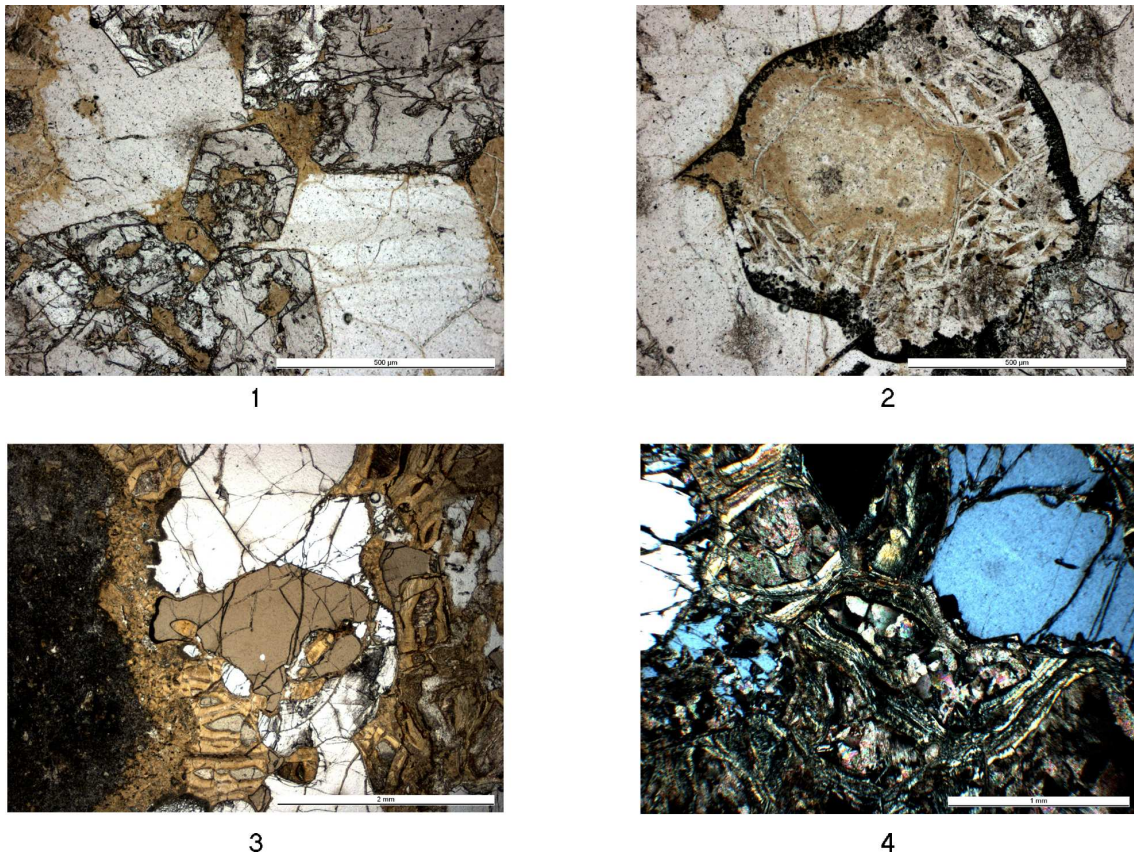
Figure 5. Mount Oxley xenolith petrology (T16). 5.1: Cumulate-textured micrograbbo, showing euhedral diopside intergrown with large plagioclase crystals, with altered olivine in interstitial grains and inclusions in diopside; 5.2: Altered, reacted olivine grain (centre) in cumulate-textured microgabbro. Note original grain is marked by opaque iron oxide rims, a prominent reaction zone of alkali feldspar laths, intersertal amphibole, partly surrounding a smectitic clay altered core, with coarser trachytic material, bottom right; 5.3: Spinel meta-harzburgite xenolith in basanite host (dark material, left), showing spinel (grey crystal, centre) intergrown with orthopyroxene (lighter crystals, centre top and bottom) and altered olivine (mesh-textured material, centre bottom and right side); 5.4: Meta-harzburgite showing altered olivine, with magnesite replacements (mesh-textured diagonal zone, with mosaic cores), intergrown with orthopyroxene grains (left and right sides). Photomicrographs (PPL): Ian Graham.

ANALYTICAL TECHNIQUES

Because the Mount Oxley basalt is invaded by ubiquitous late-stage baryte-bearing trachytic patches and veins and is riddled with xenocrysts and xenoliths, no bulk chemical analysis of the material was attempted. The mineralogy of the basalts, and a range of xenocryst and xenolith minerals from Mount Oxley and Mullagalah were investigated using a Leica DMLP polarising microscope. Electron microprobe (EMP) analysis, supplemented with back scattered electron (BSE) imaging confirmed the mineralogy. Because several EMP facilities were used over a protracted time, the analytical results come from several sources and operators. These include a JEOL probe fitted with wavelength dispersive spectrometers (WDS) at the University of Melbourne (I.R. Plimer and D. Sewell analysts), an automated ETEC probe at Macquarie University, North Ryde (B.J. Barron analyst), a CAMECA system in the Division of Exploration Geoscience, CSIRO, North Ryde (F.L. Sutherland and K. Kinealy analysts)and a JXA super probe with 3 WDS detectors at the School of Natural Sciences, University of Western Sydney, North Parramatta (A.R. McKinnon and F.L. Sutherland analysts).
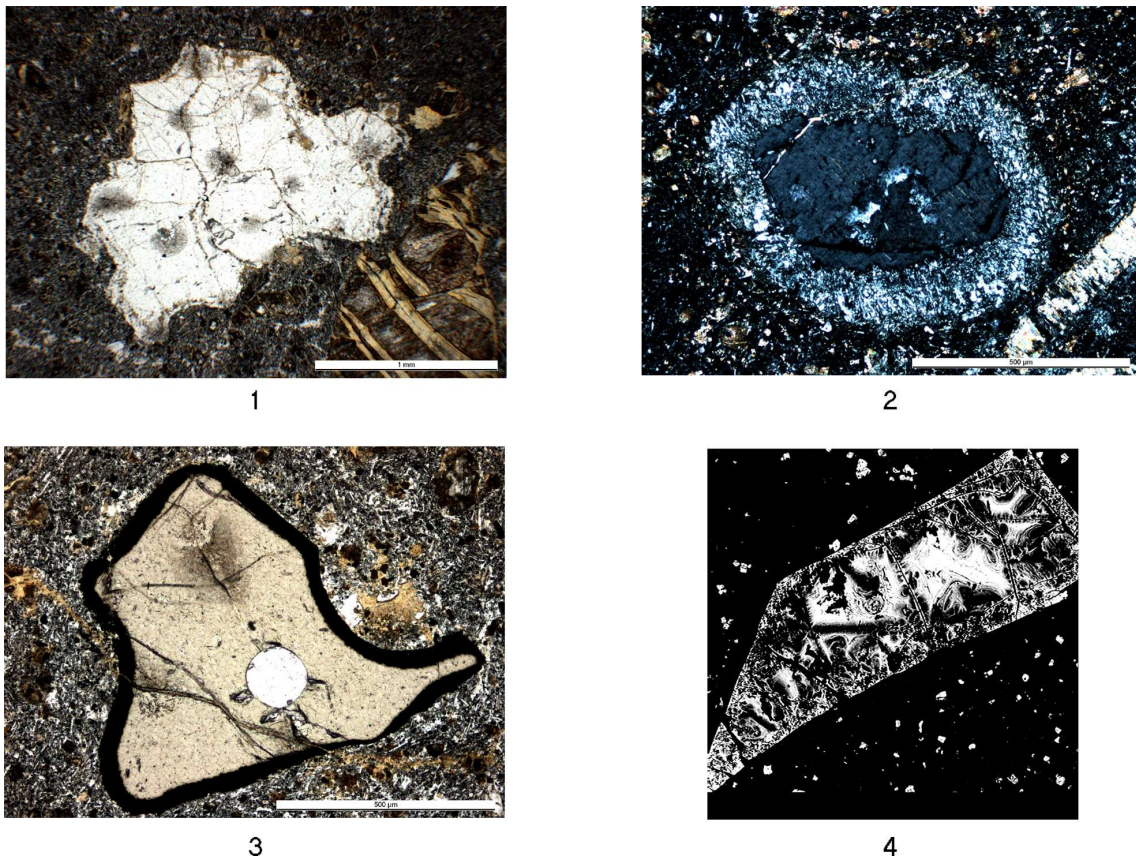
Figure 6. Mount Oxley xenocryst minerals (T16). 6.1: Plagioclase composite xenocryst (centre) in basanite (PPL), showing incipient melting, marked by patchy opaque Fe oxide dustings and invasions along grain boundaries. Note altered olivine phenocryst (bottom right); 6.2: Enstatite xenocryst (dark coloured core) with plagioclase-rich reaction zone (lighter rim) in basanite (XPL); 6.3: Spinel xenocryst (light coloured core) with prominent Fe-oxide reaction zone (opaque rim) in basanite (PPL); 6.4: Resorbed Ti-rich magnetite micro xenocryst (crystal is 1.1 mm long) with more Ti-rich reaction rims, in basanite. Photomicrographs: Ian Graham; Back scattered SEM image: A. McKinnon

Operating procedures and conditions for the EMP analyses mostly utilised a 15 kV acceleration voltage, beam current of 20 nA, Bence-Albee corrections and natural mineral standards. Analytical precision was usually within 1% for elements above 10 wt% as oxides, within ± 5% at 1–10 wt% oxides and within ± 10% at < 1 wt% oxides. Because several different instruments provided EMP analyses incorporating a range of variations in base line drift during the runs, as well as potential differences related to surface polish in the samples and operator factors, the results are presented here as normalised 100% totals. Most results represent anhydrous minerals, while the few hydrous minerals were normalised by assigning a volatile content equivalent to the difference from 100% in the total. The accuracy of the representative analyses listed in Tables 1 to 5 can be judged by the closeness of the calculated cation totals to the theoretical cation total of the unit cell for the analysed mineral. In most cases, cation totals for the anhydrous minerals fell within 0.0–0.5% of the theoretical cation total, while cation totals for the hydrous minerals were usually within 1% of the theoretical totals.
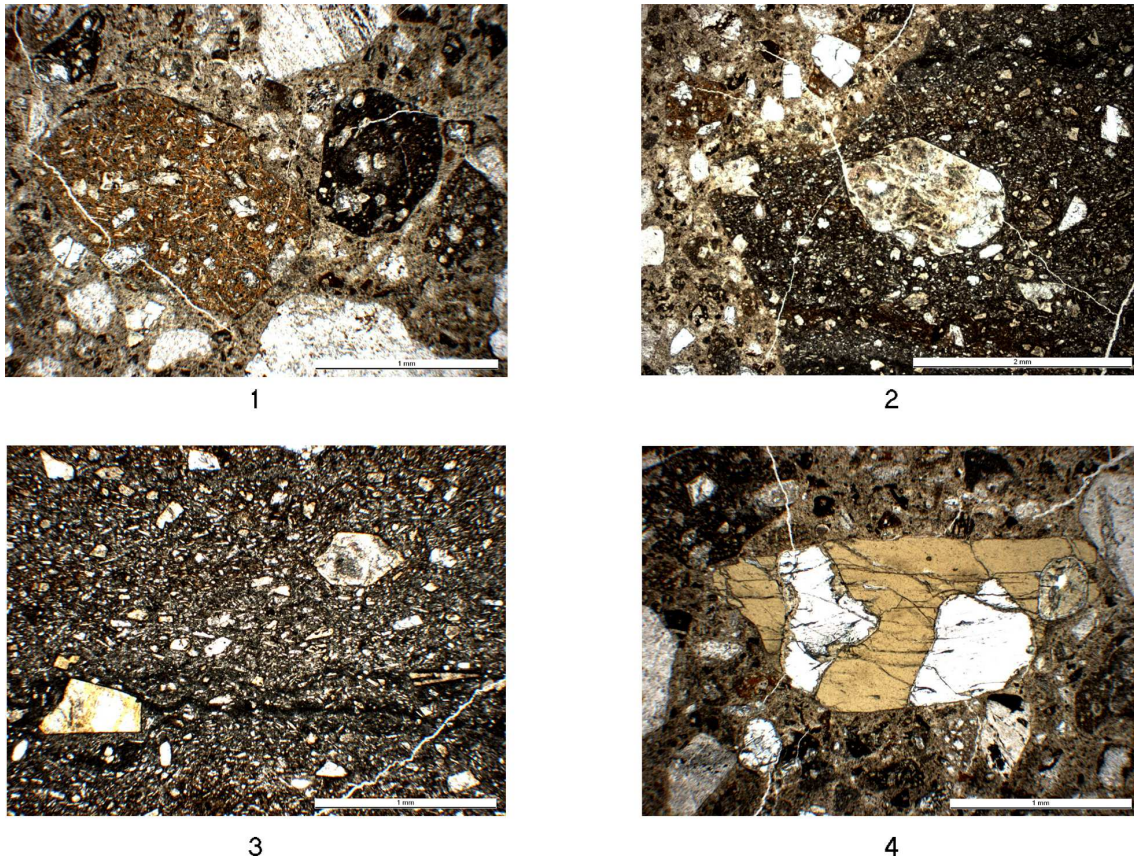
Figure 7. Mullagalah basalt breccia petrology (MUI 647). 7.1: Basalt fragments in breccia. Note microphenocrysts and plagioclase microlites in ground mass (left fragment) and dark glassy matrix (right fragments), with qaurtzitic fragments (top and bottom); 7.2: Contact of basalt fragment with breccia (left). Note large altered olivine phenocryst in the basalt (centre); 7.3: Flow-textured basalt fragment. Note alignment of olivine (altered grain, top right), clinopyroxene, microlitic plagioclase crystals and glassy bands; 7.4: Cumulate-like olivine-bearing amphibole (grey zones) and clinopyroxene (light zones) xenolith within breccia. Photomicrographs (PPL): Ian Graham.

End members for the pyroxene group minerals were calculated after the method of Yoder and Tilley (1962) and the computer program of Cebeira (1990). Amphibole compositional names were determined using the computer program of Yavuz (1996). Spinel group end members were calculated from a computer program written by Ross Pogson, Australian Museum. Two-pyroxene temperatures for the co-existing pyroxenes in the ultramafic meta-assemblages used Wells (1977) thermometry which provides the most reliable results for such assemblages (generally within $\pm 50°C$ at temperatures $< 1300°C$; Taylor 1998, Trebaudino and Bruno, 1993). For comparison, Wood and Banno (1973) two-pyroxene temperatures were also calculated and generally yielded results 15–95°C higher.

RESULTS

Representative photomicrographs and mineral analyses of the Mount Oxley and Mullagalah basalt breccias are presented in Figures 2–7 and Tables 1–5.

Mount Oxley Basalt

The phenocryst assemblage is dominated by altered olivine and clinopyroxene (Figure 3.1 and Table 1). The clinopyroxene is zoned Al-rich diopside (di_{50-56} hd_{19-22} $tsch_{20}$ jd_{0-8} ac_{0-5}), with more calcic, Fe- and Ti-rich rims (di_{40} hd_{29} $tsch_{26}$ jd_6). Sparse opaque oxide phenocrysts belong to a Cr-bearing, Ti-rich magnetite-ulvospinel series (usp_{62} mt_{17} mf_8 mc_7 sp_7). Rare large nepheline phenocrysts (Figure 2) are K-bearing (ne_{84} ks_{14}). They include co-existing zoned alkali feldspar, largely anorthoclase (ab_{69} or_{28} an_3), which shows a reaction rim marking the alkali feldspar / nepheline boundary. Alkali feldspar microphenocrysts (Figure 3.1) and twinned, zoned anorthoclase crystals ($\sim ab_{60-75}$ or_{20-32} an_{5-8}) may also represent this phenocrystic phase. The groundmass contains plagioclase laths of intermediate composition ($\sim an_{48-52}$ ab_{46-49} or_{2-3}), small ulvospinel grains and rare calcic amphibole grains (alumino-edenite) and variable amounts of glassy matrix. Overall, the mineralogy represents a porphyritic, evolved 'nepheline'-bearing basanite.

The invasive late-stage trachytic crystallisations that infiltrate the basalt (Figures 3.2 and 3.3) are dominated by mosaics, tablets and laths of K-rich alkali feldspar, largely sanidine in composition ($\sim or_{55}$ ab_{40} an_5). In places the alkali feldspar is inter-grown with clinopyroxene, calcic amphibole (titano-magnesio-hastingsite), interstitial and clustered baryte grains and secondary carbonate fillings. The baryte is Sr-bearing (up to 2%) in coarser crystals (Table 2). Rare isolated green sodic clinopyroxene grains may also belong to this assemblage and classify as hedenbergite, after Yoder and Tilly (1962) (hd_{60} di_{27} jd_{10} $tsch_2$), or as aegirine-augite under IMA nomenclature (Cebeira 1990).The high jd value favours aegirine-augite over typical hedenergite.

The last-formed veins that cut across all the basalt-trachyte features, incorporated xenoliths and host breccia are dominated by carbonate minerals including magnesite, Al, Fe-rich serpentinitic clay (Wicks and O'Hanley 1988) and nontronitic clay (Güven 1988) (Table 2).

Mount Oxley Xenoliths / Xenocrysts

Xenoliths and xenocrysts in the basalt and breccias represent various lithologies and mineral compositions. Those of interest to the basalt genesis and mantle source include the cumulate-textured magmatic equivalents and high pressure ultramafic metamorphic-textured xenolithic assemblages.

Coarse olivine-clinopyroxene-plagioclase and medium grained olivine-plagioclase cumulates (Figure 4.1) contain similar mineralogy to phenocryst and matrix phases in the basalt and probably represent near-cognate early crystallisations formed prior to basalt eruption. Such crystallisations presumably also provided xenocrysts such as a strongly resorbed ulvospinel which shows increased Ti contents in the rim zone (Figure 5.4). Other igneous-textured alkali feldspar-rich xenoliths may represent early dismembered K-rich feldspathic cumulates related to the late-stage feldspathic

veins which were introduced into and broken up in the host basalt.

Ultramafic meta-assemblages in the xenoliths include spinel meta-websterites (Figure 4) and spinel meta-harzburgite (Figures 5.3 and 5.4). Two types of meta-websterite differ in the range of Mg contents within the phases (Table 3). One type contains Al-rich enstatite (en_{88-89} fs_{9-10} wo_{1-2}), Al-rich augite (di_{66-67} $tsch_{16-17}$ jd_{6-7} ac_{6-7} hd_{3-4}) and Cr-bearing spinel (sp_{74-75} cm_{13-14} hc_{8-9} mt_{2-3} usp_{0-1}). Mg numbers for the phases range from 0.90 to 0.72. This type is more magnesian and Cr-rich than in the second type, which contains Al-rich enstatite (en_{76-77} fs_{21-22} wo_2), Al-rich augite (di_{59-60} hd_{18-19} $tsch_{12-13}$ jd_{8-9} ac_{1-2}) and Cr-

bearing spinel (sp_{81-82} hc_{9-10} cm_{7-8} mt_{1-2} usp_{0-1}). Mg numbers for the phases range from 0.81 to 0.60. Despite the different ranges in Mg numbers, the two types give similar re-equilibrated temperature ranges, based on Wells 2-Pyroxene thermometry (990° ± 5°C, using Fe^{3+} recalculated T).

The Mg-rich spinel harzburgite (Table 4) contains Al-rich enstatite (en_{89} fs_{9-10} wo_{1-2}), Al-rich diopside (di_{65-66} $tsch_{14-15}$ jd_{9-10} hd_{5-6} ac_{4-5}) and Cr-bearing spinel (spl_{81-82} hc_{9-10} cm_{6-7} mt_{1-2} usp_{0-1}). Mg numbers for these phases range from 0.91 to 0.78. The Wells 2-Pyroxene T estimates (1005 to 1035°C, Fe3+ calculation) are higher than those for the spinel meta-websterite assemblages (985–1000°C).

Mineral	Phenocryst Assemblage, Oxide wt%					
	Cpx	Cpx (core)	Cpx (rim)	Spl	Nep	Alk
SiO_2	48.71	48.90	46.18	0.72	43.39	68.16
TiO_2	0.93	1.65	2.70	20.88	-	-
Al_2O_3	6.92	8.36	7.95	3.07	33.33	17.99
Cr_2O_3	0.83	0.13	0.01	4.77	-	-
Fe_2O_3	2.60	-	-	48.02	-	-
FeO	5.79	6.86	8.95	17.78	0.31	-
MnO	0.18	0.23	0.22	0.65	-	-
MgO	14.27	13.02	11.02	3.35	-	-
CaO	18.94	19.70	22.17	0.34	0.90	0.63
Na_2O	0.71	1.15	0.76	0.20	17.39	8.09
K_2O	-	0.01	0.05	0.02	4.68	4.95
NiO	0.14	-	-	0.17	-	-
Cation Sum	3.999	4.009	4.034	23.912	24.096	19.950
(Oxygens)	6	6	6	32	32	32
Cation Ratios %	Ca 44.0	Ca 45.6	Ca 49.8	Fe 74.4	Na 83.9	Na 69.2
	Mg 42.0	Mg 41.9	Mg 34.5	Ti 19.5	K 14.2	K 27.7
	Fe 14.0	Fe 12.4	Fe 15.7	Mg 6.0	Ca 1.8	Ca 3.0
Name	Augite	Diopside	Diopside	Ulvospinel	Nepheline	Anorthoclase
$Mg/(Mg+Fe^{2+})$	0.815	0.771	0.687	0.254	-	-

Table 1. Representative normalised EMP analyses, phenocryst phases, basanite host (T16, 4C 3/5). Cpx Clinopyroxene, Spl Spinel, Nep Nepheline, Alk Alkali feldspar. Fe_2O_3 and FeO by stoichiometry. Oxygen nos. are based on respective unit cells. Cpx ($di_{56.1}$, $tsch_{20.0}$, $hd_{18.5}$, ac 5.1); Cpx core ($di_{50.2}$, $hd_{21.8}$, $tsch_{19.7}$, $jd_{8.2}$) and Cpx rim ($di_{39.9}$, $hd_{28.7}$, $tsch_{25.6}$, $jd_{5.7}$); Spl ($usp_{61.6}$, $mt_{16.7}$, $mf_{8.0}$, $mc_{7.1}$, $sp_{6.8}$); Nep ($ne_{83.9}$, $ks_{14.2}$); Alk ($ab_{69.2}$, $or_{27.7}$, $an_{\sim3.0}$). Dashes indicate concentrations below the level of detection.

Mineral	Late Vein Assemblage (S89), Oxide wt%				Late Alterations (T16) Oxide wt%	
	Alk	Amp	Cpx	Bar	Ser	Smc
SiO_2	64.52	42.02	51.16	-	48.60	44.07
TiO_2	0.13	3.53	0.40	-	0.12	0.08
Al_2O_3	19.62	14.78	2.28	-	6.69	11.96
Cr_2O_3	0.00	0.47	-	-	0.03	0.05
Fe_2O_3	-	-	4.81	-	-	15.05
FeO	1.04	8.48	13.38	-	13.69	-
MnO	0.00	0.13	0.77	-	0.04	0.01
MgO	0.41	14.45	5.63	-	15.81	1.23
CaO	1.06	10.77	18.69	-	0.72	0.64
Na_2O	4.29	2.95	2.88	-	0.24	0.49
K_2O	8.87	1.36	0.02	-	0.18	0.21
F2O	-	0.09	-	-	-	-
(H_2O)	-	(0.97)	-	-	(13.76)	(26.21)
BaO	-	-	-	63.69	-	-
SrO	-	-	-	1.47	-	-
SO3	-	-	-	34.84	-	-
Cation Sum	4.992	16.202	3.976	0.990	5.780	10.217
(Oxygens)	32	23	6	4	9	22
Cation Ratios %	K 54.5	Mg 53.6	Ca 46.3	Ba 96.7	Mg 54.9	Al 51.7
	Na 40.1	Ca 28.7	Fe 34.3	Sr 3.3	Fe 26.7	Fe 41.5
	Ca 5.5	Fe 17.6	Mg 19.4	-	Al 18.4	Mg 6.7
Name	Sanidine	Hastingsite	Hedenbergite	Baryte	Serpentine	Nontronite
$Mg/(Mg+Fe^{2+})$	-	0.835	0.429	-	0.673	0.140

Table 2. Representative normalised EMP analyses, baryte-bearing veins, Mt Oxley basanite (S89). Alteration rims, veins, basanite (T16). Alk Alkali Feldspar, Amp Amphibole, Cpx Clinopyroxene, Bar Baryte, Ser Serpentine group, Smc Smectite group. Fe_2O_3 and FeO by stoichiometry. H_2O by difference from 100%. Oxygen nos. from respective unit cells. Alk ($or_{54.5}$, $ab_{40.1}$, $an_{5.5}$); Amp (titano-magnesio-hastingsite); Cpx ($hd_{59.7}$, $di_{27.1}$, $jd_{10.2}$, $tsch_{0.2}$); Bar (Sr-bearing baryte); Ser (Al-Fe-rich 'serpentinite'); Smc (nontronite).

Xenocrysts in the basalt such as Mg-Al-rich pyroxenes and spinels show reaction rims (Figures 5.2 and 5.3) and resemble phases in the ultramafic meta-assemblages (Table 4). Compositions are Al-rich enstatite (en_{90-91} fs_{8-9} wo_{1-2}), Al-rich diopside (di_{55-56} $tsch_{24-25}$ hd_{10-11} $jd7$ $ac7$) and Cr-bearing spinel (sp_{81-82} hc_{9-10} cm_{6-7} mt_{1-2} usp_{0-1}). Mg numbers for these phases range from 0.96–0.71 and match values for these minerals in the ultramafic xenoliths.

Mullagalah Basalt Breccia

The basalt fragments are dominated by phenocrysts of altered olivine and clinopyroxene, in a fine grained partly glassy groundmass. Only the fresh pyroxene was analysed.

The zoned clinopyroxenes have Al-rich augitic cores (di_{58-59} $tsch_{21}$ hd_{10-11} ac_{8-9} jd_{2-3}) and Al-rich diopsidic outer margins (di_{55-60} $tsch_{23-25}$ hd_{7-10} ac_{9-10}) and Mg numbers range from 0.87 to 0.92 (Table 5). In composition (Ca_{46-47} Mg_{40-47} Fe_{10-13}), they have less Mg and more Fe than clinopyroxene phenocrysts in the Mount Oxley basalt (Ca_{44-50} Mg_{35-42} Fe_{12-16}), which have lower Mg numbers (0.69–0.82). The compositions are also more aluminous (Al_2O_3 8.7–9.0 at%) and sodic (Na_2O 1.3–1.4 at%) than for Mount Oxley clinopyroxene phenocrysts (Al_2O_3 6.9–8.4 wt%; Na_2O 0.7–1.2 wt%).

Mineral	Pyroxenite Xenolith Assemblage (T16), Oxide wt%			Pyroxenite Xenolith Assemblage (S89), Oxide wt%		
	Opx	Cpx	Spl	Opx	Cpx	Spl
SiO_2	54.64	50.98	-	53.39	51.19	-
TiO_2	0.26	0.73	0.34	0.21	0.84	0.21
Al_2O_3	4.89	7.78	53.08	4.30	6.48	60.04
Cr_2O_3	0.52	0.62	12.78	0.16	0.28	7.48
Fe_2O_3	0.00	2.32	0.00	0.00	0.44	0.00
FeO	6.70	1.11	14.53	13.45	5.86	10.63
MnO	0.14	0.11	0.26	0.26	0.18	0.19
MgO	32.08	14.99	18.64	27.14	13.95	21.11
CaO	0.85	19.46	0.01	0.97	19.46	-
Na_2O	0.07	1.89	0.07	0.12	1.32	-
K_2O	0.02	-	0.01	-	-	-
NiO	0.09	0.11	0.29	-	-	0.45
Cation Sum	3.998	3.999	24.171	3.998	4.000	24.134
(Oxygens)	6	6	32	6	6	32
Cation Ratios %	Mg 88.4	Mg 45.8	Mg 56.9	Mg 76.7	Ca 44.5	Mg 53.0
	Fe 9.9	Ca 43.7	Fe 22.4	Fe 21.3	Mg 44.4	Fe 38.2
	Ca 1.7	Fe 10.4	Cr 20.7	Ca 2.0	Fe 11.1	Cr 8.1
Name	Enstatite	Augite	Spinel	Enstatite	Augite	Spinel
$Mg/(Mg+Fe^{2+})$	0.895	0.707	0.718	0.782	0.809	0.569

Table 3. Representative, normalised EMP analyses. Pyroxenite xenoliths, Mount Oxley basanite. Opx Orthopyroxene, Cpx Clinopyroxene, Spl Spinel. Oxygen nos. are based on respective unit cells. Fe_2O_3 and FeO by stoichiometry. Wells (1977) 2-pyroxene temperatures: T16 (993°C); S89 (988°C). Pyroxenite (T16) phases: Opx ($en_{88.4}$, $fs_{9.9}$, $wo_{1.7}$); Cpx ($di_{66.9}$, $tsch_{16.1}$, $jd_{6.9}$, $ac_{6.3}$, $hd_{3.7}$); Spl ($sp_{74.2}$, $cm_{13.7}$, $hc_{8.8}$, $mt_{2.9}$, $Usp_{0.6}$). Pyroxenite (S89) phases: Opx ($en_{76.7}$, $fs_{21.3}$, $wo_{2.0}$); Cpx ($di_{59.1}$, $hd_{18.5}$, $tsch_{12.6}$, $jd_{8.2}$, $ac_{1.2}$); Spl ($sp_{81.2}$, $hc_{9.4}$, $cm_{7.6}$, $mt_{1.3}$, $usp_{0.4}$).

Xenoliths in the breccia include a cumulate-like, olivine-bearing clinopyroxene-amphibole-composite (Figure 7.4). Clinopyroxene, amphibole and spinel xenocrysts are probably derived from this association. The clinopyroxene is Mg- and Al-rich diopside ($\sim$ di$_{69}$ tsch$_{12}$ jd$_{10}$ hd$_7$ ac$_2$; Mg number 0.87–0.94), the spinel is a zoned Cr-bearing member of the spinel-hercynite series (sp$_{70-74}$ hc$_{17-21}$ mt$_{4.6}$ cm$_2$ usp$_{1-2}$; Mg number 0.70–0.72) and the amphibole is K-Ti-enriched ferroan pargasite (Table 5). These phases may represent an ultramafic cumulate association, as the clinopyroxene has a higher Mg number (0.93) than for the clinopyroxene phenocrysts in the basalt (0.87–0.92).

Mineral	Xenolith Assemblage Oxide wt%			Xenocryst Assemblage Oxide wt%		
	Opx	Cpx	Spl	Opx	Cpx	Spl
SiO$_2$	54.15	51.39	0.02	54.42	51.02	0.00
TiO$_2$	0.13	0.70	0.27	0.14	0.78	0.27
Al$_2$O$_3$	5.37	7.76	59.28	4.97	7.74	61.24
Cr$_2$O$_3$	0.32	0.71	7.42	0.36	0.49	6.62
Fe$_2$O$_3$	0.94	1.68	0.00	0.86	2.55	0.00
FeO	5.72	1.66	10.79	5.53	0.99	9.48
MnO	0.15	0.15	0.41	0.18	0.12	0.14
MgO	31.96	14.90	21.15	32.42	14.78	21.59
CaO	0.90	19.03	-	0.83	19.47	0.03
Na$_2$O	0.14	1.99	-	0.10	1.98	-
K$_2$O	0.01	0.02	0.12	-	0.01	0.01
NiO	0.21	0.04	0.54	0.19	0.08	0.49
BaO	0.02	-	-	-	-	-
Cation Sum	4.000	4.001	23.994	4.001	3.998	24.085
(Oxygens)	6	6	32	6	6	32
Cation Ratios%	Mg 89.0	Mg 50.3	Mg 70.8	Mg 90.7	Mg 50.5	Mg 70.8
	Fe 9.2	Ca 46.2	Fe 17.7	Fe 8.8	Ca 47.6	Fe 17.7
	Ca 1.8	Fe 3.4	Cr 11.5	Ca 1.6	Fe 2.1	Cr 11.5
Name	Enstatite	Diopside	Spinel	Enstatite	Diopside	Spinel
Mg/(Mg+Fe^{2+})	0.909	0.941	0.784	0.913	0.964	0.708

Table 4. Normalised representative EMP analyses, harzburgite xenolith and xenocryst phases (T16). Opx Orthopyroxene, Cpx Clinopyroxene, Spl Spinel. Oxygen nos. are based on respective unit cells. Fe$_2$O$_3$ and FeO by stoichiometry. Xenolith: Opx (en$_{89.0}$, fs$_{9.2}$, wo$_{1.6}$); Cpx (di$_{65.7}$, tsch$_{14.8}$, jd$_{9.4}$, hd$_{5.5}$, ac$_{4.6}$); Spl (sp$_{81.6}$, hc$_{8.1}$, cm$_{7.5}$, mt$_{2.2}$, usp$_{0.4}$). Xenocrysts: Opx (en$_{90.7}$, fs$_{8.8}$, wo$_{1.6}$); Cpx (di$_{55.2}$, tsch$_{24.1}$, hd$_{10.5}$, jd$_{7.0}$, ac$_{6.9}$); Spl (sp$_{81.7}$, hc$_{9.8}$, cm$_{6.6}$, mt$_{1.4}$, usp$_{0.6}$). Wells (1977) 2-pyroxene temperature: xenolith (1005°C).

Mineral	Phenocryst assemblage (fresh) Oxide wt%			Xenocryst–Xenolith assemblage Oxide wt%			
	Cpx	Cpx (core)	Cpx (rim)	Cpx	Spinel (core)	Spinel (rim)	Amp
SiO_2	47.74	49.11	48.04	52.07	0.01	0.06	39.58
TiO_2	1.49	1.25	1.37	0.52	0.54	0.62	3.77
Al_2O_3	9.03	8.67	8.87	6.66	59.56	60.03	15.05
Cr_2O_3	0.05		0.03	0.80	1.80	2.02	0.04
Fe_2O_3	3.82	2.98	4.08	0.85	5.28	3.81	12.63
FeO	3.32	3.29	2.20	2.01	13.39	14.71	-
MnO	0.08	0.11	0.09	0.16	0.27	0.22	0.05
MgO	12.39	14.55	13.40	14.85	18.91	18.32	11.89
CaO	20.59	18.58	20.57	20.23	0.02	-	11.30
Na_2O	1.38	1.43	1.32	1.73	-	-	2.41
K_2O	0.02	0.04	0.01	0.01	0.02	0.01	2.43
BaO	-	-	-	-	-	-	-
NiO	0.08	-	-	0.21	0.17	0.21	0.06
(H_2O)	-	-	-	-	-	-	(0.96)
Cation Sum	3.999	3.999	3.971	4.001	24.016	24.008	16.216
(Oxygens)	6	6	6	6	32	32	24
Cation Ratios %	Ca 47.8	Mg 46.5	Ca 47.0	Ca 47.0	Mg 62.9	61.9	Mg 46.6
	Mg 40.0	Ca 42.8	Mg 42.6	Mg 47.0	Fe 33.9	34.4	Ca 31.8
	Fe 12.2	Fe 10.7	Fe 12.2	Fe 5.0	Cr 3.2	3.6	Fe 21.5
Name	Diopside	Augite	Diopside	Diopside	Spinel	Spinel	Pargasite
$Mg/(Mg+Fe^{2+})$	0.870	0.888	0.916	0.929	0.716	0.698	1.000

Table 5. Normalised EMP analyses, phenocryst and xenolith phases, Mullagalah basalt breccia (MUI 647). Cpx Clinopyroxene, Spl Spinel, Amp Amphibole. Oxygen nos. are based on respective unit cells. Fe_2O_3 and FeO by stoichiometry. (H_2O) estimated by difference from 100%. Amphibole (average of 2 analyses). Phenocrysts: Cpx ($di_{55.2}$, $tsch_{24.1}$, $hd_{10.5}$, $ac_{10.0}$); Cpx core ($di_{58.3}$, $tsch_{21.0}$, $hd_{10.4}$, $ac_{8.2}$, $jd_{2.1}$) and Cpx rim ($di_{59.7}$, $tsch_{23.9}$, $ac_{9.4}$, $hd_{7.0}$). Xenocryst / xenolith: Cpx ($di_{68.9}$, $tsch_{11.9}$, $jd_{9.9}$, $hd_{6.6}$, $ac_{2.3}$); Spl core ($sp_{73.2}$, $hc_{17.8}$, $mt_{6.1}$, $cm_{1.8}$, $usp_{1.4}$); Spl rim ($sp_{70.8}$, $hc_{20.9}$, $mt_{4.8}$, $cm_{2.1}$, $usp_{1.1}$); Amp (potassian, titanian, ferroan pargasite).
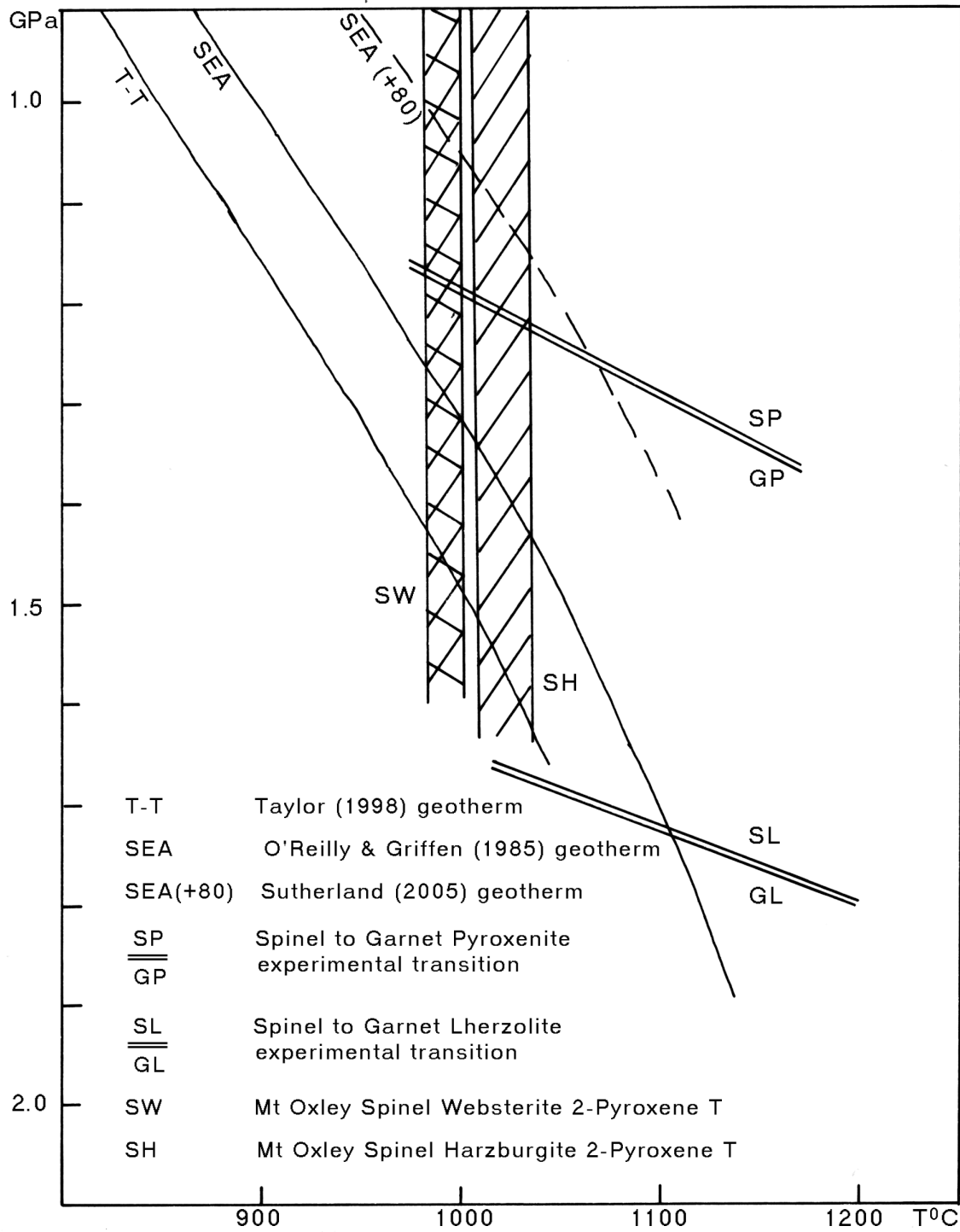
Figure 8. Pressure (GPa)–Temperature (°C) diagram showing relationships of two-pyroxene temperature estimates for Mount Oxley ultramafic xenolith meta-assemblages, with intersections of selected eastern Australian geotherms and experimental mineral assemblage transitions.

DISCUSSION

The porphyritic mafic intrusions described here were related to lamprophyres in some previous reports (Byrnes 1993), and were compared with camptonites and monchiquites. Camptonites contain amphibole together with olivine and clinopyroxene as phenocrysts, while monchquites also contain micas and feldspathoids (Rock 1991). Amphibole is absent from the Mount Oxley phenocrysts, but does occur as a groundmass phase in the hybrid late-stage trachytic crystallisations. This hybrid occurrence is insufficient to justify a camptonite nomenclature and a basaltic terminology is preferred for the mafic host. Amphibole occurs in the Mullagalah basalt, but is xenocrystic and probably derived from amphibole-clinopyroxenite xenoliths. For the ensuing discussion the Mount Oxley and Mullagalah mafic bodies are related to basanitic magmas.

Mount Oxley Basalt Petrogenesis

This basaltic intrusion displays a dual petrogenetic identity. Emplaced as a slightly evolved undersaturated magma, it become closely intermingled with a late-stage barium- and sulfur-bearing, evolved alkaline trachytic melt. The high temperature, high pressure ultramafic xenoliths within the basanite suggest initial evolution took place within the subcontinental mantle lithosphere, although the trachytic material could mark a higher level crustal fractionate. Such mantle-derived lava mingled with evolved felsic lava is rare in eastern Australian intraplate basalts. One example, however, is the meta-lherzolite and granulite xenolith-bearing nepheline hawaiite co-mingled with anorthoclase-bearing trachyte in the 3 Ma Mount St Martin volcanic centre in the Nebo Province, Queensland (Sutherland et al. 1977, Griffin et al. 1987). The hybrid lava there, however, lacked phenocrystic nepheline in the mafic component and baryte in the felsic component, which feature in the Mount Oxley association.

The Mount Oxley basanitic magma began crystallising its phenocrystic phases (olivine and diopside) at mantle depths prior to its eruption, while some crystallisation probably took place at higher levels to produce cumulate olivine microgabbros, as plagioclase joined the liquidus phases. These gabbros would crystallise at depths shallower than pressures related to the olivine + plagioclase/two pyroxene-spinel transition zone (0.6–0.9 GPa, see O'Reilly et al. 1989). Nepheline, anorthoclase and ulvospinel would form accessory crystallising phases as the magma fractionated. A further injection of basanitic magma carrying mantle fragments probably broke up the higher level cumulates and intermingled with evolved trachytic melts, which had concentrated K, Ba, S and volatiles before erupting in explosive breccias. Such melt compositions possibly link into syenitic/carbonatitic melts. The age of the explosive emplacement is uncertain on present field relationships. Miocene leucitite emplacements are known to occur to the south at Byrock and El Capitan (McQueen 2007) and are inferred to the north east for a volcanic pipe exposed in the Bokhara area (Jaques 2006 and pers. comm. 2007). Buried plugs giving magnetic anomalies are also known to the north east in the Bundabulla area (Madden 1999), where alkali basalt and mantle xenolith-bearing ankaramite were recovered in drill cores recovered below the Early Cretaceous Surat Basin sequence. These bodies suggest Mesozoic to mid-Cenozoic age limits for the Mount Oxley intrusions.

The ultramafic xenoliths in the Mount Oxley intrusives represent mantle lithologies and their thermal conditions at the time of basanite eruption. The spinel meta-harzburgite was re-equilibrated at temperatures between 1000–1035°C, while spinel meta-websterites were re-equilibrated at 985–1000°C, suggesting a slightly higher level origin within an ambient lithospheric geotherm (Figure 8). The absence of garnet in the spinel-bearing metapyroxenites and peridotites favours sampling from above the spinel-garnet pyroxenite and spinel-garnet peridotite transitions respectively (Figure 8). The lack of garnet, however, precludes precise pressure estimates and hence depths of origin, based on garnet-two pyroxene thermobarometry (see Sutherland et al. 2005). Potential pressures can

be assigned from intersections of two-pyroxene re-equilibration temperatures with a known geotherm, but this geotherm dependency produces wide variations from projected models. Several xenolith-derived geotherms proposed for eastern Australian volcanic regions include a Cenozoic South East Australia (SEA) geotherm (O'Reilly and Griffin 1985), a lower temperature variant based on different thermobarometry (Taylor 1998), a more perturbed, higher temperature variant (Sutherland 2003) and an even cooler geotherm (Gaul et al. 2003). Intersections of such geotherms with the Mount Oxley mantle xenolith re-equilibration temperatures are shown in Figure 8. These range in pressure estimate differences by up to 0.5 GPa, or about 15 km in depth for the different models. Using an estimated Moho depth of 38 km (c. 1.05 GPa) for the Bourke-Byrock section (Collins et al. 2003) allows for mantle pressures within the spinel pyroxenite and spinel-peridotite stability fields respectively, compatible with the ultramafic lithological temperatures recorded for the xenolith suite.

Mullagalah Basalt Petrogenesis

The Mullagalah basalt fragments are incompletely crystallised, but their main phenocrysts and incipient crystallites suggests they represent a similar but slightly less evolved magma than for the Mount Oxley basanite. The high pressure clinopyroxene and Cr-rich spinel xenocrysts suggest it also incorporated mantle fragments in its evolution. The common amphibole xenocrysts and amphibole-clinopyroxene cumulate assemblages indicate that a hydrous crystallisation was involved at depth, though not necessarily directly from the erupted Mullagalah magma.

Mount Oxley – Mullagalah Magmatic Links

The basanitic magmas that produced the Mount Oxley and Mallagalah intrusions are probably quasi-contemporaneous, but their age relationships to the other Mesozoic-Cenozoic mafic bodies in the area remain untested. They lie along a northern extension of the Miocene

leucitite migratory line that trends south from Byrock. If their basanitic magmas formed as part of this trail, although tapping a less potassic mantle source, they would be about 18 Ma in age on extrapolation from the 17.2 Ma age at El Capitan (McQueen et al. 2007). Alternatively, they may be linked to the pre-Early Cretaceous buried alkali basaltic plugs further north at Bundabulla (Madden 1999). The relatively fresh nature of the Mount Oxley and Mullagalah basanites and their inclusion suites, apart from post-eruptive alteration of the olivines, would suggest Cenozoic links. A fresh appearance, however, is unreliable, as similarly fresh alkali basalts and mantle xenolith suites around Dubbo, NSW, extend from Miocene to Jurassic or older ages (Meakin and Morgan, 1999). The Mount Oxley and Mullagalah breccia pipes were related to kimberlitic bodies in some exploration reports. The basanitic petrogenesis and lack of obvious garnets within the xenocryst and ultramafic xenoliths, however, weakens such origins and renders the breccias unlikely diamond prospects.

Mount Oxley Features

Distinctive features are nepheline phenocrysts in mantle-origin basanite combined with abundant baryte in hybrid trachyte. The depth of nepheline crystallisation is uncertain, but the mineral can crystallise under mantle conditions (Edgar 1984). Nepheline stability is limited by reactions with SiO_2 in the system, where albite + nepheline gives liquid and nepheline + albite gives jadeite. This gives a maximum stability around 2.4 GPa at 1250°C. Baryte is rather rare in primary magmatic rocks, but is known in late-stage vesicles in porphyritic rhyolite, and in diorite and is common in hydrothermal veins (Zussman 1998). It is also recorded in syenite-carbonatite and lamproite associations (Fitton and Upton 1987) and in lamprophyres (Rock 1991).

Secondary baryte crystals are known in Jurassic alkali basaltic diatremes (Dundas) and alkali dolerite intrusions (Prospect) that intrude the Sydney Basin Triassic beds. At Dundas, baryte is found with calcite and pyrite in vughs in the diatreme and also in veins

within metasedimentary fragments and wall rocks (Australian Museum specimens D35753, D41757). In the Prospect intrusion, baryte is rare and the last mineral to crystallise in the paragenetic sequence (England 1994), where it develops on albite, prehnite, calcite, siderite and pyrite (Australian Museum specimens D35330, D35351, D35686, D38535, D51168, D51170). It would originate from late meteoric hydrothermal fluids, rather than the earlier magmatic deuteric fluids based on oxygen isotope evidence (Williams and Carr 2005). In both the Dundas and Prospect intrusions, baryte was probably derived from barium released from the intruded Triassic shales, whereas the baryte in the Mount Oxley intrusion probably derived from Ba enrichment in fractionated trachytic magma.

ACKNOWLEDGEMENTS

REFERENCES

Byrnes, J.G., 1993. Bourke 1:250 000 Metallogenic Map SH/55-10: Metallgenic Study of Mineral Deposit Data Sheets, 127 pp. Geological Survey of New South Wales, Sydney.

Cebeira, J.M., 1990. PX: A program for pyroxene classification and calculation. *American Mineralogist* 75, 1426–1427.

Collins, C.D.N., Drummond, B.J. and Nicoll, M.G., 2003. Crustal thickness patterns on the Australian continent. Evolution and Dynamics of the Australian Plate (Hillis, R.R. and Mueller, R.D., eds), pp. 121–128. *Geological Society of Australia Special Publication 22* and *Geological Society of America Special Paper 372*.

Cundari, A., 1973. Petrology of the leucite-bearing lavas in New South Wales. *Journal of the Geological Society of Australia* 20, 465–492.

Edgar, A.D. 1984. Chemistry, occurrence and paragenesis of feldspathoids: a review. In: Feldspars and Feldspathoids, W.L. Brown (ed.) pp. 501–532. D. Reidel Publishing Company, Dordrechet.

England, B.M., 1994. Minerals of the Prospect intrusion, New South Wales, Australia. *The Mineralogical Record* 25, 185–194.

Fitton, J.G. and Upton, B.G. J., Eds, 1987. Alkaline Igneous Rocks. Geological Society Special Publication No. 30. Oxford, 568 pp.

Gaul, O.F., O'Reilly, S.Y. and Griffin, W.L., 2003. Lithosphere structure and evolution in Southeastern Australia. Evolution and Dynamics of the Australian Plate (Hillis, R.R. and Mueller, R.D., eds), pp. 185–202. *Geological Society of Australia Special Publication 22* and *Geological Society of America Special Paper 372*.

Griffin, W.L., Sutherland, F.L. and Hollis, J.D., 1987. Geothermal profile and crust mantle transition beneath east-central Queensland: volcanology, xenolith petrology and seismic

data. *Journal of Volcanology and Geothermal Research* 31, 177–203.

Güven, N., 1988. Smectites. Hydrous Phyllosilicates (exclusive of micas). S.W. Bailey (ed.), pp. 497–559. *Progress in Mineralogy* 19. Mineralogical Society of America.

Jaques, A.L., 2006. Australian diamond deposits, kimberlites, and related rocks, 1:5 000 000 scale map. Geoscience Australia, Canberra.

Johnson, R.W. (ed.), 1989. Intraplate Volcanism in Eastern Australia and New Zealand. Cambridge University Press, Cambridge.

McQueen, K.G., Gonzalez, O.R., Roach, I.C., Pillans, B.J., Dunlap, W.J. and Smith, M.L., 2007. Landscape and regolith features related to Miocene leucitite lava flows, El Capitan northeast of Cobar, New South Wales. *Australian Journal of Earth Sciences* 54, 1–17.

Madden, J., 1999. EL 5171 Bundabulla First and Final Report Angledool SH 55-07 1:250 000 New South Wales Australia. Geological Survey of New South Wales Report 1999/259.

Meakin, N.S. and Morgan, E.J., 1999. Dubbo 1:250 000 Geological Sheet SI/55-4 (2nd edition). Geological Survey of New South Wales Explanatory Notes.

North Broken Hill Ltd, 1971a. Assessment report, EL 292. Bourke-Byrock area. Geological Survey of New South Wales, File GS 1971/346 (unpubl.).

North Broken Hill Ltd, 1971b. Drilling aid, El 292, Byrock area. Geological Survey of New South Wales, File GS 1971/ 378 (unpubl.).

North Broken Hill Ltd & Pressaug Australia Pty Ltd 1982. Final report, ELs 1208 and 1209, Mt Oxley, Bourke area. Geological Survey of New South Wales, File GS 1982-339 (unpublished).

O'Reilly, S.Y. and Griffin, W.L., 1985. A xenolith-derived geotherm for southeastern Australia and its geological implications. *Tectonophysics* 111, 41–63.

O'Reilly, S.Y., Nicholls, I.A. and Griffin, W., 1989. Xenoliths and megacrysts of Eastern Australia. Intraplate volcanism in Eastern Australia and New Zealand. Johnson, R.W.

(ed.), pp. 249–288. Cambridge University Press.

Paul, B., Hergt, J.M. and Woodhead, J.D., 2005. Mantle heterogeneity beneath the Cenozoic volcanic provinces of central Victoria inferred from trace-element and Sr, Nd, Pb and Hf isotope data. *Australian Journal of Earth Sciences* 52, 243–260.

Preussag Australia Pty Ltd & North Broken Hill Ltd, 1981a. Exploration reports, 3 and 4, ELs 1208 and 1209, Mount Oxley, Bourke area. Geological Survey of New South Wales, File GS 1981/ 095.

Preussag Australia Pty Ltd & North Broken Hill Ltd, 1981b. Exploration reports, ELs 1208 and 1209, Mount Oxley, Bourke area. Geological Survey of New South Wales, File GS 1981/ 565.

Rock, N.M.S., 1991. Lamprophyres. Blackie, Glasgow & London, 285 pp.

Sutherland, F.L., 1985. Regional controls in eastern Australian volcanism. *Geological Society of Australia, New South Wales Division, Proceedings* 1, 13–32.

Sutherland, F.L., 2003. Boomerang migratory intraplate Cenozoic volcanism, eastern Australia rift margins and the Indo-Pacific mantle boundary. Evolution and Dynamics of the Australian Plate (Hillis, R.R., and Müller, R.D., eds), pp. 203–221. *Geological Society of Australia Special Publication 22* and *Geological Society of America Special Paper 372.*

Sutherland, F.L., Raynor, L.R. and Pogson, R.E., 2005. Table Cape vent xenolith suite, northwest Tasmania: Mineralogy and implications for crust-mantle lithology and Miocene geotherms in Tasmania. *Papers and Proceedings of the Royal Society of Tasmania*, 139, 7–22.

Sutherland, F.L., Stubbs, D. and Green, D.C., 1977. K-Ar ages of Cainozoic volcanic suites, Bowen-St Laurence hinterland, north Queensland (with some implications for genetic models). *Journal of the Geological Society of Australia* 24, 447–460.

Tadros, N. (Victor) (Compil. and ed.), 1993. The Gunnedah Basin New South Wales. *Ge-*

ological Survey of New South Wales Memoir Geology 12.

Taylor, W.R. 1998. An experimental test of some geothermometer and geobarometer formulations for upper mantle peridotites with applications to the thermometry of fertile lherzolite and garnet websterite. *Neues Jahrbuch für Mineralogie, Abhandlungen* 172, 381–408.

Trebaudino, M. and Bruno, E., 1993. Effects of Al on enstatite solubility in CMAS clinopyroxenes: 1-Experimental results in the clinopyroxene-othopyroxene two phase field at P=18kbar. *European Journal of Mineralogy* 5, 123–131.

Wells, P.R.A. (1977). Pryoxene thermometry in simple and complex systems. *Contributions to Mineralogy and Petrology* 62, 129–139.

Wicks, F.J. and O'Hanly, D.S., 1988. Serpentine minerals: structures and petrology. Hydrous Phyllosilicates (exclusive of micas), S.W. Bailey, (ed.), pp. 91–167. *Reviews in Mineralogy* 19, Mineralogical Society of America.

Williams, M.L. and Carr, P.F., 2005. Isotope systematics of secondary minerals from the Prospect intrusion, New South Wales. *Australian Journal of Earth Sciences* 52, 799–806.

Wood, B.J. and Banno, S., 1973. Garnet orthopyroxene and orthopyroxene-clinopyroxene relationships in simple and complex systems. *Contributions to Mineralogy and Petrology* 42, 109–121.

Yavuz, F., 1996. Amphcal: A quickbasic program for determining the amphibole name from electron microprobe analysis using the IMA rules. *Computers and Geosciences* 22 (2), 101–107.

Yoder, H.S., and Tilly, C.E. 1962. Origin of basalt magmas: an experimental study of natural and synthetic rock systems. *Journal of Petrology* 3, 342–532.

Zhang, M. and O'Reilly, S.Y., 1997. Multiple sources for basaltic rocks from Dubbo, eastern Australia: geochemical evidence for plume-lithosphere mantle interaction. *Chemical Geology* 136, 33–54.

Zussman, J. 1998. Baryte In Chang L.L.Y, Howie, R.A. and Zussman, J. eds. Rock Forming Minerals. Volume 5B Second Edition. Non-silicates: Sulphates, Carbonates, Phosphates, Halides, pp. 3–29. The Geological Society, London.

* School of Natural Sciences
BCRI Campus, University of Western Sydney
Locked Bag 1797, Penrith South DC
NSW 2197
Australia

† B.J. Barron
7 Fairview Avenue,
St. Ives NSW 2075
Australia

Author for correspondence.
Dr Lin Sutherland
email: `L.Sutherland@uws.edu.au`

Applications and Limitations of Independent Component Analysis for Facial and Hand Gesture Surface Electromyograms

GANESH R. NAIK AND DINESH K. KUMAR

Abstract: In the recent past, there has been an increasing trend to use blind source separation (BSS) or independent component analysis (ICA) algorithms for biomedical data. This paper reviews the concept of ICA and demonstrates its usefulness and limitations in the context of surface electromyograms (sEMG) related to hand movements and facial muscles. In the first experiment ICA has been used to separate the electrical activity from different hand gestures. The second part of the study considers separating electrical activity from facial muscles. In both instances the surface electromyogram has been used as an indicator of muscle activity. The theoretical analysis and experimental results demonstrate that ICA is suitable for identification of different hand gestures using sEMG signals. The results identify the unsuitability of ICA when a similar technique is used for facial muscles with respect to different vowel classifications.

Keywords: Independent component analysis, surface electromyogram, motor unit action potentials, human-computer interaction, blind source separation

INTRODUCTION

Independent component analysis (ICA) has recently received a lot of attention both in biomedical signal processing and statistical signal processing. Independent component analysis is a useful method for blind source separation (BSS) and unsupervised learning, where the observation vectors are assumed to be linear mixing of independent components. Efficient new ICA algorithms have been introduced to solve the blind source separation problems. ICA algorithms are successfully utilised for removing artefact and noise from recorded biosignals, especially sEMG. Research that isolates motor unit action potential (MUAP) originating from different muscles and motor units has been reported in 2004 (Nakamura et al. 2004), where success is reported in the isolation of the different MUAP with applications for decomposing the sEMG at low levels of muscle activation. ICA has also been proposed for unsupervised cross talk removal from sEMG recordings of the muscles of the hand (Greco et al. 2003). Recently ICA had been utilised to identify different hand gestures (Naik et al. 2006). From the literature, ICA appears to be the emerging technology with solutions to most of the sEMG applications. Myo-electric activity originating from different muscles can be considered to be independent, making the use of ICA a suitable method for the separation of muscle activity originating from different muscles.

Surface Electromyography (sEMG) is a surface recording of muscle activity. It is a result of the spatial and temporal integration of the MUAP originating from different motor units. Being non-invasive and an important indicator of muscle activity, sEMG is useful, but the presence of multiple muscle activity and the random nature of the transmission path makes the signal difficult to use reliably when muscle activity is small, and actions are complex. It is difficult to separate muscle activity originating from different muscles due to similarity in the signals. Earlier work by the authors has used sEMG to identify unspoken vowels with success (Kumar et al. 2004), but reliability issues exist. This paper reports research conducted to identify the applications of ICA in hand gesture identification, and to determine some of the limitations of using ICA for separation of sEMG from facial muscle activity originating from other muscles (cross talk). The paper reports theoretical analysis and experimental results and discusses the apparent discrepancies between the two.

FACIAL MOVEMENT AND MUSCLES RELATED TO SPEECH

The face can communicate a variety of information including subjective emotion, communitive intent, and cognitive appraisal. The facial musculature is a three-dimensional assembly of small pseudo-independently controlled muscles performing a variety of complex or facial functions such as speech, mastication, swallowing and mediation of motion (Lapatki et al. 2003, Parsons 1986).

When using facial sEMG to determine the shape of the lips and the mouth, there arises the issue of the proper choice of muscles and their corresponding best location of electrodes. Face structure is more complex than that of the limbs due to a large number of overlapping muscles. It is thus difficult to identify the specific muscles that are responsible for specific facial actions and shapes. There is also the difficulty of cross talk due to the overlap between different muscles. This is made more complex because of the temporal variation in the activation and deactivation of the different muscles. It is impractical to consider the entire facial musculature and record its electrical activity. In this study, only four facial muscles have been selected. The *Zygomaticus major* arises from the front surface of the zygomatic bone and merges with the muscles at the corner of the mouth. The *Depressor anguli oris* originates from the mandible and inserts into the skin at an angle to the mouth and pulls the corner of mouth downward. The *Masseter* originates from the maxilla and zygomatic arch and inserts to the ramus of the mandible to elevate and protrude; it assists in side-to-side movements of the mandible. The *Mentalis* originates from the mandible and inserts into the skin of the chin to elevate and protrude the lower lip, to pull skin into a pout (Fridlund and Cacioppo 1996).

SURFACE EMG AND INDEPENDENT COMPONENT ANALYSIS

The EMG signal is widely used as a suitable means to have access to physiological processes involved in producing joint movements. The information extracted from the EMG signals can be exploited in several different applications. sEMG is a non-invasive and painless procedure in which EMG signals are measured from electrodes on the skin. This technique has clear advantages over needle EMG. Most importantly it is painless for the patient and avoids health hazards for patient and doctor. Furthermore, sEMG is a quick and easy process that facilitates sampling of a large number of MUPs (Fujimoto and Nishizono 1993). One major barrier is that, due to the wide pickup area of surface electrodes, sEMG waveforms exhibit significant interference. Surface EMG recordings provide a practical means to record from several muscles simultaneously but tend to be unreliable, i.e., recordings from a subject performing the same movement repetitively tend to have considerable trial-to-trial variability. sEMG recordings are also affected by crosstalk whereby several muscles may contribute to the recording of a given electrode, making the source of the signal difficult to identify. Recently, ICA has been proposed as a method to analyze sEMG recordings, and this addresses many of these concerns. One property of the sEMG is that the signal originating from one muscle can generally be considered to be independent of other bioelectric signals such as an electrocardiogram (ECG), electro-oculargram (EOG), and signals from neighbouring muscles. This opens an opportunity for the use of ICA in this application (Hyvarinen et al. 2001).

BSS aims at recovering the sources from a set of observations. Applications include separating individual voices at a cocktail party. In the BSS problem, two processes are involved (Hyvarinen 1997, Comon 2001). These are the mixing and un-mixing processes. First, we observe a set of multivariate signals $[x_1(t), x_2(t) \ldots x_n(t)]$ that are assumed to be linearly mixed with a set of source signals $[s_1(t), s_2(t) \ldots s_n(t)]$. The mixing process is hidden so we can only observe the mixed signals. The task is to recover the original source signals from the observations through an un-mixing process. Equation (1) and (2) describe the mixing and un-mixing processes mathematically

(Bell and Sejnowski 1995, Hyverinen and Oja 1997).

Mixing $x = As$ (1)
Unmixing $Wx = WAs$ (2)

For solving the BSS it is assumed that the number of observations is equal to the number of source signals. Matrix s contains the original source signals driving the observations, whereas the separated signals are stored in matrix u. They are both $[n \times t]$ matrices. A and W are both $[n \times n]$ matrices, the mixing and un-mixing matrix, respectively. If the separated signals are the same as the original sources, the mixing matrix is the inverse of un-mixing matrix, i.e., $A = W^{-1}$.

METHODOLOGY

Experiments were conducted to evaluate the performance of the hand gesture recognition and facial muscle activity using surface EMG.

Recording and Processing of Hand Gesture sEMG

For the hand gesture experiments 5 subjects whose ages ranged from 21 to 32 years (4 males and 1 female) were chosen. The experiments were conducted on two different days on all five subjects. For the data acquisition a proprietary surface EMG acquisition system by Delsys (Boston, MA, USA) was used. Four electrode channels were placed over four different muscles as indicated in Table 1 and Figure 1. A reference electrode was placed at the *Epicondylus Medialis*.

The experiments were repeated on two different days. Subjects were asked to keep the forearm resting on the table with the elbow at an angle of 90 degree in a comfortable position. Three hand actions were performed and repeated 12 times in each instance. Each time the raw signal sampled at 1024 samples/second was recorded. The gestures used for the experiments are listed below and details are provided in Table 1.

- Wrist flexion (without flexing the fingers)
- Finger flexion
- Finger and wrist flexion together but normal along centre line

The hand actions and gestures represented low level muscle activity. The hand actions were selected based on small variations between the muscle activities of the different digitas muscles situated in the forearm.
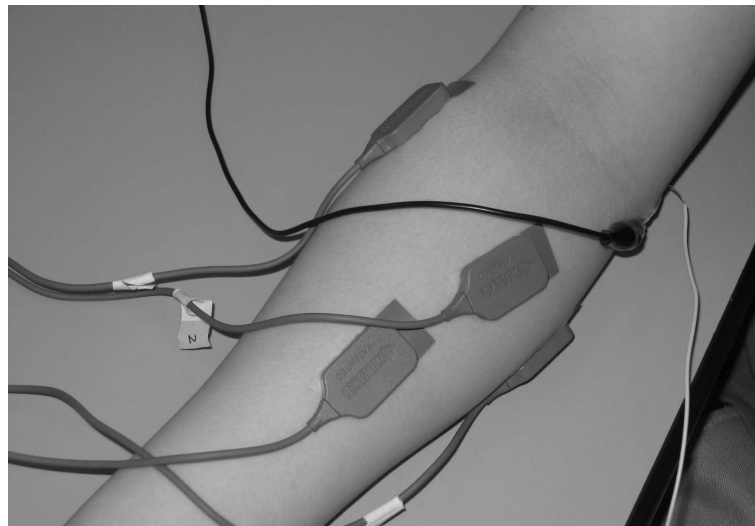

Figure 1. Hand gesture experimental set up with four electrodes.

Channel	Muscle	Function
1	Brachioradialis	Flexion of forearm
2	Flexor carpi radialis (FCR)	Abduction and flexion of wrist
3	Flexor carpi ulnaris (FCU)	Adduction and flexion of wrist
4	Flexor digitorum superficialis (FDS)	Finger flexion while avoiding wrist Flexion

Table 1. Placement of electrodes over the skin of the forearm.

Recording and Processing of Facial sEMG

Experiments were conducted on a single subject on two different days to test inter-day variations. A male subject participated in the experiment. The experiment used 4 channel EMG configurations as per the recommended recording guidelines (Fridlund and Cacioppo 1996). A four channel, portable, continuous recording MEGAWIN equipment (MEGA Electronics, Finland) was used. Raw signal sampled at 2000 samples/ second was recorded. Ag/AgCl electrodes (AMBU Blue sensors from MEDICOTEST, Denmark) were mounted at appropriate locations close to the selected facial muscles (on the right side *Zygomaticus major*, *Masseter* and *Mentalis*, and on the left side *Depressor anguli oris*). The inter-electrode distance was kept constant at 1 cm for all channels and experiments.

Controlled experiments were conducted where the subject was asked to speak 5 English vowels (/a/, /e/, /i/, /o/, /u/). Each vowel was spoken separately such that there was a clear start and end to the utterance. During utterance, facial sEMG from the muscles was recorded. sEMG from four channels were recorded simultaneously. The experiment was repeated ten times. A suitable resting time was given between each experiment.

Data Analysis

The aim of these experiments wase to test the use of ICA along with known properties of the muscles for separation of sEMG signals to identify hand gestures and to test the use of ICA on the facial sEMG signals for identifying speakers. Similar data analysis was performed on facial sEMG and hand gesture sEMG. For both experimental datasets, there were four channel (recordings) electrodes and four active muscles associated, forming a square 4×4 mixing matrix. The sEMG recordings were separated using a fast ICA matlab algorithm which has been developed by a team at the Helsinki University of Technology (Hyvarinen and Oja 1997). The mixing matrix A was computed for the first set of data only. Independent sources of motor unit action potentials that mix to make the EMG recordings were computed using equation (3),

$$s = Bx \qquad (3)$$

where B is the inverse of the mixing matrix A. This process was repeated for each of the three hand gesture experiments. Four sources were estimated for each experiment. After separating the four sources sa, sb, sc and sd, each of these was segmented to sample length. Root Mean Squares (RMS) were computed for each separated sources using equation (4),

$$S_{rms} = \sqrt{\frac{1}{N}\sum_{i=1}^{n} s_i^2} \qquad (4)$$

where s is the source and N is the number of samples. This results in one number representing the muscle activity for each channel for each hand action and muscle activity for facial muscle. The RMS value of muscle activity of each source represents the muscle activity of that muscle and is an indicator of the force of contraction generated by each muscle. The above process was repeated for all 3 different hand actions 12 times and for each of the participants and repeated for the facial muscle sEMG for the 5 vowels. The outcome was 10 sets of examples, each pertaining to speech of 5 vowels. Results were used further for neural network analysis.

Neural Network Analysis

As a first step, the networks were trained using the randomly chosen training data. Performances were monitored during the training phase in order to prevent overtraining. Similar ANN architecture was used to test the reliability of hand gesture sEMG and facial sEMG. The ANN consisted of two hidden layers with a total of 20 nodes. A sigmoid function was the threshold function and the type of training algorithm for the ANN was gradient descent.

For hand gesture actions 12 sets of examples were used to train a back-propagation neural network. Inputs to the network were the 4 RMS values for each gesture and the output of the network were the three gestures. A back propagation neural network was then trained with the RMS values as the inputs and the gesture numbers as the targets. This network was then tested for the test data. For facial sEMG we used 10 sets with 4 inputs and 3 outputs by taking different combinations of vowels (a/i/u), (i/o/u), (a/o/u), (e/i/u), etc. Ihe inputs to the network were the 4 RMS values for each vowel utterance and the output of the network were the three vowels. Similar to the hand gesture analysis, a back propagation neural network was trained and tested with the RMS values as the inputs and the vowel utterance numbers as the targets.

RESULTS AND DISCUSSION

The aim of this research was to test the reliability and to determine the efficacy of the ICA technique to decompose sEMG into muscle activity from individual muscles and to classify the activity from these muscles to identify the hand gestures and speakers. The ability of the system to accurately classify the decomposed sEMG against the known hand gestures is given Table 2. Classification of different vowels using facial sEMG is shown in Table 3.

In hand gesture identification experiments, the accuracy was computed based on the percentage of correct classified data points to the total number of data points. These results indicate an overall classification accuracy of 100%. Results for two different set of vowels are shown in Table 3. Accuracy was computed based on the percentage of correct classified data points to the total number of data points. The results indicate an overall average accuracy of about 60%.

Number of participants	Wrist flexion		Finger Flexion		Finger flexion and wrist flexion	
	Day one	Day two	Day one	Day two	Day one	Day two
Subject 1	100%	100%	100%	100%	100%	100%
Subject 2	100%	100%	100%	100%	100%	100%
Subject 3	100%	100%	100%	100%	100%	100%
Subject 4	100%	100%	100%	100%	100%	100%
Subject 5	100%	100%	100%	100%	100%	100%

Table 2. Experimental results for hand gesture identification using muscle activity separated from sEMG using ICA.

Correctly classified vowels	Day 1	Day 2
/a/	60%	60%
/e/	60%	55%
/i/	60%	65%
/o/	55%	55%
/u/	65%	60%

Table 3. Experimental results for vowel classification using muscle activity separated from facial sEMG using ICA.

Comparative Evaluation of Hand sEMG with Facial sEMG

In order to measure the quality of the separation of hand gesture muscle activities in comparison to facial muscle activities, we used mixing matrix analysis. Generally, the efficiency of the ICA estimation stage for the un-mixing matrix can be verified by the following cross check. If a temporal wide-band source signal is split into, e.g., two consecutive narrow band signals p and q, the un-mixing matrix can be estimated independently twice from different raw data sections.

Then, processing quality can be validated by multiplying two of the independently retrieved matrices Wp and Wq, while one of the two has to be inverted. The result of this multiplication should be the identity matrix I (theoretically, in practice it should be close to I due to noise contributions), if everything in the process works correctly, and if the input source signal vector contains independent signals, as in equation (5).

$$I \approx G = W_p W_q^{-1} \qquad (5)$$

In the comparative experiments here, performing these evaluation steps for hand gesture signals as well as for facial muscle signal captures yielded the following result matrices.

Due to the intrinsic order ambiguity of ICA, the order of unit vectors in the resulting matrix may be permuted, but from this sample measurement it appears confirmed that full dimensionality is achieved in the hand gesture application. On the other hand, for the facial application the validation result obviously contains dependent vectors and doesn't match the theory. This result shows a fundamental issue in the facial setup. One explanation for this effect may be that the facial signal components are not independent to the required extent. To validate this, a systematic experimental series was performed to evaluate the behavior of the dimensionality of the matrix G. In this supplementary investigation it turned out that the computational rank (Meyer 2000) of the matrix is not a valid measure in this signal-processing application. Instead the determinant value of the multiplication matrix was found being a valuable indicator in the sense that if this measure is close to zero there are problems with the recorded signal compound (in mathematical interpretations the determinant value would have to be exactly zero, but due to noise contributions this is never achieved even in constructed and obvious dependency cases). In the above sample, the determinant values are $\mathbf{det}(G_{hand}) = 2.2588$, while $\mathbf{det}(G_{facial}) = 0.0013$ is close to zero.

$$G_{hand} = \begin{bmatrix} 0.0800 & -1.0094 & 0.0271 & 0.0927 \\ 0.0670 & -0.0046 & 0.0307 & -1.2610 \\ 0.0143 & 0.0295 & 0.8062 & 0.0273 \\ 2.1595 & 0.3787 & -0.0729 & 0.0686 \end{bmatrix}, \mathbf{det}(G_{hand}) = 2.2588$$

$$G_{facial} = \begin{bmatrix} 0.0485 & -1.1738 & 0.0891 & -1.1105 \\ -0.8019 & 1.0171 & 0.7873 & 0.1669 \\ -0.8377 & 0.0142 & 1.1837 & -1.0169 \\ -1.4905 & 0.0192 & -1.3557 & 0.4750 \end{bmatrix}, \mathbf{det}(G_{facial}) = 0.0013$$

Overall, this comparative investigation shows that the high recognition rate for hand gestures can be considered as being reasonable, since in an inappropriate experimental setup the new technique doesn't work efficiently. Another notable aspect is that this technique can be applied in real-time mode, because of easy to use algorithms like fast ICA (Hyvarinen and Oja 2001) and back propagation neural networks (Fausett 1994). Quick computation times for these algorithms make the system suitable for day-to-day application.

Numbers of researchers have reported attempts to identify hand and body gestures from sEMG recordings but with low reliability. This may be attributed to low signal to noise ratios and high levels of cross-talk between different simultaneously active muscles. ICA is a recently developed signal processing and source separation tool and has been employed to separate the muscle activity and remove artefacts to overcome this difficulty. While ICA has been extremely useful for audio-based source separation, its application for sEMG is questionable due to the random order of the separated signals and magnitude normalisation. This paper reports research that overcomes this shortcoming by using prior knowledge of the anatomy of muscles along with blind source separation. Using a combination of the model and ICA approaches with a neural network configured for the individual overcomes the order and magnitude ambiguity.

The results demonstrate that the proposed method provides interesting results for inter-experimental variations in facial muscle activity during different vowel utterance. The accuracy of recognition is poor when the system is used for testing the training network for all subjects. This shows large variations between subjects (inter-subject variation) because of different styles and speeds of speaking. This method has only been tested for limited vowels. This is because the muscle contraction during the utterance of vowels is relatively stationary while for consonants there are greater temporal variations. The results show that for such a system to succeed, the system needs to be improved. Some possible improvements would include improved electrodes, site preparation, electrode location, and signal segmentation. This current method also has to be enhanced for large sets of data with many subjects in future. The authors intend to use this method for checking the inter-day and inter-experimental variations of facial muscle activity for speech recognition in the near future to test the reliability of ICA for facial SEMG

CONCLUSIONS

Independent component analysis (ICA) is a technique that is suitable for blind source separation and has been considered for decomposing sEMG to obtain individual muscle activities. This paper proposed applications and limitations of ICA on hand gesture actions and vowel utterance. Results on hand gesture identification indicate that the system is able to perfectly (100% accuracy) identify the set of selected complex hand gestures for each of the subjects. These gestures represent a complex set of muscle activation and can be extrapolated for a larger number of gestures. Nevertheless, it is important to test the technique for more actions and gestures, and for a large group of people. Results on vowel classification using facial sEMG indicate that while there is similarity between muscle activities, there are inter-experimental variations. Possible reasons are that people use different muscles even when they make the same sound, and cross talk due to different muscles makes the signal quality difficult to classify. Normalisation of the data reduced the variation of magnitude of facial sEMG between different experiments. The work indicates that people use same set of muscles for the same utterances, but there is a variation in muscle activities. It can be used in preliminary analysis for using facial sEMG-based speech recognition.

ACKNOWLEDGEMENTS

REFERENCES

Bell, A. and Sejnowski, T. 1995. An information-maximisation approach to blind separation and blind deconvolution. *Neural Computation*, **7**, 1129–1159.

Comon, P. 2001. Independent Component Analysis, a New Concept. John Wiley, New York.

Fausett, L. 1994. Fundamentals of Neural Networks: Architectures, Algorithms, and Applications. Prentice Hall, New Jersey.

Fridlund, A.J., and Cacioppo, J.T. 1996. Guidelines for human electromyographic research. *Journal of Psychophysiology*, **23**, 567–589.

Fujimoto, T. and Nishizono, H. 1993. Muscle contractile properties by surface electrodes compared with those by needle electrodes. *Electroencephalography and Clinical Neurophysiology*, **89**, 247–251.

Greco, A., Costantino, D., Morabito, F.C. and Versaci, M.A., 2003. Morlet wavelet classification technique for ICA filtered SEMG experimental data. *Neural Networks*, **1**, 166–171.

Hyvarinen, A., Karhunen, J. and Oja, E. 2001. Independent Component Analysis. John Wiley, New York.

Hyvarinen, A. 1997. A fast and robust fixed-point algorithm for independent component analysis. *IEEE Transaction on Neural Networks*, **10**, 626–634.

Hyvarinen, A. and Oja, E. 1997. Fast fixed-point algorithm for independent component analysis. *Neural Computations*, **9**, 1483–1492.

Hyvarinen, A. and Oja, E. 1997. Fast fixed-point algorithm for ICA. The Fast ICA matlab software package `http://www.cis.hut.fi/projects/ica/fastica/index.shtml`

Kumar, S., Kumar, D.K., Alemu, M. and Burry, G. 2004. EMG based voice recognition. Proceedings of the 2004 Intelligent Sensors, Sensor Networks and Information Processing Conference, pp. 593–597.

Lapatki, G., Stegeman, D.F. and Jonas, I.E., 2003. A surface EMG electrode for the simultaneous observation of multiple facial muscles. *Journal of Neuroscience Methods*, **123**, 117–128.

Meyer, C.D. 2000. Matrix Analysis and Applied Linear Algebra, Cambridge University Press, Cambridge.

Naik, G.R., Kumar, D.K., Singh, V. and Palaniswami, M.,2006. SEMG for identifying hand gestures using ICA. Proceedings of the Workshop on Biosignal Processing and Classification at the 2nd International Conference on Informatics in Control, Automation and Robotics, pp. 61–67.

Nakamura, H., Yoshida, M., Kotani, M., Akazawa K. and Moritani, T. 2004. The application of independent component analysis to the multi-channel surface electromyographic signals for separation of motor unit action potential trains. *Journal of Electromyography and Kinesiology*, **14**, 423–432.

Parsons, W.T., 1986. Voice and Speech Processing. McGraw-Hill, New York.

Ganesh R. Naik* and Dinesh K. Kumar
School of Electrical and Computer Engineering
RMIT University
GPO BOX 2476V Melbourne
Victoria 3001, Australia
email: ganesh.naik@rmit.edu.au & dinesh@rmit.edu.au

* Author for correspondence.

Subtle Hand Gesture Identification for Human-Computer Interaction using Independent Component Analysis of Surface Electromyography

GANESH R. NAIK AND DINESH K. KUMAR

Abstract: Surface electromyography (sEMG) is an indicator of muscle activity and is related to body movement and posture. One common shortcoming in the use of sEMG is to distinguish between small actions that require simultaneous contraction of number of adjoining muscles. This paper presents a method for subtle hand gesture identification from sEMG of the forearm by decomposing the signal into components originating from different muscles. The processing requires the decomposition of the surface EMG by independent component analysis (ICA) technique. Pattern classification of the separated signal is performed in the second step with a back propagation neural network. The focus of this work is to establish a simple, yet robust system that can be used to identify subtle complex hand actions and gestures for control of prostheses and other computer-assisted devices. The proposed model-based approach is able to overcome the ambiguity problems (order and magnitude problems) of ICA methods by selecting an *a priori* mixing matrix based on known hand muscle anatomy. Testing was conducted using several single shot experiments conducted with five subjects. The results indicate that the system is able to classify the data with 97% accuracy.

Keywords: Independent component analysis, surface electromyogram, motor unit action potentials, human-computer interaction, blind source separation

INTRODUCTION

Surface electromyography (EMG) is the electrical manifestation of contracting muscle activity and is thus an obvious choice for control of prostheses and other control applications. While there are number of possible applications of EMG, one common shortcoming is the difficulty in identifying small and subtle muscle contractions related to actions or maintained gestures and postures. Many attempts have been made to use the surface EMG signal as the command to control a prosthesis (Doerschuk et al. 1983, Kermani et al. 1995), but none of them takes explicit advantage of its subtlety, the fact that commands can be issued without the generation of observable movements. Hand actions and maintained gestures are a result of complex combination of contraction of multiple muscles in the forearm. Since all these muscles present in the forearm are close to each other, myoelectric activity observed from any muscle site comprises the activity from neighbouring muscle as well, referred to as cross-talk. The cross-talk problem is greater when muscle activation

is relatively weak (subtle). Extraction of useful information from such surface EMG becomes difficult mainly due to the low signal to noise ratio. At low levels of contraction, EMG activity is hardly discernible from background activity. Therefore to correctly classify the movement and gesture of the hand more precisely, EMG needs to be decomposed to identify contraction of individual muscles. There is little or no prior information of muscle activity, and signals have temporal and spectral overlap, making the problem suitable for independent component analysis (ICA).

Blind source separation (BSS) techniques, especially in ICA, have found numerous applications in audio- and bio-signal processing. ICA has been proposed for unsupervised cross-talk removal from surface EMG recordings of muscles of the hand (Greco et al. 2003). Research that isolates motor unit action potential (MUAP) originating from different muscles and motor units was reported in 2004 (Nakamura et al. 2004). Muscle activity originating from different muscles can be considered to be independent, and this gives suggests the use of

BSS methods for separation of muscle activity. The spatial location of the active muscle activity is the determining factor of the hand action and gesture. One technique that has been reported is the use of prior knowledge of the anatomy. The advantage of this approach is that the method removes ambiguity of the order and magnitude. This paper proposes the use of ICA for separation of muscle activity from the different muscles of the forearm to identify subtle hand gesture where a pre-trained neural network classifier is used to identify hand gestures.

HAND GESTURE IDENTIFICATION FOR HCI

The use of hand gestures provides an attractive alternative to cumbersome interface devices for human-computer interaction (HCI). HCI requires the design and implementation of interactive computing systems for human use. The intent is to provide a seamless and natural interface that allows the human user to control and interact with computers and computer-based devices. Human hand gestures are a mean of non-verbal interaction. They range from simple actions like pointing at objects to more complex ones that express feelings and communicate ideas. The main applications of gesture recognition are communicative (e.g., sign language recognition) and manipulative (e.g., controlling robots without any physical contact between human and computer). Some examples of applications include control of consumer electronics, interaction with visualization systems, control of mechanical systems and computer games. Numerous approaches have been applied to the problem of visual interpretation of gestures for HCI. Many have focussed on a particular aspect of gesturessuch as hand tracking, pose classification, or hand posture interpretations (Rehg and Kanade 1996). Trejo et al. (2003) developed a technique for a multimodal neuroelctric interface. Recent studies focus on the use of EMG for the recognition of an alphabet of discrete gestures. To improve reliability, a number of efficient solutions to ges-

ture input in HCI exist, such as restricting the recognition situation, use of input devices (e.g. a data glove), restricting the object information and restricting the set of gestures.

In traditional HCI, most attempts have used some external mechanical device such as an instrumented glove. If the goal is natural interaction in everyday situations this might not be acceptable. A vision-based approach to hand-centered HCI has been proposed in recent years. However vision-based techniques require restricted backgrounds and camera positions and are suitable for a small set of gestures performed with only one hand (Pavlovic et al. 1997). In this report we propose the identification of maintained hand gesture based on muscle activity using the decomposition of surface EMG. It is a combination of a model-based approach with the BSS technique.

SURFACE ELECTROMYOGRAPHY

Surface electromyography is the electrical recording of the spatial and temporal integration of the MUAP originating from different motor units. It can be recorded non-invasively and used for dynamic measurement of muscular function. It is typically the only *in vivo* functional examination of muscle activity used in the clinical environment. The close relationship of surface EMG with the force of contraction of the muscle is useful for number of applications such as sports training, prostheses and for machine control. The EMG signals contain a lot of important information such as muscle force, operator's intended motion, and muscle impedance. Gross properties of sEMG such as magnitude and spectrum parameters are a good indicator of the overall magnitude of contraction, but these are unable to differentiate between muscle activities originating from different adjoining muscles.

Decomposition of sEMG has been attempted with the aim of determining the number of MUAP. Such methods are designed to identify the MUAP based on the shape, and are not suitable for determining the closely located muscles from where the MUAP originates.
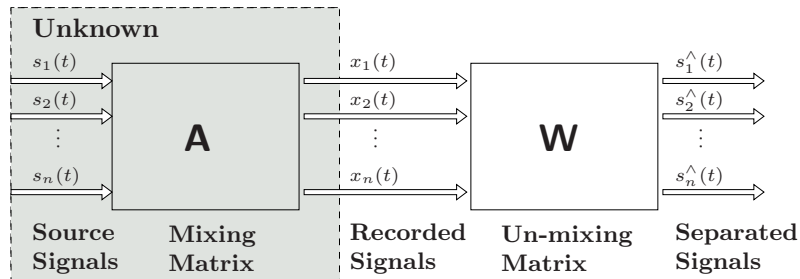
Figure 1. Block diagram describing the system concept; $s(t)$ are the sources, $x(t)$ are the recordings, A is the mixing matrix, W is the estimated un-mixing matrix and $u(t)$ are the estimated separated signals.

One property of the surface EMG is that the signal from one muscle can generally be considered to be independent of other bioelectric signals such as electrocardiogram (ECG), electro-oculargram (EOG), and signals from neighbouring muscles. This opens the opportunity for using BSS methods.

INDEPENDENT COMPONENT ANALYSIS

ICA consists in recovering unobserved signals or 'sources' from several observed mixtures. Typically the observations are obtained at the output of a set of sensors, each sensor receiving the different combination of source signals. The simplest ICA technique aims at transforming an input vector into a signal space in which the signals are statistically independent (Hyvarinen et al. 2001). The simplest ICA model assumes that the mixing process as linear, so it can be expressed as in equation (1),

$$x(t) = As(t) \qquad (1)$$

where $x(t) = [x_1(t), \ldots, x_n(t)]^T$ are the recordings, $s(t) = [s_1(t), \ldots, s_n(t)]$ the original signals, and A is the $n \times n$ mixing matrix. This mixing matrix and each of the original signals are unknown. To separate the recordings to the original signals (estimated original signals, u), the task is to estimate an un-mixing matrix W as in equation (2).

$$s = Wx(t) = WAs(t) \qquad (2)$$

The ICA source recovering process is shown schematically in Figure 1. ICA is a difficult task because we do not have any information about the sources and the mixing process. ICA is a method to tackle this problem and is based on the assumption that the sources are independent from each other (Hyvarinen 1999, Comon 2001). BSS iteratively determines the un-mixing matrix W and thus estimates the corresponding independent signals u from the observations x. There are numbers of possible functions that may be considered for making the separated signals as independent as possible. The choice is based on the statistical independence of the sources s.

Relevance of ICA for sEMG Signal Evaluation

The aim of this section is to demonstrate that there is a strong theoretical basis for applying BSS techniques especially using ICA to sEMG signals. The assumptions that underpin the theory of ICA discussed in the previous section and indicate that BSS methods are ideally suited to separating sources when the sources are statistically independent, independent components have non-Gaussian distributions and the mixing matrix is invertible. These assumptions are well satisfied for sEMG data as MUAPs are statistically independent, have non-Gaussian distributions and we can be (virtually) certain that the mixing matrix will be invertible.

There are, however, two other practical issues that must be considered. First, to ensure that the mixing matrix is constant, the sources must be fixed in space (this was an implied assumption as only the case of a constant mixing matrix was considered). This is satisfied by sEMG as motor units are in fixed physical locations within a muscle, and in this sense applying ICA to sEMG is much simpler than in other biomedical signal processing applications such as EEG or fMRI in which the sources can move (Jung et al. 2000). Secondly, in order to use ICA techniques it is essential to assume that the signal propagation time is negligible. Volume conduction in tissue is essentially instantaneous (Makeig et al. 1997) and hence this assumption is also well satisfied. Based on the, it is reasonable to be confident that ICA can be effectively applied to EMG data. The validity of using ICA is examined below.

METHODOLOGY

Experiments were conducted to evaluate the performance of the proposed subtle hand gesture recognition system from hand muscle surface EMG. We propose a technique to classify small levels of muscle activity to identify hand gestures using a combination of ICA, known muscle anatomy and a neural network configured for the individual.

Data Acquisition

In the hand gesture experiments, seven subjects participated. For data acquisition a proprietary surface EMG acquisition system from Delsys (Boston, MA, USA) was used. Four electrode channels were placed over four different muscles as indicated in Table 1 and Figure 2. Subjects were asked to keep the forearm resting on the table with the elbow at an angle of 90 degree in a comfortable position. Four subtle hand actions were performed and repeated 12 times in each instance. Each time the raw signal sampled at 1024 samples/second was recorded. Markers were used to obtain the subtle contraction signals during recording. Complex actions were chosen to determine the ability of the system when similar muscles are active simultaneously. The four different hand actions performed weremiddle and index finger flexion, little and ring finger flexion, all finger flexion and finger and wrist flexion together. These hand actions and gestures represented low levels of muscle activity (subtle hand gestures). The hand actions were selected based on small variations between the muscle activities of the different digitas muscles situated in the forearm. The subtle hand muscle recordings were separated using the Fast ICA algorithm.

Data Analysis

The aim of these experiments was to test the use of an ICA algorithm (Hyvarinen and Oja 1997) along with known properties of the muscles for separation of muscle activity from sEMG recordings for the purpose of identifying subtle hand gestures. These require no more than 4 independent muscles. Each experiment lasted approximately 2.5 seconds and was repeated 12 times. The sampling rate was 1024 samples per second to give approximately 2500 samples. There were four channel (recordings) electrodes and four active muscles associated with the hand gesture, forming a square 4×4 mixing matrix. The mixing matrix A was computed using the Fast ICA, BSS algorithm for the first set of data only and kept constant throughout the experiment. The independent sources of motor unit action potentials that mix to make the EMG recordings were estimated using equation (3),

$$s = Bx \qquad (3)$$

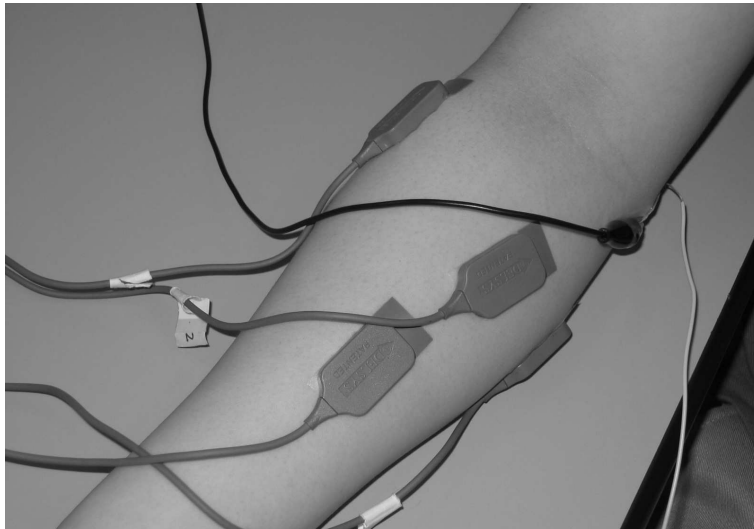| Channel	Muscle	Function
1	Brachioradialis	Flexion of forearm
2	Flexor carpi radialis (FCR)	Abduction and flexion of wrist
3	Flexor carpi ulnaris (FCU)	Adduction and flexion of wrist
4	Flexor digitorum superficialis (FDS)	Finger flexion while avoiding wrist Flexion

Table 1. Muscle electrode configuration.

Figure 2. Hand gesture experimental set up with four electrodes.

where, B is the inverse of the mixing matrix A. This process was repeated for each of the four hand gesture experiments. Four sources sa, sb, sc and sd were estimated for each experiment. Root mean squares (RMS) was computed for each of the separated sources using equation (4),

$$S_{rms} = \sqrt{\frac{1}{N} \sum_{i=1}^{n} s_i^2} \qquad (4)$$

where s are the estimated sources and N is the number of samples. This results in one number representing the muscle activity for each channel for each hand action. RMS values of muscle activity of each source represent the muscle activity of that muscle and are indicative of the strength of contraction.

Classification of Data

The above process was repeated for all four different hand actions 12 times and for each of the participants. These 12 sets of examples were used to train a back-propagation neural network with 4 inputs and 4 outputs. The 4 RMS values of the muscles were the input and the 4 RMS values were the output. In the first part of the experiment, RMS values of 4 recordings for each subject were used to train the artificial neural network (ANN) classifier with a back-propagation learning algorithm. The second part of the experiment (testing) was to verify the performance of the network. For that purpose a subset of all the input vectors different from the learning set (an independent data set) was selected. Performance was also monitored during the training phase in order to prevent overtraining of the network. The ANN consisted of two hidden layers with a total of 20 nodes. A sigmoid function was the threshold function and the type of training algorithm for the ANN was gradient descent. During testing, the ANN with a weight matrix generated during training was used to classify the RMS of the muscle activity. The ability of the network to correctly classify the inputs against known subtle hand actions was used to determine the efficacy of the technique.

RESULTS AND DISCUSSION

The results of the experiment demonstrate the performance of the described system. To compare the performance of the system analysis of RAW sEMG and traditional ICA were performed. In the traditional ICA method, a mixing matrix was computed for each instance. Results demonstrate the ability of the semi-blind ICA method in source separation and identification.

Hand Gesture Identification Results on Raw sEMG

The results of the experiment on raw EMG signals for three different hand gestures are shown in Table 2. The accuracy was computed based on the percentage of correctly classified data points with respect to the total number of data points. Results shows an overall efficiency of 60% for all experiments.

Hand Gesture Identification Results using Traditional ICA

To compare the proposed system with the use of traditional ICA, analysis was performed where RMS of the four channels of sEMG separated using ICA were tabulated for each experiment and classified. This experiment was conducted for four hand gestures where the accuracy was observed to be only 65% (Table 3). These results demonstrate that standard BSS-based separation is not suitable for classifying sEMG.

Hand Gesture Identification Results using Semi-blind ICA

The classification of sEMG after pre-processing using ICA-based separation for four subtle hand gestures are presented in Table 4. The accuracy

was computed based on the percentage of correct classified data points with respect to the total number of data points. The experiments were repeated for different numbers of hand gestures to be classified. Results indicate an overall classification accuracy of 97% for all experiments and demonstrate that this technique can be used for the classification of different subtle hand gestures.

The proposed technique is suitable for classify small levels of muscle activity even when there are multiple, simultaneously active muscles. Such a system may be suitable for being used for HCI, even when the actions are so slight that they may not be observable by other people. The technique has been tested with 7 volunteer participants and with experiments repeated on different days, thus indicating the robustness of the system. We believe that the reason the technique succeeded where others have failed is because the other techniques are not suitable when the signal-to- noise ratio is low and there is significant cross-talk between different, simultaneously active muscles. Use of ICA alone is not suitable for sEMG due to the nature of sEMG distribution and order ambiguity. Prior knowledge of muscle anatomy combined with suitable semi-blind ICA has overcome the abovementioned shortcomings.
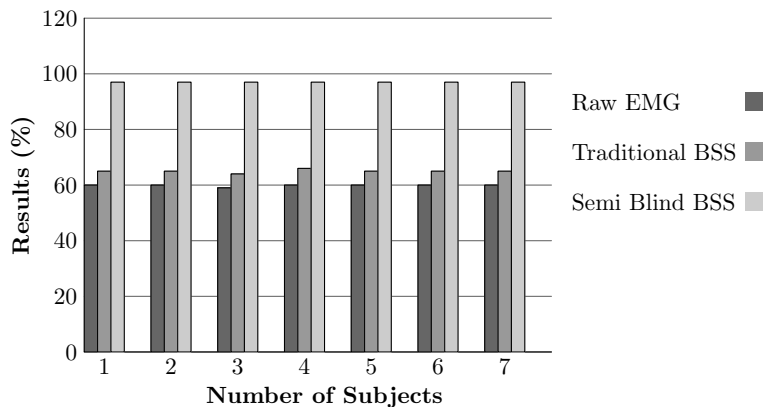

Figure 3. Results showing hand gesture identification results for 7 subjects.

Number of participants	Middle and index finger flexion	Little and ring finger flexion	All finger flexion	Finger and wrist flexion together
Subject 1	60%	60%	61%	60%
Subject 2	60%	62%	60%	60%
Subject 3	58%	60%	60%	60%
Subject 4	60%	60%	60%	60%
Subject 5	60%	60%	60%	60%
Subject 6	60%	60%	60%	60%
Subject 7	60%	60%	60%	60%

Table 2. Experimental results for hand gesture identification without using independent component analysis.

Number of participants	Middle and index finger flexion	Little and ring finger flexion	All finger flexion	Finger and wrist flexion together
Subject 1	66%	65%	65%	65%
Subject 2	64%	65%	64%	65%
Subject 3	65%	65%	65%	66%
Subject 4	65%	66%	65%	66%
Subject 5	66%	64%	66%	64%
Subject 6	66%	64%	66%	64%
Subject 7	66%	64%	66%	64%

Table 3. Experimental results for hand gesture identification using traditional independent component analysis.

Number of participants	Middle and index finger flexion	Little and ring finger flexion	All finger flexion	Finger and wrist flexion together
Subject 1	97%	97%	97%	97%
Subject 2	96%	97%	96%	97%
Subject 3	97%	98%	97%	97%
Subject 4	98%	97%	98%	98%
Subject 5	97%	97%	97%	98%
Subject 6	97%	97%	97%	98%
Subject 7	97%	97%	97%	98%

Table 4. Experimental results for isometric hand gesture identification using the semi-blind ICA algorithm.

CONCLUSIONS

We have shown that a combination of a known biological model with ICA along with neural networks for classification can effectively be applied to classify small muscle activities for identifying subtle hand actions and gestures. Experimental results demonstrate that ICA is highly efficient in performing classification of subtle, motionless gestures. Results indicate that ICA can be successfully employed for the separation of highly correlated, low level muscle activity. Overall, the purpose of this project is to develop new perceptual interfaces for human-computer interaction based on hand gesture identification, and to investigate how such in-

terfaces can complement or replace traditional ones. Possible applications include rehabilitation, prostheses, control of consumer electronics, interaction with visualization systems, control of mechanical systems and computer games.

ACKNOWLEDGEMENTS

REFERENCES

Doerschuk, P.C., Gustafson., D.E. and Willsky, A.S. 1983. Upper extremity limb function discrimination using EMG Signal analysis, *IEEE Transactions on Biomedical Engineering*, **30**, 18–28.

Greco, A., Costantino, D., Morabito, F.C. and Versaci, M.A. 2003. Morlet wavelet classification technique for ICA filtered SEMG experimental data. *Neural Networks*, **1**, 166–171.

Hyvarinen, A., Karhunen, J. and Oja, E. 2001. Independent Component Analysis. John Wiley, New York.

Hyvarinen, A. 1999. A fast and robust fixed-point algorithm for independent component analysis. *IEEE Transaction on Neural Networks*, **10**, 626–634.

Hyvarinen, A. and Oja, E. 1997. Fast fixed-point algorithm for ICA. The Fast ICA matlab software package. `http://www.cis.hut.fi/projects/ica/fastica/index.shtml`

Jung, T., Makeig, S., Lee, T., McKeon, M., Brown, G., Bell, A. and Sejnowski, T. 2000. Independent component analysis of biomedical signals. Proceedings of the Second International Workshop on Independent Component Analysis and Blind Signal Separation, pp. 633–644.

Kermani., M.Z., Wheeler, B.C., Badie K. and Hashemi, R.M. 1995. EMG feature evaluation for movement control of upper extremity prostheses. *IEEE Transactions on Rehabilitation Engineering*, **2**, 1267–1271.

Makeig, S., Jung, T., Bell, A. and Sejnowski, T. 1996. Independent component analysis of electroencephalographic data. *Advances in Neural Information Processing*, **8**, 145–151.

Nakamura, H., Yoshida, M., Kotani, M., Akazawa K. and Moritani, T. 2004. The application of independent component analysis to the multi-channel surface electromyographic signals for separation of motor unit action potential trains. *Journal of Electromyography and Kinesiology*, **14**, 423–432.

Pavlovic, V.I., Sharma, R. and Huang, T.S. 1997. Visual interpretation of hand gestures for human computer interaction: a review. *IEEE Transactions on Pattern Analysis and Machine Intelligence*, **19**, 677–695

Rehg, J.M. and Kanade, T. 1994. Vision-based hand tracking for human-computer interaction. Proceedings of the IEEE Workshop on Motion of Non-Rigid and Articulated Objects, pp. 16–22

Trejo, L.J., Wheeler, K.R., Jorgensen, C.C., Rosipal, R., Clanton, S.T., Matthews, B., Hibbs, A.D., Matthews, R. and Krupka, M. 2003. Multimodal neuroelectric interface development, *IEEE Transactions on Neural Systems and Rehabilitation Engineering*, **11**, 199–204.

Ganesh R Naik* and Dinesh K Kumar
School of Electrical and Computer Engineering
RMIT, GPO BOX 2476V Melbourne
Victoria 3001, Australia
email: ganesh.naik@rmit.edu.au, & dinesh@rmit.edu.au

* Author for correspondence.

Status of Non-native Freshwater Fishes in Tropical Northern Queensland, Including Establishment Success, Rates of Spread, Range and Introduction Pathways

ALAN CHARLES WEBB

Abstract: At least 20 non-native fishes have been reported from northern Queensland fresh waters, a 75% increase since 1994. Eleven of these species have established breeding populations and some are locally abundant and highly invasive, such as the tilapiine cichlids (*Oreochromis mossambicus* and *Tilapia mariae*) and the poeciliids (*Gambusia holbrooki* and *Poecilia reticulata*). Besides the continued introduction of non-native species, of great concern is the further spread of the tilapias, especially *Oreochromis mossambicus* and its hybrid form, and of another invasive, the three-spot gourami, *Trichopterus trichogaster*. Initial introductions are most probably releases of unwanted aquarium fish directly into open waters, or indirectly from ornamental ponds by flood waters. While natural dispersal is occurring, most of the range expansion of the tilapiine cichlids, particularly into impoundments in flood-prone areas, has been as a result of human translocation, and possibly the use of live bait by anglers.

Keywords: Cichlidae, distribution patterns, Gambusia, Gourami, introduction pathways, invasive fishes, *Oreochromis mossambicus*, Poeciliidae, Tilapia

INTRODUCTION

The history of non-native fishes, i.e., those originating from overseas, introduced into northern Queensland fresh waters has been well documented (McKay 1978, 1984, 1989; Arthington et al. 1984, Lear 1987, Blühdorn et al. 1990, Arthington and Blühdorn 1994, Milward and Webb 1990, Webb 1994, Webb et al. 1997, Canonico et al. 2005). Introductions began in the early 1940s with the widespread release of the poeciliid, *Gambusia holbrooki*, for biological control of mosquito larvae (McKay 1984). In the 1950s and 60s there was a massive expansion in numbers of non-native fishes imported into Australia for the aquarium trade as the keeping of tropical fishes increased in popularity. There was subsequently a large increase, especially in the late 1970s and onwards, in the number of species, notably cichlids, reported from open fresh waters in tropical northern Queensland.

Five non-native species (*G. holbrooki, P. reticulata, X. maculatus, Hemichromis* sp. (cf. *guttatus*), *O. mossambicus* and *T. mariae*) were reported during the first surveys of non-native fishes in northern Queensland (McKay (1978, 1989, Arthington et al. 1984, Lear 1987), while McKay (1989) also referred to a previous, though unsuccessful, introduction of *Jordanella* sp. (*floridae*) (Family Cyprinodontidae) in Harvey Creek. These surveys found *P. reticulata* and *X. maculatus* to be common in several rivers, creeks, urban and rural drains north of Innisfail, while recently introduced populations of *O. mossambicus*, in Townsville and Cairns, and *T. mariae*, in Cairns, were rapidly spreading from their original points of introduction. Mather and Arthington (1991) reported that there were two genetically distinct populations of *O. mossambicus* in northern Queensland, a 'pure' strain occurring in the Townsville region and a polymorphic hybrid strain occurring in the Cairns region. Webb (1994) reported that the number of cichlids in open waters in northern Queensland had increased to at least six with the addition of the oscar (*Astronotus ocellatus*), green severum (*Heros severum*), the red devil *Amphilophus cf. labiatum (citrinellum)* and the jewel cichlid (*Hemichromis guttatus*).

This paper presents the results of surveys by the author and others conducted since 1996 between the Burdekin and Endeavour River catchments in northern Queensland. It documents the current status of non-native fishes in the region, their establishment success and current distributions, and discusses the rate and probable manner of spread, with particular reference to two tilapiine cichlids, the Mozambique mouthbrooder (*O. mossambicus*) and the spotted mangrove cichlid (*T. mariae*), and the osphronemid, the three-spot gourami (*Trichogaster trichopterus*).

METHODS

Between January 1997 and February 2007, 321 sites were surveyed between the Burdekin and Daintree catchments by the author, including 84 sites by others (see Acknowledgements). The location, GPS coordinates, habitat type, habitat condition and exotic species present were recorded at each site. A variety of survey methods was used including seine and gillnets, electroshocking, bait-traps, underwater snorkelling and visual observation from the water's edge using binoculars fitted with polarised lenses when water conditions allowed.

Establishment success was defined as successful and continued breeding of a species observed during the survey period. The relative occurrence of each species was defined as the number of sites where a species was observed as a percentage of the total number of sites where non-native species were present. An estimate of the distribution of each tilapiine species was calculated as the percentage occurrence in the total catchment area, including Cape York Peninsula, for all the major river systems in the North East Coast Drainage Division north of the Burdekin River (Table 1; catchment area data from Jacobson et al. 1983).

River System	Catchment Area (km^2)	Occurrence of Tilapia OM	TM
Jacky-Jacky	2770		
Olive-Pascoe	4350		
Lockhardt	2825		
Stewart	2795		
Normanby	24605		
Jeanie	3755		
Endeavour	2200	✓	
Daintree	2125		
Mossman	490		
Barron	2175	✓	✓
Mulgrave-Russell	2020		✓
Johnstone	2330		✓
Tully	1685		
Murray	1140		
Herbert	10125	✓	
Black-Alice	1025	✓	
Ross	1815	✓	
Haughton-Barrattas	3650		
Burdekin	129860	✓	
$\sum$ catchment area	201740		
$\sum$ % OM occurrence	73.0		
$\sum$ % TM occurrence	3.2		

Table 1. Catchment areas of major rivers in the North East Coast Drainage Division, north of the Burdekin River and reported occurrence of tilapia, *O. mossambicus* (OM) and *T. mariae* (TM); data from Jacobson et al. (1983).

RESULTS

Nineteen non-native fish species were recorded during surveys (Table 2). These included 12 cichlids, five poeciliids, one osphronemid and one cyprinid. The distributions of these species are shown in Figures 1 to 4. Poeciliids were the most frequently encountered group (60.4% of all sites surveyed) compared with cichlids (48.3%). The dominant poeciliids, as a percentage occurrence of all sites surveyed, were the Mosquitofish (41.7%) and the Guppy (19.3%), while the dominant cichlids were the Mozambique mouthbrooder (46.1%) and the spotted mangrove cichlid (7.2%). Eleven species were reported from five or fewer sites. Of the 19 species, at least 11 (58%) have established breeding populations (Table 2). The Ross River catchment had the largest number of non-native species (15) reported from all sites surveyed.

The total number of reported non-native fish species introduced into northern Queensland fresh waters (20) represents about 69% of all reported introductions in Queensland (29) and 50% of all reported introductions in Australian fresh waters (40). The number of established species (11) represents about 48% of all species known to have breeding populations in open fresh waters in Australia (23) (Kailola et al. 1999, Webb 2003, this paper, Koehn and MacKenzie 2004, T. Rayner, School of Tropical Biology, James Cook University, Townsville, pers. comm.). Between 1930 and 1980 the rate of introduction of non-native fishes into northern Queensland fresh waters was approximately linear, but during the past 25 years has entered an almost exponential phase (Figure 5). This pattern is comparable with other tropical regions (e.g., Hawaii and Florida) with similar introduction histories and well-established domestic aquarium fish industries (Figures 6 and 7). The majority of countries in tropical regions (e.g., Sri Lanka, Indonesia, and Taiwan), also have experienced increased post-1945 rates of fish introduction, but with imports principally for fisheries production rather than for a domestic aquarium trade, which is either lacking or in an early phase of development (Figures 8, 9 and 10. Data for Figures 6 to 10 obtained from De Silva 1989, de Zylva 1999, Radtke 1995, Froese and Pauly 2007).
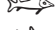
Family	Genus/Species	Common Name	Estab	% sites
Poeciliidae	*Gambusia holbrooki*	Mosquitofish	🐟	50.4
	Poecilia reticulata	Guppy	🐟	27.8
	P. latipinna	Molly		0.4
	Xiphophorus maculatus	Platy	🐟	10.0
	X. helleri	Swordtail	🐟	1.7
Cichlidae	*Oreochromis mossambicus*	Mozambique tilapia	🐟	40.7
	Tilapia mariae	Spotted mangrove cichlid	🐟	10.4
	Thorichthys meeki	Firemouth		0.4
	Hemichromis sp. (cf. *guttatus*)	Jewel cichlid	🐟	0.8
	Haplochromis burtoni	Burton's haplochromis	🐟	0.8
	Astronotus ocellatus	Oscar	🐟	2.6
	Aequidens rivulatus	Green terror		0.4
	Heros severus	Green severum		0.4
	Archocentrus nigrofasciatum	Convict cichlid		1.3
	Amphilophus citrinellum	Midas cichlid	🐟	3.0
	Geophagus brasiliensis	Pearl cichlid		0.4
	Archocentrus spilurus	Blue-eye cichlid		0.4
Belontiidae	*Trichogaster trichopterus*	Three-spot gourami	🐟	7.0
Cyprinidae	Cyprinid sp. A	Unknown 'carp' species		0.4
Cyprinodontidae	*Jordanella* sp. (*floridae*)	Flagfish		-

Table 2. Non-native fish species reported from northern Queensland fresh waters (🐟 = established breeding population).

Tilapiine Cichlids (O. mossambicus and T. mariae)

Between 1978 and 2000, the range of *O. mossambicus* and *T. mariae* has increased from approximately one per cent (Ross River catchment) to about 75% of the total catchment area in the North-East Drainage Division. Of the two species, *O. mossambicus* is more widespread. It has been reported from six of the major river systems (about 73% of total catchment area; Table 1) and with a latitudinal range of 3.9°, extending between the Endeavour and Burdekin Rivers. The main populations occur in the Barron River, including Lake Tinaroo, in some small creeks to the north and south of Cairns and in almost every waterway in the Townsville-Thuringowa region.

The rate of new site reports for the species in northern Queensland has also accelerated since its initial introduction to the Ross River in the late 70s (Arthington et al. 1984), and especially since 2000 (Figure 11). Based on morphology and colour pattern, most of the recent range expansion of *O. mossambicus* is possibly of the hybrid form. Fish collected from the upper Barron River, Herbert River and Burdekin River catchments tend to have more orange-red body colour, a shallow body depth, and long posterior anal and dorsal fin extensions, while Townsville fish tend to have a dull grey-green body colour, a deeper body and shorter posterior anal and dorsal fin extensions.

O. mossambicus has established large populations in the Ross River, Townsville, and neighbouring Black and Alice River catchments, Thuringowa, and virtually all smaller creeks between Sleeper Log Creek to the north and Alligator Creek to the south of Townsville. The species was observed by the author in farm dams in 2001 in the upper catchment of Sachs Creek and then in Ross River Dam in 2004 following downstream dispersal. Other local reports of the species from farm dams at Cungulla and Harvey's Range in 2001 and 2004, respectively, were also confirmed by the author.

In 2003, a single specimen of *O. mossambicus* was collected from Jensen's Crossing, Endeavour River, near Cooktown, and is the first confirmed report of the species north of the Daintree River (J. Russell, Northern Fisheries Centre, Cairns, pers. comm.). In 2004, the species was found in weirs in the upper reaches of the Herbert River (A. Hogan, QDPI&F, Walkamin, Atherton Tablelands, pers. comm.). Between February 2004 and March 2005, the species was confirmed from the Burdekin River catchment in Keelbottom Creek (D. Burrows, ACTFR, pers. comm.) and its feeder streams (Speed Creek and Two Mile Creek), and from Gladstone and Milchester Creeks, Charters Towers, that flow into the Burdekin River approximately 50 km downstream from its junction with Keelbottom Creek.

Further surveys between March 2005 and November 2006 found *O. mossambicus* in the main channel of the Burdekin, in the Star River, Fanning River, Kirk River, Basalt River, Allingham Creek and Fletcher Creek (ACTFR and QDPI&F, unpublished data). The species has spread through more than 300 km of waterways in the middle reaches of the Burdekin River catchment over a period of at least three years, although the exact timing of the first introduction is not known. These reports suggest that the species is rapidly dispersing throughout the Burdekin catchment from one or possibly a few points of introduction. Observations were made during a period of low but consistent flow in the Burdekin River, with above average dry season rainfall in the Running River, Star River and Keelbottom Creek catchments in 2006, but below average wet season rainfall in 2004/5 and 2005/6. As a result of the low flows, upstream migration has probably been restricted by natural barriers such as rock bars on the Burdekin River adjacent to Mt Foxton and in the Basalt River, Fletcher Creek and Lolworth Creek (see Figure 1). It is likely that *O. mossambicus* will continue to disperse further downstream and upstream beyond such barriers when these are drowned out during wet seasons with higher rainfall. It is also probable that the species will spread to neighbouring catchments, either by 'creek-hopping' via coastal waters or during localised flooding.

In April 2005, two adult male specimens were collected from the irrigation channel leading from Lake Tinaroo into the Mitchell River

irrigation system, fortunately upstream from a screening station installed to prevent downstream passage of eggs or fry of tilapia. According to A. Hogan (QDPI&F, Walkamin, Atherton Tablelands, pers. comm.), the location of the fish suggested that they were deliberately released rather than the result of accidental translocation (e.g., by fish-eating birds) or natural dispersal from Lake Tinaroo.

Tilapia mariae has a more restricted latitudinal range (0.7°) than *O. mossambicus* and occurs in three of the major river systems (about three per cent of total catchment area) (Table 1). The species occurs in the Barron River catchment, including Lake Tinaroo, and small creeks in the Cairns region (Lear 1987, Mather and Arthington 1991, Webb et al. 1997), and with large populations also in the Russell-Mulgrave Rivers system and Johnstone Rivers system (Russell and Hales 1993, Russell et al. 1996). Figure 12 shows a relatively rapid, approximately linear rate of new sites reported for *T. mariae* over a period of 20 years, but with no new site locations confirmed in the last four years. In February 2005 there were unconfirmed reports of tilapia in marine conditions – observed by divers about 1 km north of the mouth of the Russell River (possibly *T. mariae*) and caught by fishers off Fitzroy and Double Island (possibly *O. mossambicus*) (B. Rossi, Marine Advisory Group, Cairns, pers. comm.).

Other Cichlids

Of the ten, non-tilapiine cichlids, six species (*T. meeki*, *A. rivulatus*, *H. burtoni*, *A. nigrofasciatum*, *A. ocellatus* and *A. citrinellum*) were reported only from the Townsville region, the majority from the Ross River weirs. A jewel cichlid, *Hemichromis* sp. (cf., *guttatus*), was found at two locations (Cairns and Ross River Townsville), while two species (*G. brasiliensis* and *A. spilurus*) were found at only one location (Didgeridoo Lagoon, Lower Burdekin region). Of these ten species, at least four (*Hemichromis* sp. (cf., *guttatus*), *A. citrinellum*, *A. ocellatus*,

H. burtoni) have established breeding populations, while the other species were reported in very low numbers.

Unidentified Cyprinid sp. A

In March 2003, an approximately 4 kg specimen of a cyprinid was found among a large number of dead fish in Gleeson's Weir, Ross River (M. Cappo, Australian Institute of Marine Science, Townsville, pers. comm.). These fish were presumably killed by anoxic conditions created by a combination of bacterial decomposition of aquatic vegetation, high water temperatures and lack of flushing of the weirs. The fish was identified as a cyprinid, possibly a wild variant of the European carp, *Cyprinus carpio*, or a member of the African-Asian carp genus, *Labeo*. Full identification, however, was not possible as the fish was in an advanced state of decomposition when found. Further surveys by QDPI&F personnel using a boat-mounted electroshocker failed to detect any further specimens.

Three-spot Gourami

The species was first reported in 1998 from a sugar cane channel and several lagoons associated with Sheep Station Creek (C. Perna, Australian Centre for Tropical Freshwater Research, Townsville, pers. comm.) and has now established breeding populations in the lower Burdekin region. A new introduction was reported by Webb (2003) from Aplin Weir, Ross River, and in 2005 the species was collected from Didgeridoo Lagoon that flows into East Barrattas Creek (M. Pearce, Department of Primary Industry & Fisheries, Mackay, pers. comm.) and from Upper Barratta Creek (Woodhouse Lagoon) a neighbouring catchment to Sheep Station Creek (C. Perna, pers. comm.). In February 2007, the species was reported from Horseshoe Creek to the north of the Barrattas system and in close proximity to the Haughton River and its catchment (V. Veitch, Australian Centre for Tropical Freshwater Reseasrch, pers. comm.).

Poeciliids

The mosquitofish, *G. holbrooki* and the guppy, *P. reticulata*, were the most widespread and abundant poecillids observed. Apart from populations in a stormwater drain and in Avondale Creek, Smithfield, in northern Cairns, *G. holbrooki*, was the dominant poeciliid south from Ingham, while *P. reticulata* was dominant north of Ingham, although several populations of the latter species were present to the south, in the Townsville-Thuringowa region (Little Crystal Creek, Alice-Black River, Campus Creek and Alligator Creek), with new site records for Charters Towers and Didgeridoo Lagoon, in the Lower Burdekin region.

G. holbrooki was reported for the first time in May 2004 from the upper reaches of the Burdekin River at Reedybrook, approximately 250 km upstream, and Blue Range, approximately 105 km upstream from the junction of the river with Keelbottom Creek (B. Pusey, Griffith University, Brisbane, pers. comm.). The species was observed after heavy rains in mid-December in the lower reach of Keelbottom Creek and approximately 8 km downstream in the Burdekin River at Deep Bend. In March 2005, the species was found in the lower reach, but not in the middle or upper reaches, of Sheep Station Creek, at its junction with the Burdekin River, approximately 25 km downstream from Deep Bend. The species was also reported by the author for the first time from the upper catchment of the Herbert River, in the Wild River and The Millstream, Atherton Tablelands, in December 2005, although the origins and residency time of this population are unknown.

X. maculatus was found mainly in Cairns and in several creeks southward to Innisfail and in small creeks and stormwater drains in the Townsville region. Small populations of *X. helleri* were found at two sites in Cairns (Delaney's Creek and Saw Pit Gully), at one site in Townsville (Cranbrook Creek) and a large population in ponds at a crocodile farm at Flying Fish Point, Innisfail, and in adjoining cane drains. Of the five poeciliid species reported, only the sailfin molly has not established a breeding population. The species was found at only one site in Majors Creek, approximately 50 km to the south-east of Townsville.

DISCUSSION

The number of non-native fish species reported from open waters in northern Queensland has increased by 75 percent during the past decade with many of these fish establishing breeding populations. Northern Queensland now has approximately half of all reported non-native species introductions and half the number of all established exotic species recorded from Australian fresh waters. To date, all exotic species in northern Queensland have been reported from fresh waters in the North-East Drainage Division and none from the Gulf of Carpentaria Drainage Division. The Ross River, Townsville, now has the highest percentage of reported species introductions (15) and number of established species (11) in Australia. In comparison, the Burdekin River system has three non-native species, the Brisbane River in south-eastern Queensland has six non-native species (McKay and Johnson 1990, J. Johnson, Ichthyology Section, Qld Museum, Brisbane, pers. comm.), while Australia's largest river system, the Murray-Darling, many times larger than the Ross River, has 10 non-native species present (Clunie et al. 2002, Murray Darling Basin Commission 2004).

Genetic evidence indicated at least three separate introductions of tilapias in northern Queensland (Mather and Arthington 1991), while human translocation has clearly been responsible for the subsequent large-scale spread of these fishes in the region. In many instances tilapia have been released into standing water bodies such as ornamental ponds or farm dams and weirs with fish escaping into open waterways in floodwaters, e.g., tilapia in the upper Barron River, Atherton Tablelands (Webb et al. 1997), in Ross Creek (Arthington et al. 1984), Ross River (McKay 1984, Blühdorn et al. 1990) and Sachs Creek and Ross Dam, Townsville (Webb, this paper). The majority of new reports of non-native species introductions are probably a result of dumping unwanted aquarium fishes (e.g., several cichlids in the

Ross River weirs) or are due to other human activity, including use of the fish as live bait and stocking for aquaculture.

Tilapia collected in the Cairns region were used as live bait by anglers in Cape York rivers (M. Tilse, Cairns, pers. comm.). The *O. mossambicus* specimen collected from the Endeavour River in 2004 may have been used, or intended for use as live bait, but either escaped or was discarded. (J. Russell, Northern Fisheries Centre, Cairns, pers. comm.). The report of tilapia (*O. mossambicus*) from Gladstone Creek, Charters Towers, in March 2005 was also due to a local angler collecting fish for live bait. Fortunately, a colleague recognised tilapia among the catch and these fish were then destroyed and thus prevented from possible further spread.

While some stocking may occur inadvertently, it is possible that these releases, along with those directly into open waters, are deliberate. Such stocking may be for production of fish (e.g., tilapias) for domestic consumption, or harvesting ornamental species for sale. In the case of tilapia, some individuals may have opportunistically exploited the concern about the spread and impacts of the species, and even assisted the process by deliberately releasing fish, the objective being to apply political pressure so that removal of the prohibited status of the species is viewed as an environmentally and economically beneficial management option, i.e., to allow harvesting from open waters to get rid of a pest species and to establish an aquaculture industry based on tilapia providing rural employment opportunities.

The recent unconfirmed reports of tilapia observed about 1 km north of the mouth of the Russell River and caught by fishers off Fitzroy and Double Island are not unexpected as both tilapiine species are euryhaline and *O. mossambicus*, in particular, can survive in marine and even hypersaline conditions (Whitfield and Blaber 1979, Stickney 1986). It is possible, therefore, that both species may eventually spread throughout all of the northern section of the North East Drainage Division by creek-hopping along the coast, especially after heavy rains lower salinities in coastal waters.

It is probable that *O. mossambicus* dispersed throughout the small creeks to the north of Townsville by this process (see Arthington et al. 1984, 1994, Webb 2003).

Of particular concern is that the recent, major range expansion of *O. mossambicus*, is possibly that of the Cairns hybrid now present in the upper Barron and Herbert Rivers and the Burdekin River system. The genetic identity of these populations needs to be confirmed, although the general morphology and colour of these fishes are quite different from those of the 'pure' strain of *O. mossambicus* from the Townsville region. The study by Mather and Arthington (1991) indicated that genes from one or more of *O. aureus*, *O. niloticus* and *O. honorum* were present in the Cairns hybrid. *O. aureus* has been used to improve cold tolerance (Cnaani et al. 2000), *O. niloticus* to increase growth characteristics (Kamal and Mair 2005) and *O. honorum* to alter sex ratios (Lovshin 1982) of *O. mossambicus*. Mather and Arthington (1991) argued that this species, due to hybrid vigour, may pose an even greater threat than the pure mossambicus strain, and suggested that there was potential for spread of tilapia to parallel that of hybrid carp in southern states in the 1970s. To date, there has been no examination of the ecological attributes of the *O. mossambicus* hybrid and assessment of its invasive potential or impacts.

The three-spot gourami is another popular aquarium species and has established breeding populations at two locations in the lower Burdekin and Townsville regions. The recent report from Didgeridoo lagoon may be another aquarium release as guppies and a small number of two cichlid species (*G. brasiliensis* and *H. spilurus*) were found at this site. Rapid natural dispersal of the species in floodwaters is occurring throughout the system of lagoons and low-lying coastal areas especially to the north of the Burdekin River, and is likely to continue dispersal into the Haughton River system and its catchment. Gouramis are anabantids with special respiratory structures associated with the gills that allow air breathing (Burggren 1979). This species is therefore well-adapted to survive in many of northern Queensland

waterways that have been highly modified by human activity, for example, where eutrophic conditions result in excessive aquatic plant growth, and subsequent high biological oxygen demand creating virtually stagnant water, conditions that are unfavourable for many native fish species. The three-spot gourami is likely to disperse during floods throughout the network of drains and irrigation channels and lagoons in the lower Burdekin region. The species is carnivorous, feeding mainly on small invertebrates (Rainboth 1996), and is territorial and aggressive. According to Liao and Chiu (1989), the species was strongly suspected, as a resource competitor, to have adversely impacted on populations of the endangered Chinese barb, *Puntius semifasciolata*, although its impacts on resident aquatic communities, in Queensland or overseas, are unknown.

The poeciliids as a group are the longest established non-native fishes in northern Queensland, with introductions beginning about sixty years ago (McKay 1978, 1984). The mosquitofish, *G. holbrooki* and the guppy, *P. reticulata*, were the most frequently encountered and widespread non-native species surveyed, while the platy, *X. maculatus*, was largely restricted to the Cairns and Townsville regions, but with locally common to abundant populations. *G. holbrooki*, was the dominant poeciliid south of Ingham to the Burdekin, while *P. reticulata* was dominant in creeks and rivers to the north of Ingham, including the Atherton Tablelands, where, apart from recent reports from the Upper Burdekin, *G. holbrooki* are absent.

The distribution of the poeciliids, particularly of *P. reticulata* and *X. maculatus* suggests that these species were also used with *G. holbrooki* for control of mosquito larvae during World War II and in the immediate postwar period. McKay (1984) stated that only *G. holbrooki* was introduced by military personnel in the 1940s, although the largest concentration of Allied troops in northern Queensland was located on the Atherton Tablelands where *G. holbrooki* is virtually absent, but *P. reticulata* is widespread. This suggests that both species may have been used during this period

as biocontrol agents. Other poeciliids, *X. maculatus* and *X. helleri*, may also have been introduced at this time, or in the immediate post-war period, by local councils that continued introductions, while some populations may have originated during this time from aquarium releases. Swordtails, along with guppies were found in the ponds of a crocodile farm near Innisfail, and escapees from these ponds were found in cane drains adjacent to the farm. The farm manager stated that these fish had been stocked in the ponds to 'eat the mosquito larvae'.

The recently reported populations of *P. reticulata* from Charters Towers may also be long-established and have simply gone unreported because of a lack of surveys in the area. The population of *G. holbrooki* observed in the mouth of Sheep Station Creek near Charters Towers is more recent and probably derived from fish moving downstream from the upper Burdekin, although the timing of original introductions into this catchment is unknown. The few specimens of the sailfin molly, *Poecilia latipinna*, found at one location in Majors Creek, were undoubtedly an aquarium dumping. No further specimens or other exotic species were detected during subsequent surveys at this site.

Since the vast majority of fish species used in the aquarium trade are tropical species, northern Queensland is at a greater risk from these fish, which, if released into open tropical waters, are likely to develop self-maintaining populations. This is evidenced by the relatively high proportion (55%) of species that, once introduced, have established breeding populations. While the focus tends to be upon those species that become 'invasive' – that rapidly spread and become a dominant component of fish communities in receiving waters – the cumulative impact of all non-native species on aquatic biodiversity and ecosystem function within a catchment needs to be considered. The rate of introductions into tropical northern Queensland fresh waters is alarming and could result, if the trend continues in the coming decades, in many freshwater fish communities being dominated by these and probably other exotic species.
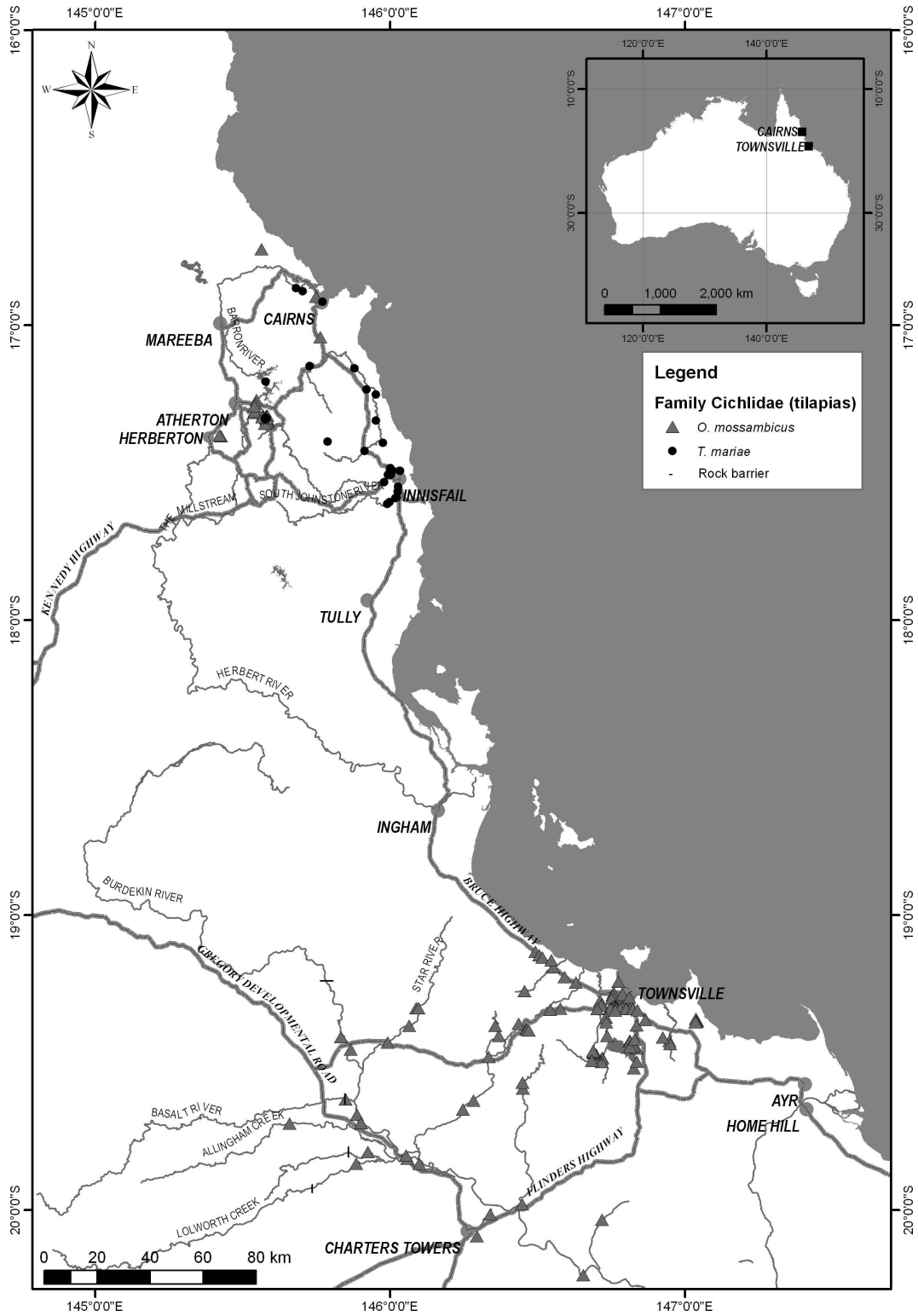
Figure 1. Distribution map for tilapiine cichlids, *O. mossambicus* and *T. mariae* (Family Cichlidae), in fresh waters of tropical northern Queensland
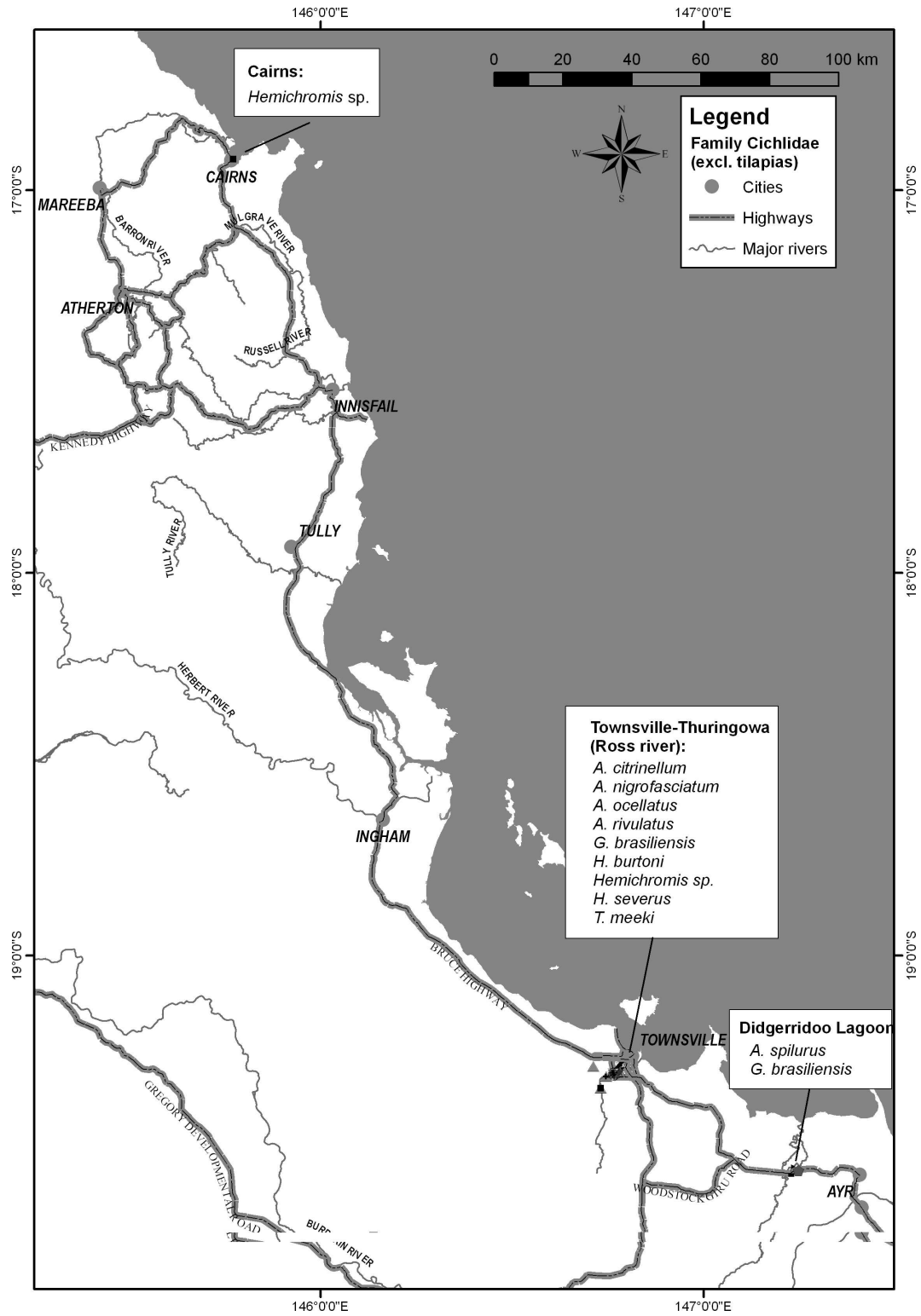
Figure 2. Distribution map for cichlids (excluding tilapias) (Family Cichlidae) in fresh waters of tropical northern Queensland.
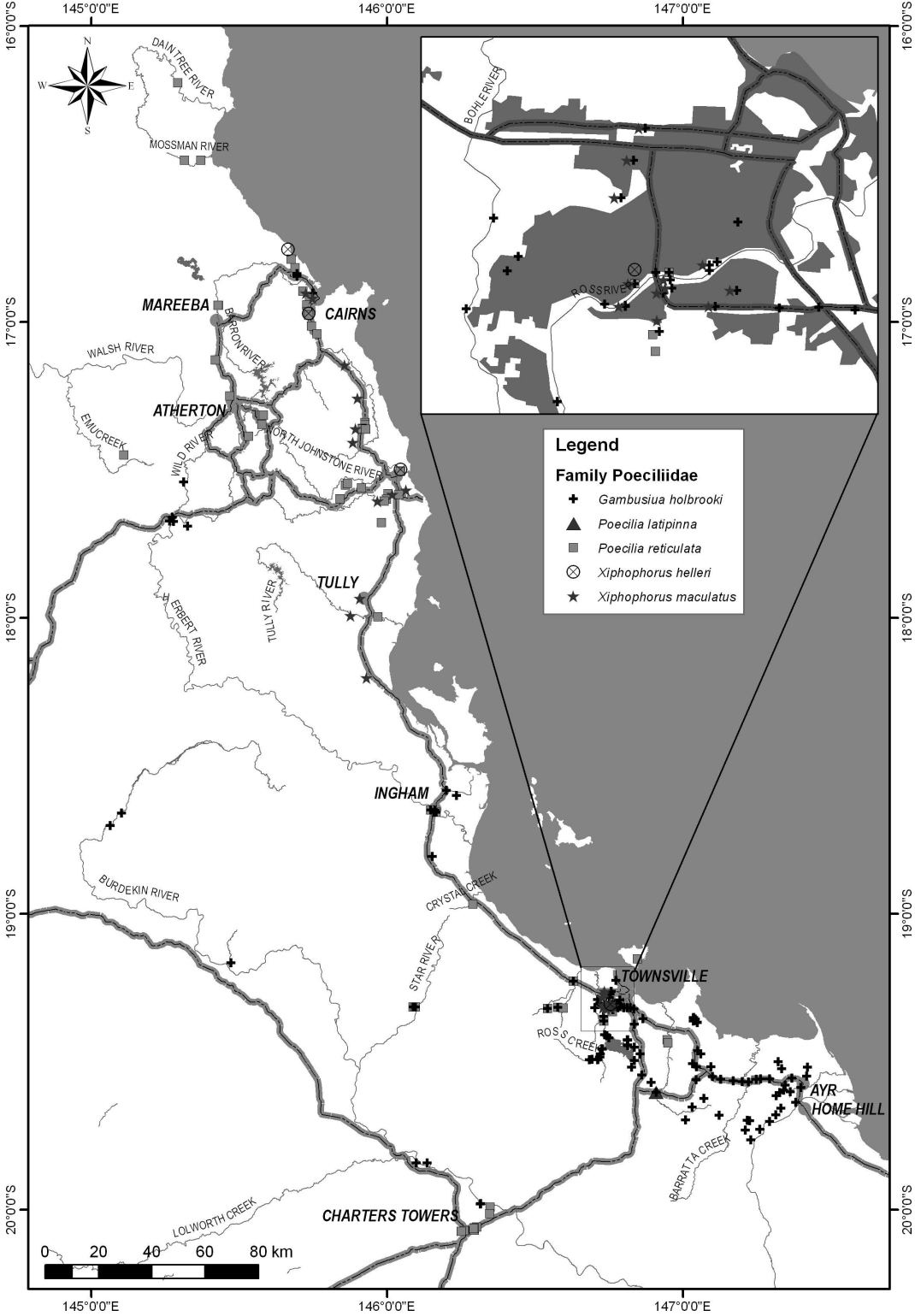
Figure 3. Distribution map for live-bearers (Family Poeciliidae) in fresh waters of tropical northern Queensland.
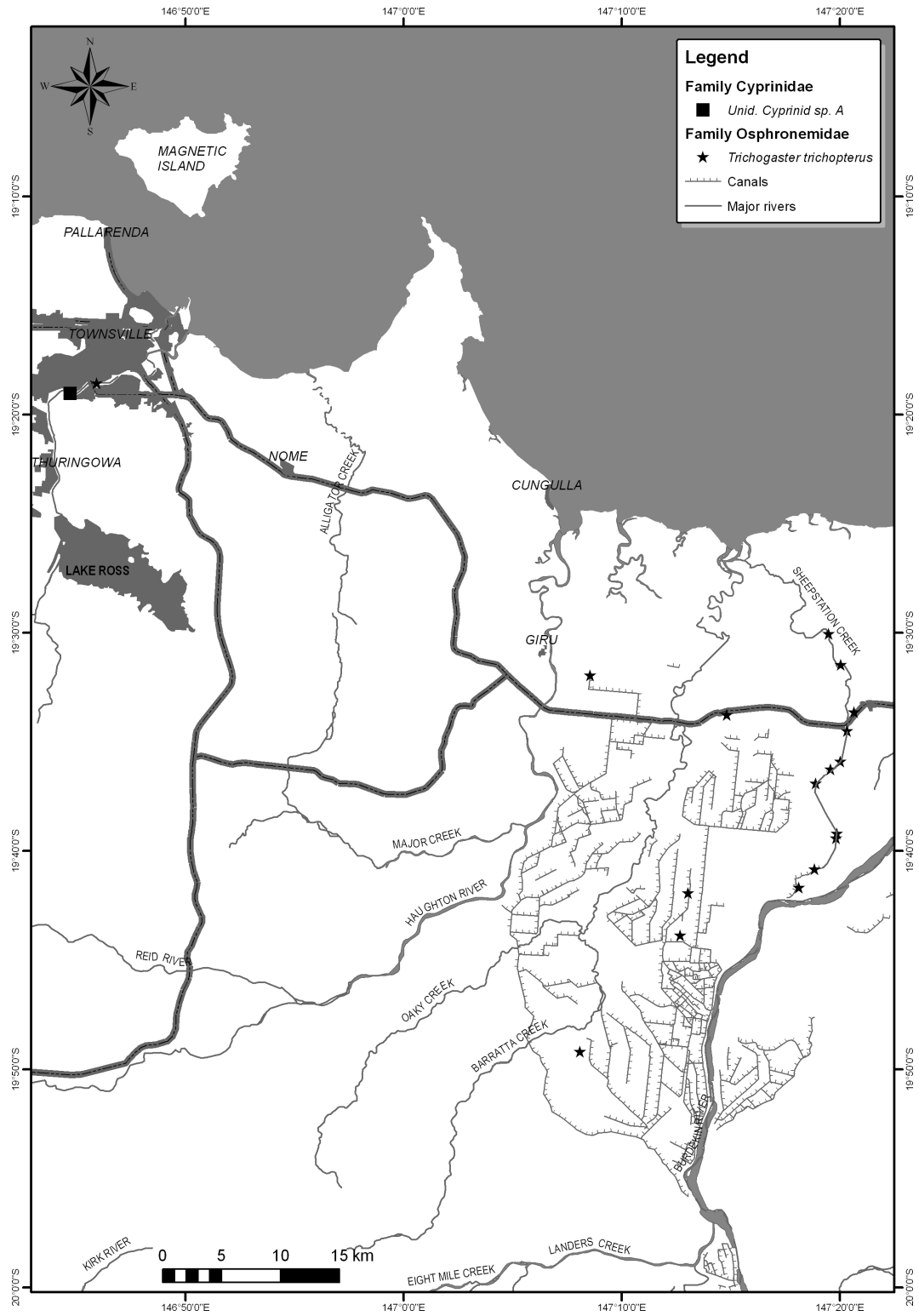
Figure 4. Distribution map for unidentified cyprinid sp. A (Family Cyprinidae) and three-spot gourami, *T. trichopterus* (Family Osphronemidae), in fresh waters in tropical northern Queensland.
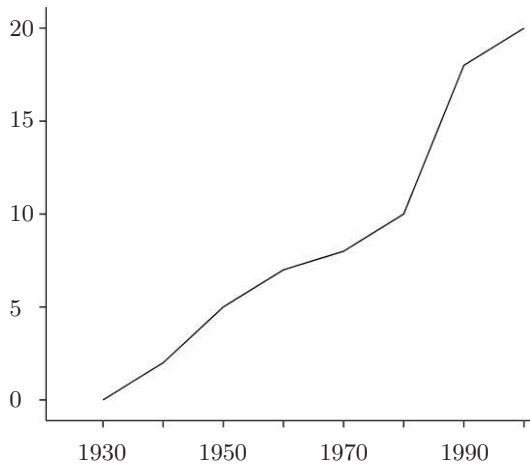
Figure 5. Cumulative number of non-native freshwater fish species introduced per decade into northern Queensland.
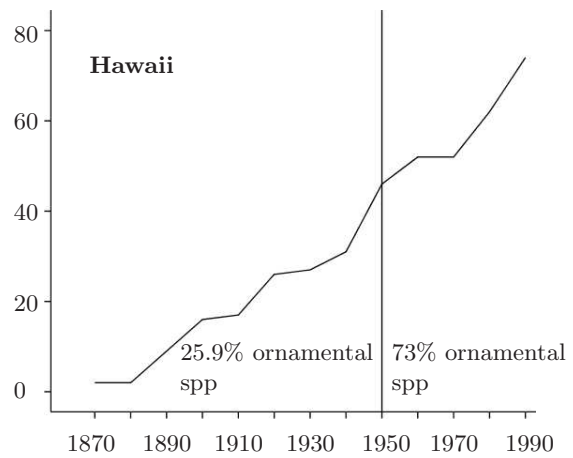
Figure 6. Cumulative number of introduced fish species per decade for Hawaii.
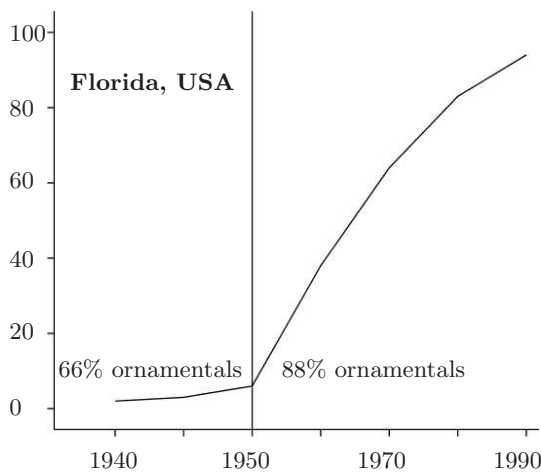
Figure 7. Cumulative number of introduced fish species per decade for Florida, USA.
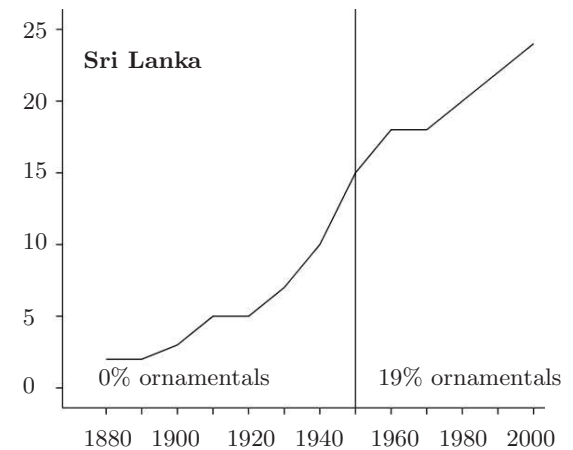
Figure 8. Cumulative number of introduced fish species per decade for Sri Lanka.
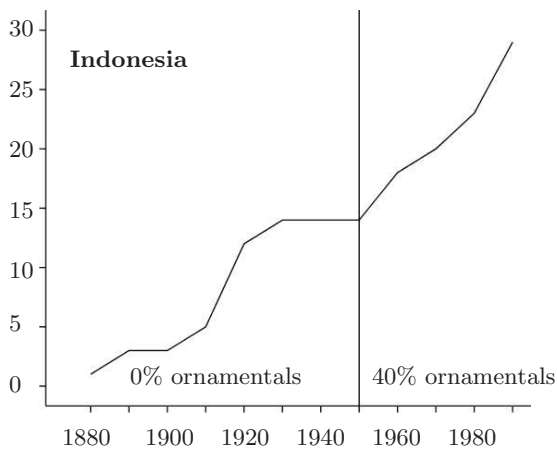
ACKNOWLEDGEMENTS

Figure 9. Cumulative number of introduced fish species per decade for Indonesia.
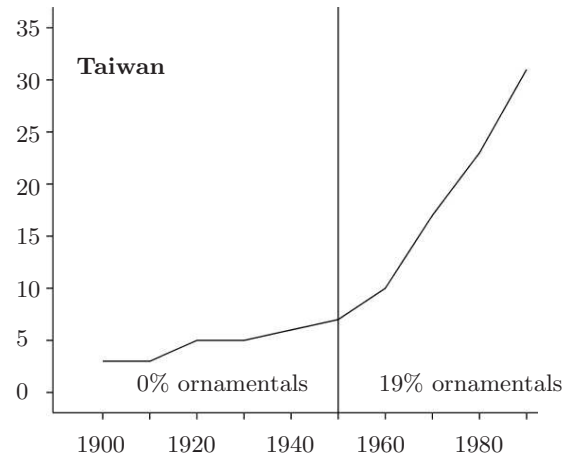

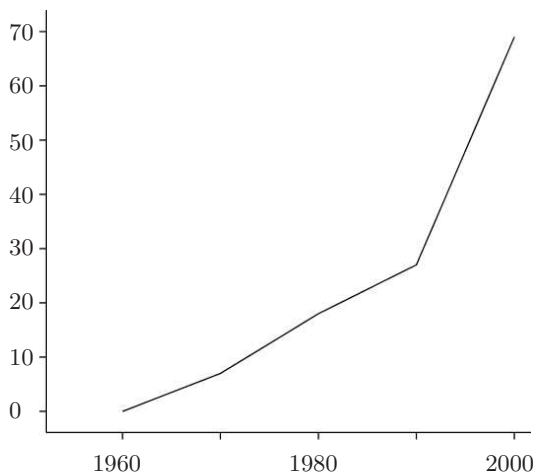Figure 10. Cumulative number of introduced fish species per decade for Taiwan.

Figure 11. Cumulative number of new site reports per decade for the Mozambique tilapia, *O. mossambicus*, in northern Queensland fresh waters.
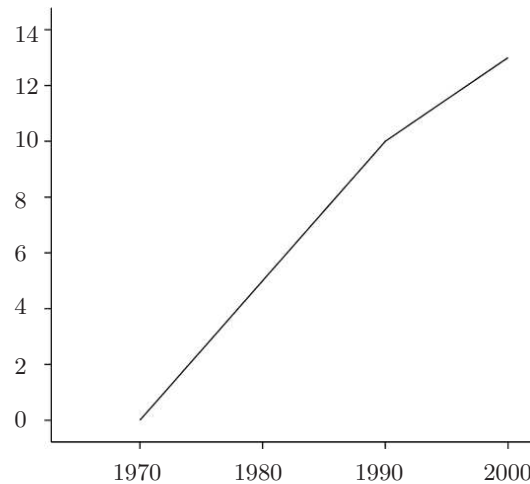

Figure 12. Cumulative number of new site reports per decade for the spotted tilapia, *T. mariae*, in northern Queensland fresh waters.

REFERENCES

Arthington, A.H., McKay, R.J., Russell, D.J. and Milton, D.A., 1984. Occurrence of the introduced cichlid *Oreochromis mossambicus* (Peters) in Queensland. *Australian Journal of Marine and Freshwater Research* **35**, 267–272.

Arthington, A.H. and Blühdorn, D.R., 1994. Distribution, genetics, ecology and status of the introduced cichlid, *Oreochromis mossambicus*, in Australia. *Mitteilungen Internationale Vereinigung für Theoretische und Angewandte Limnologie* **24**, 53–62.

Blühdorn, D.R., Arthington, A.H. and Mather, P.B., 1990. The introduced cichlid, *Oreochromis mossambicus*, in Australia: a review of distribution, population genetics, ecology, management issues and research priorities. In: D.A. Pollard (ed.) Introduced and Translocated Fishes and their Ecological Effects. Proceedings No. 8, Australian Government Publishing Service, Canberra, pp. 83–92.

Burggren, W.W., 1979. Bimodal gas exchange during variation in environmental oxygen and carbon dioxide in the air breathing fish, *Trichogaster trichopterus*. *Journal of Experimental Biology* **82**, 197–213.

Canonico, G.C., Arthington, A.H., McCrary, J.K. and Thieme, M.L., 2005. The effects of introduced tilapias on native biodiversity. *Aquatic Conservation: Marine and Freshwater Ecosystems* **15**, 463–483.

Clunie, P., Stuart, I., Jones, M., Crowther, D., Schreiber, S., McKay, S., O'Connor, J., McLaren, D., Weiss, J., Gunneskera, J. and Roberts, J., 2002. A risk assessment of the impacts of pest species in the riverine environment in the Murray-Darling Basin. Report prepared for the Murray Darling Basin Commission, Strategic Investigations and Riverine Program, Project R2006. Department of Natural Resources and Environment, Victoria.

Cnaani, A., Gall, G.A.E. and Hulata, G., 2000. Cold tolerance of tilapia species and hybrids. *Aquaculture International* **8**, 289–298.

De Silva, S.S. (ed.), 1989. Exotic Aquatic Organisms in Asia. Proceedings of a Workshop on Introduction of Exotic Aquatic Organisms in Asia. Asian Fisheries Society, Manila, Philippines.

De Zylva, E.R.A., 1999. The introduction of exotic fish in Sri Lanka with special reference to Tilapia. *Naga* **22**, 4–8.

Froese, R. and Pauly, D. (eds), 2007. FishBase. World Wide Web electronic publication. `http://www.fishbase.org`, version 02/20070.

Jacobson, G., Habermehl, M.A. and Lau, J.E., 1983. Australia's Groundwater Resources. Water 2000: Consultant Report No. 2, Bureau of Mineral Resources, Geology and Geophysics, Australian Government Publishing Service, Canberra.

Kailola, P.J., Arthington, A.H., Woodland, D.J. and Zalucki, J.M., 1999. Non-native Finfish Species Recorded in Australian Waters. Report to the Australian Quarantine and Inspection Service, `http://www.aqis.gov.au/docs/qdu/Environmental-report.pdf`, cited 25 January 2007.

Kamal, A.H.M.M. and Mair, G.C., 2005. Salinity tolerance in superior genotypes of tilapia, *Oreochromis niloticus*, *Oreochromis mossambicus* and their hybrids. *Aquaculture* **247**, 189–201.

Koehn, J.D. and MacKenzie, R.F., 2004. Priority management actions for alien freshwater fish species in Australia. *New Zealand Journal of Marine and Freshwater Research* **38**, 457–472.

Lear, R.J., 1987. Survey of the Introduced Tilapia in the Cairns Region, North Queensland. Queensland National Parks and Wildlife Service, Cairns.

Liao, L.-C. and Chiu, H.-C., 1989. Exotic aquatic species in Taiwan. In: S.S. De Silva (ed.) Exotic Aquatic Organisms in Asia. Asian Fisheries Society, Darwin, Australia, pp. 101–118.

Lovshin, L.L., 1982. Tilapia hybridization. In: R.S.V. Pullin and R.H. Lowe-McConnell (eds), The Biology and Culture of Tilapias. ICLARM, Manila, pp. 279–308.

Mather, P.B.and Arthington, A.H., 1991. An assessment of genetic differentiation among

feral Australian Tilapia populations. *Australian. Journal of Marine and Freshwater Research* **42**, 721–728.

McKay, R.J., 1978. The Exotic Freshwater Fishes of Queensland. Australian National Parks and Wildlife Service, Canberra.

McKay, R.J., 1984. Introductions of exotic fishes in Australia. In W.R. Courtenay Jr and J.R. Stauffer (eds), Distribution, Biology, and Management of Exotic Fishes. The John Hopkins University Press, Baltimore, pp. 117–199.

McKay, R.J., 1989. Exotic and translocated freshwater fishes in Australia. In: S.S. De Silva (ed.), Workshop on Introduction of Exotic Aquatic Organisms in Asia. Asian Fisheries Society, Darwin, Australia, pp. 21–34.

McKay, R.J. and Johnson, J., 1990. The freshwater and estuarine fishes. In P. Davie, E. Stock and D. Low Choy (eds), The Brisbane River. A Source Book for the Future. Australian Littoral Society, Queensland Museum, Brisbane, pp. 153–166.

Murray Darling Basin Commission, 2004. Native Fish Strategy for the Murray-Darling Basin 2003-2013. MDBC Publication No. 25/04, Murray Darling Basin Commission, Canberra.

Milward, N.E. and Webb, A.C., 1990. The Status of the Introduced Tilapia Species *Oreochromis mossambicus* in the Townsville Region: Distribution, Feeding and Reproduction. Report for the Council of the City of Townsville from the Zoology Department, James Cook University of North Queensland, Townsville.

Radtke, R.I., 1995. Forensic biological pursuits of exotic fish origins: piranha in Hawaii. *Environmental Biology of Fishes* **43**, 393–399.

Rainboth, W.J., 1996. Fishes of the Cambodian Mekong. FAO Species Identification Field Guide for Fishery Purposes. FAO, Rome.

Stickney, R.R., 1986. Tilapia tolerance of saline waters: a review. *Progressive Fish Culturist* **48**, 161–167.

Webb, A.C., 1994. Ecological Aspects of the Mozambique Mouthbrooder, *Oreochromis mossambicus*, and Other Introduced Cichlids in Northern Queensland. MSc dissertation, Zoology Department, James Cook University of North Queensland, Townsville.

Webb, A.C., 2003. The Ecology of Invasions of Non-indigenous Freshwater Fishes in Northern Queensland. PhD dissertation, School of Tropical Biology, James Cook University, Townsville.

Webb, A.C., Hogan, A. and Graham, P., 1997. The Distribution of the Mozambique Mouthbrooder, *Oreochromis mossambicus*, and its Future Management in the Upper Barron River Catchment. QDPI Fisheries Research Centre, Walkamin.

Whitfield, A.K. and Blaber, S.J.M., 1979. The distribution of the freshwater cichlid *Sarotherodon mossambicus* in estuarine systems. *Environmental Biology of Fishes* **4**, 77–81.

Alan Charles Webb
Australian Centre for Tropical Freshwater Research
Kevin Stark Building
James Cook University
email: alan.webb@jcu.edu.au

Micropropagation of Elite Sugarcane Planting Materials from Callus Culture in Vitro

PATRICK S. MICHAEL

Abstract: Many plants including sugarcane (*Saccharum* spp.) has been successfully regenerated from callus culture *in vitro* worldwide and a varying range of explants were used. Presented in this paper is a procedure in which segments of the young innermost rolled leaves (2–3 cm) of four sugarcane cultivars (Q77N1232, Cadmus, Co997 and a local cutltivar (Lae1) cultured onto Murashige and Skoog (MS) medium supplemented with $3\,\mathrm{g\,L^{-1}}$ 2,4-D, $0.5\,\mathrm{g\,L^{-1}}$ PVP, $2\,\mathrm{ml\,L^{-1}}$ BAP, $100\,\mathrm{ml\,L^{-1}}$ coconut water, $30\,\mathrm{g\,L^{-1}}$ sucrose and $8\,\mathrm{g\,L^{-1}}$ agar (MSC3). Using this procedure, successful initiation of large amounts of contaminant-free, embryogenic callus ranging from 80–90 per cent was obtained which were potentially capable of efficient plantlet regeneration. Plantlets were regenerated by transferring the embryogenic callus onto regeneration media of same composition as MSC3 but without auxin (2,4-D). Adequate multi-shooting was achieved using no more than $2\,\mathrm{ml\,L^{-1}}$ BAP and prior to acclimatization, rooting was achieved by sub-culturing the plantlets onto medium lacking cytokinin (BAP). Ninety to ninety five percent of the plantlets were successfully acclimatized in the green house and field planted after 6 weeks. There was no indication of morphological deviation from the parents.

Keywords: Tissue culture, embryogenic callus, micropropagation, elite planting materials

INTRODUCTION

Man has utilized 3,000 species of plants for food, of which 150 have entered world commerce. However, only 16 crops feed the World's population, among them being sugarcane (*Saccharum* hybrids) (Chaudhary, 1994). This crop is vegetatively propagated and is grown in many different countries across the World. Sugarcane provides about 65–70% of sugar produced in the World (Adam et al. 1995) and 90% in Papua New Guinea (Wagih and Musa, 2000).

The importance of this crop is demonstrated by the bulk volume produced, amount of energy provided, income generated and the type and number of people involved in sugarcane production. In PNG, sugarcane is used for commercial production as well as co-staple food together with other root and tuber crops. A significant portion, however, is commercially-based production of sugarcane. In the future, consumption of sugarcane is expected to increase sharply as the population increases; hence there will be an increase in production and demand for elite and improved planting materials.

Despite the importance of sugarcane, seed multiplication and propagation through cut-

tings by conventional method is slow, present risks of pest and disease transmission, and takes some years before a new cultivar is released and cultivated fully on a commercial basis (Dookun et al. 1996). Additionally, the time spent is considered as an economic loss and requires huge investment in improving elite propagative planting materials from the few parent stocks available. Sugarcane micropropagation has been reported by many workers using callus culture (Barba et al. 1977), bud culture (Wagih et al. 1995) and culture segment of young leaves (Alam et al. 1995). Among the many *in vitro* propagation techniques for sugarcane, Hendre et al. (1983) reported that it was possible to produce some 260,000 shoots from single shoot tips in four months and Comstock (1988) reported that about 20,000 plantlets could be multiplied weekly using shoot apex.

The latest advances in plant tissue culture and biotechnology, and the ability to regenerate improved planting materials from any portion of a plant using plant tissue culture techniques, means that there is now the potential to make propagation improvements much more quickly than by conventional methods. Such rapid sugarcane improvement could be very impor-

tant in PNG today where the population is growing at a fast rate. For this to be successful, sugarcane plants must be manipulated at the tissue level, and thus an understanding of the aims and techniques of sugarcane tissue culture is therefore essential. This paper describes an efficient and rapid method of micro-propagating elite sugarcane planting materials using callus culture *in vitro*.

MATERIALS AND METHODS

Field Practices and Sources of Material

Plant material

Three varieties of sugarcane (*Saccharum* spp. hybrids), Q77N1232, Cadmus, Co997 and a local cutltivar (Lae1) of unknown origin but widely cultivated by locals in Lae were grown at the Experimental Farm of the University of Technology, Lae, PNG, located at an altitude of 54 m above sea level at $147°\,00'$ E and $6°\,45'$ S. Canes were planted at a spacing of 1.5×0.5 m. Young shoots 10 ± 2 months old were used as the source of explant. Tops stalks of these varieties were cut at the third node from the top visible dewlap, collected in paper bags and taken to the laboratory for immediate use.

Callus culture

Embryogenic callus (EC) was established as described by Wagih et al. (1998). The spindle cylinder of the innermost young rolled leaves just above the meristem tips (approximately 3 cm long) were surface-sterilized by dipping ino ethanol and flaming, then dipping in 1.5% sodium hypochlorite (NaOCl) for 15 minutes and washing three times with distilled water. A sterile scalpel blade removed the outer rolled leaves and the edge of the cylinder. The remainder of the cylinder (about 2 cm long) was cut transversally into four equal segments and cultured onto callus induction medium (MSC3). This medium consisted of MS (Murashige and Skoog, 1962), supplemented with $3\,\mathrm{mg\,L^{-1}}$ 2,4-D, $0.5\,\mathrm{g\,L^{-1}}$ polyvinylpyrroli- done (PVP), $0.5\,\mathrm{ml\,L^{-1}}$ BAP, $100\,\mathrm{ml\,L^{-1}}$ co- conut water, $30\,\mathrm{g\,L^{-1}}$ sucrose; $8\,\mathrm{g\,L^{-1}}$ agar (Sigma Products) was used as the gelling agent. The pH was adjusted to 5.8 and a manual dispenser was used to dispense 20 ml into 7 cm plastic vials, then autoclaved at 15 psi ($121°$C) for 15 minutes.

Cultured vials were incubated in the dark at $26\pm2°$C and routinely sub-cultured 2 times in the first week of culture (Bhojwani and Razdan, 1983) onto fresh medium to avoid toxicity of leached phenolics. It was then sub-cultured at 3 week intervals for further callus induction. Selected ECs were sub-cultured twice a month until abundant calli were obtained. ECs for plantlet regeneration were transferred onto the same media lacking 2,4-dichlorophenoxyacetic acid (2,4-D) (MSC) and incubated under photo- periods of 16 hours and $30\,\mathrm{mol}\,\mu\mathrm{E\,m^{-2}s^{-1}}$ of illumination at $28\pm2°$C. Fifty percent of the shoots about 3–5 cm long with small roots were singled out and placed in 1.5 cm diame- ter test tubes with sterile distilled water un- der natural daylight (Wagih, 1999) and 50% were sub-cultured onto media lacking cytokinin (BAP) (Anderson, 1975) until abundant roots developed. Plantlets were then transferred to the green house for acclimatization (hardening) prior to field planting.

Acclimatization of Tissue Cultured Plants in the Greenhouse

Hardening of tissue cultured plants

Rooted plantlets were washed under running tap-water and transferred into a substrate mix- ture of sterile soil, 1 part farmyard manure, 1 part sand and 1 part top soil (ratio 1:1:1) in ger- minating trays. As the humidity is constantly high in Lae, no cover was provided to minimize transpiration. Careful watering twice a day was performed, ensuring that the soil was damp, but not wet and water logged up to 2 weeks and allowed to grow for 3–4 weeks until they reached a favourable height. At this age, the plants were watered once a day.

Four week old plants were then taken outside the greenhouse under shade, had their older roots and leaves trimmed once and transplanted into new soil of the composition; performance was monitored based on plant growth charac-

teristics under greenhouse conditions. There was no artificial light, both at night and in the day. This condition was considered an analogue of the field situation where the plants receive sunlight only during the day and less or nothing at night. Watering was done twice (8 am and 4 pm) a day, and adequate watering was carried every Friday afternoon to cater for requirements during weekends.

Growth Performances of the in vitro Regenerated Plants in the Greenhouse

Monitoring of plant growth

The growth performances of 100 plants in greenhouse conditions were monitored by assessing the development of leaves and roots, increase in height, tillering ability and phenotypic variations. Total number of leaves and roots per hill were and measured. The leaf lengths were measured from the base of leaf zero (first rolled leaf) to the tip of the longest leaf. The tillering ability was assessed manually by counting the tillers per hill. These plants were then uprooted, gently rocked to remove access soils and the roots washed under tap water. The roots per hill were counted and the longest roots measured. Broken roots were not considered for measurement and average data are presented in Table 2. The data collected were analyzed using the analytical software package *Statistix*.

RESULTS AND DISCUSSION

For the four varieties, callus induction, plantlet regeneration, shoot and root development including contamination and plant growth performance and characteristics recorded show large variability. The influence of the two media types (MSC3 and MSC) on callus initiation and regeneration including phenotypic variations based on plant characteristics observed are discussed below.

Cultivar	TCT TW	Iw (g)	Fw (g)	CG (g)	Ga	SD	Va	C.V.
Q77N1232	10 1–3	453.92	460.31	6.39	14.58	8.95	80.16	61.39
	10 3–6	460.31	473.53	13.22				
	10 6–9	473.53	497.67	24.14				
	10 9–12	497.67	492.50					
Cadmus	10 1–3	459.17	466.41	7.24	15.69	9.32	86.90	59.42
	10 3–6	466.41	480.55	14.14				
	10 6–9	480.55	506.24	25.69				
	10 9–12	506.24	506.21					
Co997	10 1–3	461.79	469.37	7.59	16.52	10.05	101.09	60.86
	10 3–6	469.37	483.96	14.56				
	10 6–9	483.96	511.37	27.41				
	10 9–12	511.37	511.34					
Lae1	10 1–3	456.55	462.84	6.29	14.39	8.88	78.91	61.73
	10 3–6	462.84	475.83	12.99				
	10 6–9	475.83	499.72	23.89				
	10 9–12	499.72	253.61					

Table 1. Growth determination of EC on MSC3 media by fresh weights (g). Total number of culture tubes (TCT), time in weeks (TW), initial weights (Iw), final weight (Fw) and callus growth (CG) are given. All initial weights include the weight of the culture tubes and the media $(20\,\mathrm{ml\,L^{-1}})$. Grand average (Ga), standard deviation (SD), variance (Va) and coefficient of variation (C.V.) are also shown. The former three are the average weights of callus (g) and the four are calculated based on the CG figures. Grand average is sum of the average CG for each cultivar between 1–3, 3–6 and 6–9 weeks. Callus growth in the period 9–12 weeks was not considered for statistical analysis as weight differences were negative.

Characters	Varieties			
	Q77N1232	Cadmus	Co997	Lae1
Plant heights (cm)				
Range	7–8.0	6.5–7	7–8.5	7–80
Average	7.50	6.50	7.40	7.00
Mean	7.50	6.52	7.36	7.10
SD	0.35	0.19	0.47	0.63
Variances	0.13	0.04	0.22	0.40
C.V.	4.71	2.95	6.42	8.91
Leaves (no)				
Range	6.50	7.50	6.00	5.00
Average	6.00	7.00	7.50	6.50
Mean	5.98	6.98	7.48	6.46
SD	0.55	0.38	0.22	0.11
Variance	0.31	0.14	0.05	0.01
C.V.	9.27	5.40	2.90	1.77
Leaf length (cm)				
Range	12–15.8	17–20.6	16–20.4	14–22.3
Average	10–13.6	14–18.4	14–18.2	12–20
Mean	11.78	16.18	16.06	15.95
SD	1.74	1.51	1.53	2.66
Variances	3.01	2.28	2.34	7.05
C.V.	14.73	9.34	9.53	16.65
Roots (no)				
Range	6–80	4.5–6.4	8–10.2	6.8–10.4
Average	8–10	5.4–8.0	8–11.4	9–10.2
Mean	9.04	6.66	9.66	9.60
SD	0.86	0.89	1.28	0.39
Variances	0.73	0.79	1.63	0.16
C.V.	9.47	13.37	13.21	4.10
Root Length (cm)				
Range	6.0–8.0	8–10.4	8–10.6	8–12.8
Average	6.5–7.0	7–8.8	8–12.4	10–11.6
Mean	6.76	7.86	10.18	10.78
SD	0.21	0.63	1.57	0.94
Variances	0.04	0.40	2.46	0.88
C.V.	3.08	8.08	15.41	8.71

Table 2. Growth assessment of greenhouse-grown plants by growth characters. For the selected 100 plants (25 per cultivar), range was calculated by subtracting shortest from longest average lengths and the average was calculated by dividing the total number and lengths of parameters considered by 100. Standard deviation (SD) and coefficient of variation (C.V.) are calculated based on the average data obtained (full data not shown).

Callus Development and the Influence of MSC3 Media

The protocol used in this project was found to yield large amounts of contamination-free callus with a high regeneration rate. After 11 days of sub-culture, callus initiation began with small white clusters of callus with creamy surfaces. After 6–9 weeks of cultivation, a considerable mass of white, compact and yellow, fast-growing, friable callus had accumulated on all the explants cultured (Figure 1). The rate of contamination of explants cultured due to the incidence of microbes, media, culture tubes or non-aseptic techniques was low (Figure 1) except during the first three weeks of sub-culture when 20–30% of the explants were lost. This was mainly due to leaching of browning substances onto the culture media. The incidence of grey, non-embryogenic mucilaginous callus was negligible except when cultures were prolonged.

At the end of the second sub-culture, more than 95% of the explants were contamination-free and had produced a considerable mass of callus. Observation has shown that callus proliferation was not restricted to the areas close to cut surfaces, but was observed where a wound has occurred. When calli were sub-cultured at three week intervals on MSC3 medium for 3–6 weeks, callus growth remained vigorous. It was found that continued sub-culturing for 6–9 weeks and beyond resulted in dehydration, a decreases in callus growth and loss of regenerative ability (Figure 2). Only 3–6 weeks old callus had a high regeneration potential and germination was detected 12 days after transfer to the MSC media. Analysis of variance showed that observed variation among mean callus growth of the four cultivars was highly significant ($p = 0.99$). The mean callus growth of the cultivars was 14.58 (Q77N1232), 15.7 (Cadmus), 16.5 (Co997) and 14.4 g (Lae1), respectively (Table 1).
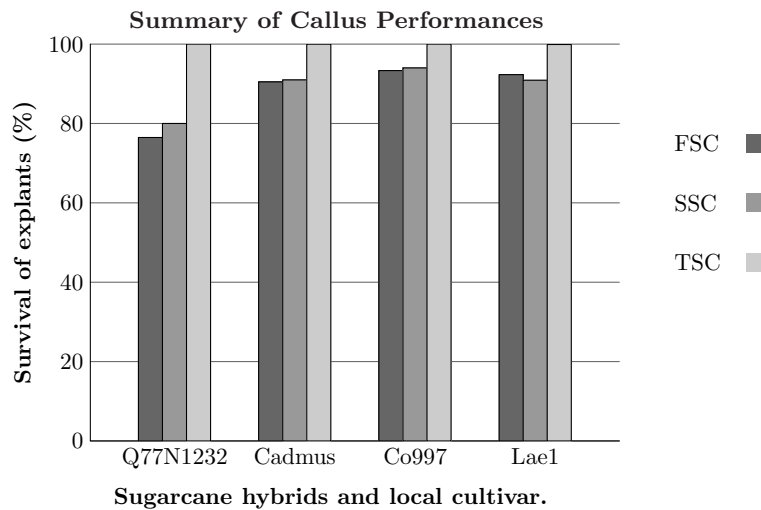

Figure 1. Survival of explants as percentage from first, second and third subcultures (FSC, SSC, TSC) at 3, 6 and 9 weeks. Percentage calculations are based on contaminated explants versus the total number cultured.
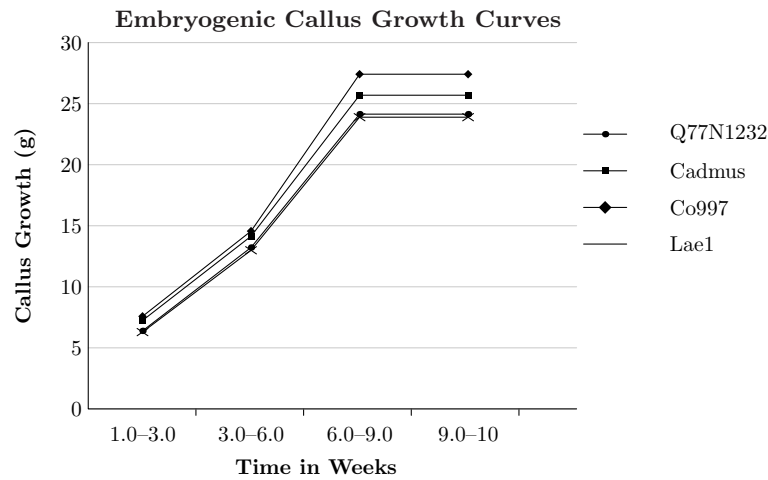
Figure 2. Callus growth of the four sugarcane cultivars at 3, 6 and 9 weeks. There was no further callus growth after 9 weeks of culture.

Minimizing the Effects of Browning Substances Leached into the Culture Media

Dookun et al. (1996) have detoxified phenols by either modifying the redox potential, inactivating phenolase enzymes, reducing phenolase activativation or substrate availability. Adams et al. (1995) reported that light activated polyphenoloxidases to form oxidates; less than 4% browning occurred under a light intensity of 150 Lux and 18% at 500 Lux with cultured garlic meristem clone explants. Given limited resources, an addition of $0.5–1\,\mathrm{g\,L^{-1}}$ of polyvinylpyrrolidone (PVP) to cultures exposed to 16 hours light and 8 hours darkness and continuous subcultures (cultures in the dark) has proven to be a cheap and efficient means of reducing tissue browning.

The degree of browning was found to be variety-specific and in more than 5% of the explants necrosis started from the younger rolled leaves rather than older ones. This indicated that using older explants (2–3 years old) would be advisable to avoid the leaching of phenols. Additionally, it was obvious that necrosis occurred more frequently in the early days of the initial culture, both in explants, calli, young shoots and rooted plants. This indicated that phenols were present wherever there was active plant growth (the meristematic regions of shoots and roots), except in the mature part of a plant such as the stem.

Shoot Regeneration, Root Development and Dedifferentiation on MSC Media

Following the transfer of EC onto MSC, numerous embryoids or miniature shoots (green-purplish) started to develop on callus surfaces. Most callus turned purple to purplish-green and within 3 to 4 weeks the entire EC surfaces were covered with green and healthy shoots. Four week old isolated shoots on MSC media developed a few or no roots and special effort had to be made to stimulate root development. For these shoots, the method of Wagih and Musa (2000) was adopted. Shoots without any forms of roots were transferred to $2\,\mathrm{mL}$ of sterile distilled water and within 14 days developed abundant roots. Rooting in MSC media in the presence of $2\,\mathrm{ml\,L^{-1}}$ BAP resulted in certain root development.

Genetic Variation on Regenerated Plantlets

Individual plantlets showed great variation with such differing phenotypic characters as pale green, wide and thick and hairy or arrow leaves. Dwarf plantlets and albino plantlets as reported

by Wagih and Musa (2000) were obvious in many cases. Many researchers, including Wagih and Adkins (1989) and Liu and Chen (1974), have reported similar types of variation in their work with sugarcane tissue cultures. An attempt to pin point the cause of these variations was impossible at the time of this project, but current work on sugarcane tissue culture at the University of Technology Biotechnology Centre is addressing this problem. Greenhouse-grown plants have shown no variations like those observed *in vitro* and the plants were clones of their mother plants.

Multiplication of Shoots in Vitro

So far as lack of planting materials is concerned, induction of multi-shoots is all that was required. Induction at a BAP concentration of $2\,\mathrm{ml\,L^{-1}}$ resulted numerous plantlets, which were potentially capable of growing into mature plants. In this project, a total of 750 plantlets on average per month were regenerated and would have regenerated as many as 9000–10000 in 12 months. This demonstrates that thousands of plants can be micro-propagated for commercial sugarcane production from a few available parent stocks.

Assessment of Plant Growth and Development

Growth as indicated by leaf development, root formation, multishoots and height increase of sub-cultured plantlets was favorable, and there was numerous multiplication of shoots with huge variation in leaf length, color and venation, thickness and plant height. Determination of actual leaf and root lengths, shoot heights and multishoots while in the culture tubes was impossible and Table 2 shows some of the variation of 100 randomly selected plants in the greenhouse. Some 95–100% of the plants grown successfully reached maturity. One-way analysis of variance showed that all the plant parameters used for assessing growth and development of glasshouse grown plants (Table 2) were significantly different with p-values of the plant parameters heights (0.02), leaves (0.00), leaf length (0.01), root (0.00) and root length

(0.00). The observed variations had probability values of less than 1 percent.

ACKNOWLEDGEMENTS

REFERENCES

Alam, M.Z., Haider, S.A., Islam, R. and Joarder, O.I. 1995. Higher frequency *in vitro* plant regeneration in sugarcane. *Sugar Cane*, **6**, 20–21.

Anderson, W.C. 1975. Propagation of rhododendrons by tissue culture. Part I. Development of a culture medium for propagation for multiplication of shoots. Combined Proceedings of the International Society for Plant Propagation, 25, 129–135.

Barba, R.C., Zambora, A.B., Mallion, A.K. and Linga, C.K. 1977. Sugarcane tissue culture research. Proceedings of the 16th Conference of the International Society of Sugar Cane Technologists, Sao Paulo, Brazil, pp. 843–863.

Bhojwani, S.S. and Razdan, M.K. 1983. Plant Tissue Culture. Theory and Practice. Elseiver Science Publishers, Amsterdam.

Chaudhary, R.C. 1994. Introduction to Plant Breeding. Mohan Primiani, Oxford, and IBH Publishing, New Delhi.

Chen, W.H., Liu, M.C. and Chao, C.Y. 1979. The growth of sugarcane downy mildew fungus in tissue culture. *Canadian Journal of Botany*, **57**, 528–533.

Comstock, J.C. (1988). Micropropagation plantlet project. Laboratory production, nursery operations, and field aspects. Proceedings of the 47th Annual Conference of Hawaiian Sugar Technologists, Honolulu, Hawaii, pp. A38–39.

Dookun, A., Moutia, M., Mulleegadoo, K. and Autrey, L.J.C. 1996. Constraints in sugarcane micropropagation by tissue culture. Proceedings of the 22nd Conference of the International Society of Sugar Cane Technologists, Cartagena, Colombia, pp. 434–440.

Hendre, R.R., Mascarenhas, A.F., Nadgir, A.L., Pathak, M. and Jagamathan, V. 1975. Growth of Mosaic Virus-free sugarcane plants from apical meristems. *Indian Phytopathologist*, **28**, 175–178.

Liu, M.C. and Chen, W.H. 1974. Historical studies on the origin and process of plantlet differentiation in sugarcane callus mass. Proceedings of the 15th Conference of the International Society of Sugar Cane Technologists, Durban, South Africa, pp. 118–128.

Murashige, T. and Skoog, F. 1962. A revised medium for rapid growth and bioassay with tobacco tissue culture. *Plant Physiology*, **15**; 473–497.

Wagih, M.E. 1999. AgBiotechnology. Phyto-Technology Approach to Plant Breeding. Course Guide for Final Year Bachelor Science Agriculture Students, Agriculture Department, PNG University of Technology.

Wagih, M.E., Ala, A. and Musa, Y. (2000). Rapid mass propagation of sugarcane by combined in vitro and nursery methodologies. A doctors thesis program at the PNG University of Technology, Papua New Guinea. An abstract read.

Wagih, M.E. and Adkins, S.W. 1998. Embryogenic culture for Fiji disease virus elimination in sugarcane. Proceedings of the 4th Breeding and Germplasm Workshop of the International Society of Sugar Cane Technologists, Mauritius, pp. 1–15.

Patrick S. Michael
Department of Agriculture
PNG University of Technology
Private Mail Bag Services
Lae, MP 411
Papua New Guinea.
email: pmichael@ag.unitech.ac.pg

Thesis Abstract: Investigation of the Therapeutic Potential of Transgenic CD40 Ligand Expression

MICHAEL P. BROWN

Abstract of a Thesis submitted for the Degree of
Doctor of Philosophy, University of Adelaide

The CD40 ligand (CD40L) molecule is central to innate and adaptive immunity. CD40L expression is very tightly regulated whereas its CD40 receptor is constitutively expressed by many different cell types. CD40L is expressed transiently on helper T cells (Th) only after activation by specific immune recognition molecules carried by professional antigen presenting cells, in particular, dendritic cells (DC). CD40L subsequently binds to CD40 on DC to enable full Th activation. CD40 ligated DC produce interleukin-12 (IL-12) and contribute both to the development of IFNγ-secreting natural killer cells, a vital component of innate immunity, and of IFNγ-secreting type 1 Th (Th$_1$) cells. CD40 ligated DC also contribute to the development of IL-4- and IL-10-secreting Th$_2$ cells. CD40L on Th cells also binds CD40 on macrophages to enhance their cytotoxic functions. CD40L-expressing Th cells provide the 'help' pivotally required to activate other components of adaptive immunity responsible both for clearing invading pathogens and generating the memory cells required to prevent re-infection. Th-supplied CD40L binds (i) B cell CD40 to switch production of antibodies to more potent effector molecules that have higher avidity for antigen, and (ii) DC CD40 to prime then expand antigen-specific cytotoxic T lymphocytes (CTL). Activated NK cells and CTL are required both to eradicate malignant cells and cells infected with viruses or other intracellular pathogens.

Genetic CD40L deficiency causes the very rare HyperIgM Syndrome Type 1 (HIGM1), which is realistically modelled by genetically engineered CD40L-deficient mice. Neither CD40L-deficient patients nor mice make effective antibodies or mount cellular immune responses that would defend them against intracellular pathogens such as parasites. Consequently, the only potentially curative therapy is allogeneic stem cell transplantation or CD40L gene replacement. Here, we used a retroviral vector, which constitutively expressed CD40L, to genetically modify CD40L-deficient bone marrow cells, which were used to reconstitute partially the immunity of CD40L-deficient mice. The crucial importance of tight regulation of CD40L expression was revealed when these mice later developed lethal thymic T cell malignancy.

Growing tumours escape immune vigilance by genetic alterations that reduce their sensitivity to IFNγ. Using murine tumour models, we incorporated transgenic CD40L expression in therapeutic tumour vaccines to show that CD40L gene transfer augmented the immunogenicity of the host's tumour thus reducing its tumorigenicity. We translated this finding clinically to safety and immunogenicity testing of a transgenic CD40L- and IL-2-expressing leukaemia vaccine.

Finally, the common viral respiratory pathogen, respiratory syncytial virus (RSV) mainly infects young infants and the elderly to cause potentially lethal pneumonia. Both groups have reduced cellular and humoral immunity, which predisposes them to re-infection with RSV. Using a murine model, we showed first that simultaneous adenoviral expression of CD40L augmented primary RSV-specific Th$_1$ responses that were associated with accelerated pulmonary viral clearance. Second, we showed that expression of CD40L in RSV-F and RSV-G subunit DNA vaccines elevated antibody and cellular immune responses to RSV challenge four and eight months after the initial immunisation.

These results demonstrate the potent ability of CD40L gene transfer to solve the absolute immune deficiency caused by genetic lesions of CD40L. However, physiological regulation

of the transgene is required to prevent serious adverse consequences. In contrast, no adverse effects were observed after transgenic CD40L expression was used to overcome relative immune deficiencies imposed by malignancy and RSV infection.

Dr Michael P. Brown, MB PhD FRACP FRCPA
Department of Medical Oncology
Royal Adelaide Hospital Cancer Centre
Level 7, East Wing, North Terrace
Adelaide SA 5000, Australia
email: michael.brown@health.sa.gov.au

Thesis Abstract: Compound Specific Detection of Endogenous Steroid Abuse in Sport: A Metabonomic Perspective

ADAM CAWLEY

Abstract of a Thesis submitted for the Degree of
Doctor of Philosophy, University of Sydney

The complementary application of Gas Chromatography-Mass Spectrometry (GC-MS) and Gas Chromatography-Combustion-Isotope Ratio Mass Spectrometry (GC-C-IRMS) were used in this study to provide compound specific detection of endogenous steroid misuse for improved anti-doping analysis. Administrations of synthetically derived dehydroepiandrosterone, androstenedione, 4-androstenediol, 5-androstenediol and testosterone were specifically confirmed on the basis of abnormal urinary excretions and low ^{13}C content of their respective diagnostic markers; $3\alpha,5$-cyclo-5α-androstane-6β-ol-17-one, 4OH-androstenedione, androst-2,4-diene-17-one/androst-3,5-diene-17-one, etiocholanolone sulfoconjugate and testosterone.

A comprehensive reference interval study established the natural variation, predominantly from diet, observed for δ^{13}C values in an elite athlete population (n $= 1262$) representing 13 countries. The minimum ^{13}C values recorded for the terminal androgen metabolites; androsterone and etiocholanolone were -25.3‰ and -25.8‰, respectively. A maximum of 3.8‰ was observed for the associated $\Delta\delta^{13}$C value that incorporated 11keto-etiocholanolone as the endogenous reference compound. Parametric statistics were applied to these data sets to propose high confidence (mean $\pm$ 3 standard deviations) δ^{13}C and $\Delta\delta^{13}$C limits of -27.0‰ and 4.0‰ to define endogenous steroid abuse. The use of pregnanediol as the endogenous reference compound provided a lower $\Delta\delta^{13}$C limit of 3.0‰.

The combinatorial approach to GC-MS and GC-C-IRMS data analysis was used to investigate the potential for *metabonomics* – the study of a discrete metabolite set – to improve anti-doping science. This methodology allowed the simple interpretation of all relevant information concerning an individual's metabolism in order to make an informed decision with respect to a doping violation.

Dr Adam Cawley
RQF Project Officer
University of Sydney
A14 - Main Quadrangle
NSW 2006
email: a.cawley@usyd.edu.au

Thesis Abstract: Multiple Foreign Agents IP Mobility Management in Internet Integrated Mobile Ad Hoc Networks

SHUO DING

Abstract of a Thesis submitted for the Degree of
Doctor of Philosophy, University of South Australia

Recently, *Mobile Ad Hoc Networks* (MANETs) have enjoyed a dramatic rise in popularity as potential solutions to connectivity in environments where telecommunication infrastructure is not available. Traditionally, MANETs are assumed to be stand-alone networks which do not require assistance from fixed network infrastructure (e.g. a backbone network). Based on this assumption, routing protocols for MANETs have been designed to work in stand-alone mode. However, throughput and coverage requirements of future 4G all-IP systems may require integration of MANETs into these systems to enhance the flexibility and pervasiveness of the networks. The coverage of existing infrastructure networks (wireless LAN hot-spots or 3G networks) can be effectively extended by the relaying communications via ad hoc network nodes (wireless routers). Also, the limited services available within MANET can be extended to a wider range through connecting of the MANET to the Internet infrastructure. To achieve this, effective solutions are needed to the many existing challenges in integrating MANETs with the Internet.

In this thesis, we propose solutions to three major challenges of interconnecting MANETs with Internet. The underlying research problems can be listed as follows:

Architecture options for integrating Mobile IP-based MANETs to the Internet via multiple gateways. Previous researchers rarely considered scenarios such as a MANET consisting of roaming nodes and multiple gateways to Internet. The design of protocol interfaces to achieve integration of ad hoc routing protocols and Mobile IP into the IP routing system of the Internet, was one of the most important challenges in this area. It has not been effectively addressed by research published thus far. In the thesis, we analyse the architecture options and propose effective solutions to the challenges of integration.

Internet extensions to reactive ad hoc routing protocols. Proposals for solutions published thus far have been mostly based on 'subnet' addressing strategy and single gateway scenario. This is not widely applicable to a variety of scenarios we may encounter in real-life networks, e.g., a MANET comprising roaming nodes and multiple gateways to Internet. Extensions to reactive ad-hoc routing protocols have to be defined to effectively support *External Route Discovery* and *External Route Maintenance* functions in MANET connected to Internet.

Schemes for Gateway Discovery / Handoff in MANETs. Efficient management of Mobile IP functionality supporting seamless data services in Internet integrated MANETs where ad-hoc nodes may change their association with Internet gateways, is a major challenge. The inadequacy of existing Mobile IP schemes applicable to MANETs motivated the search for more efficient gateway discovery/handoff schemes described in this thesis.

The contributions of the thesis can be listed as follows:

1. We formulate a new framework for integration of Mobile IP within the ad hoc network environment. The framework includes addressing strategies, protocol architecture, protocol interfaces, and supported communication scenarios. The issues in *Routing Interoperability* across IP, Mobile IP, and ad hoc routing protocols are

analysed, and the proposed solutions described in detail and verified via experimental development within OPNET simulation environment.

2. We design Internet extensions for DSR and AODV ad-hoc routing protocols. We contribute novel *External Route Discovery* and *External Route Maintenance* schemes suitable for DSR and AODV, operating under the *Mixed Addressing Scenario* (the addressing scenario proposed in this thesis as an effective solution to integrating ad-hoc network nodes into the Internet addressing and routing structure). The *External Route Discovery* algorithms include methods designed to distinguish between internal and external destinations of transmissions, including ARRD (*Affirmative Reply Route Discovery*), RERC (*Reactive External Route Construction*) and CERJ (*Comprehensive External Route Judgment*) algorithms. The *External Route Maintenance* algorithms are concerned with creating, accessing and maintaining multi-hop routes composed of internal (ad-hoc) and external (Internet) segments. Guidelines are also given on where and how the proposed algorithms are applicable.

3. We propose and analyse a solution for Mobile IP based *Gateway Discovery* schemes appropriate for operation within MANETs. A new, enhanced Mobile IP protocol entity operating on mobile node and gateway, i.e. the *Mobile IP Registration Controller*, is designed. We design two methods of propagating Mobile IP signalling messages in MANETs, based on broadcast and unicast respectively, with piggybacking of ad hoc routing information. Specifically, we focus on two *Gateway Discovery* approaches, *Reactive* and *Proactive Gateway Discovery*. In particular, the *Reactive Gateway Discovery* is capable of significantly decreasing the routing overhead incurred by the gateway discovery processes.

4. One of our most significant contributions deals with the handoff triggering mechanisms for a networking scenario where multiple Internet gateways serve the ad-hoc network. The Route Maintenance in both reactive ad hoc routing protocols can adaptively assist the Mobile IP gateway handoff. The triggers designed for Reactive Gateway Handoffs significantly improve the network performance.

5. Finally, OPNET simulation models are developed and simulation results obtained to demonstrate the implementability and effectiveness of the schemes proposed in this thesis. The Internet extensions for DSR and AODV are proven feasible as complete solutions to interconnection between MANET and Internet via multiple gateways. We recommend CERJ as an *External Route Discovery* algorithm suitable for the *Mixed Addressing Scenario*. Moreover, as a result of comparison with *Proactive Gateway Discovery/Handoff* scheme, the *Reactive Gateway Discovery/Handoff* is recommended as a scheme which can achieve satisfactory end-to-end performance and low routing overhead.

Dr Shuo Ding
Institute for Telecommunication Research
University of South Australia
email: shuoding@yahoo.com

Thesis Abstract: Clinical Management of Diabetes Mellitus in Dogs

LINDA FLEEMAN

This thesis presents important new findings on glycaemic monitoring, and insulin and dietary therapy of dogs with diabetes mellitus, and so provides valuable evidence on which to base treatment recommendations. Improved protocols for sampling blood glucose concentration in dogs are described, including a new method for obtaining capillary blood that has fewer technical problems than existing methods. The serial blood glucose concentration curve that is commonly used for monitoring diabetic dogs is shown to have large day-to-day variability. Pharmacological evaluation of subcutaneous porcine insulin zinc suspension indicates that the majority of diabetic dogs will require twice-daily dosing with this insulin preparation. New information reveals that hyperglycaemia-induced insulin resistance is likely a clinically relevant feature of spontaneous diabetes mellitus in dogs and has important implications for insulin therapy. Traditionally recommended high-fibre, moderate-carbohydrate, moderate-fat diets are shown to not be advantageous for diabetic dogs compared with a commercial, adult maintenance diet with moderate-fibre, ultra low-carbohydrate, and high-fat content. Finally, new evidence is presented that subclinical exocrine pancreatic disease appears to be common in dogs with diabetes mellitus and seems to be associated with hypertriglyceridaemia. These findings are expected to improve the clinical management of diabetes mellitus in dogs.

Linda Fleeman BVSc MACVSc PhD
School of Veterinary Science
The University of Queensland
St Lucia, QLD 4072
email: L.Fleeman@uq.edu.au

Thesis Abstract: Conserving and Restoring Wildlife in Fragmented Urban Landscapes: A Case Study from Brisbane, Australia

JENNIFER G. GARDEN

Native biodiversity is under threat as urban areas continue to expand and replace natural habitats, yet the processes enabling wildlife to persist in urban areas are not well understood. Consequently, urban planning and management decisions often fail to ensure the long-term conservation of urban biodiversity. This project applied a spatially-explicit, multi-scaled landscape approach to determine the relative importance of site (<1 ha), patch (1–100s ha), and landscape-level (100s–1000s ha) attributes for the occurrence of reptile and small mammal species living in fragmented forest remnants of Brisbane City, Queensland, Australia.

The study tested a set of *a priori* models to investigate the importance of site-level habitat attributes relative to patch and landscape-level attributes for native reptile and small mammal species. The occurrence of target species and the local-level habitat structure and composition were investigated at 59 sites using field based fauna and habitat surveys conducted over two consecutive years. Patch and landscape-level attributes were measured using GIS analysis and satellite imagery interpretation. Comparative analysis was used to investigate the detection success and costs associated with the different fauna survey methods employed. Cluster analysis and multi-dimensional scaling ordination were used to investigate relationships between species occurrences and local-level habitat characteristics. Generalised linear modelling and hierarchical partitioning were used to determine the importance of the area of forest habitat and its configuration relative to patch size and shape, and local vegetation composition and structure.

Nineteen native reptile and nine native mammal species were identified during surveys. Pit-fall traps and direct observations were the most successful and cost efficient method combination for detecting reptiles. Mammals were most successfully and efficiently detected using hair funnels combined with either Elliott traps (for small bodied mammals) or cage traps (for medium sized mammals). The one exception being the more successful use of pit-fall traps for detecting planigales (*Planigale maculata*).

At the local-level, species composition for both groups was influenced most by habitat structure rather than vegetation composition. When the importance of local-level habitat attributes was examined relative to patch and landscape-level attributes, attributes across each spatial level were found to be important for determining species richness. Overall, patch level attributes, such as size and shape, were less important than landscape context and local attributes of habitat quality. Reptile species richness was influenced most by attributes at the landscape and local levels, specifically, the area of forest habitat and its configuration in the surrounding landscape, and soil compaction and weed cover. Mammal species richness was influenced by attributes at all spatial levels, with the key factors being the amount of forest and rural/low density urban habitat at the landscape-level, followed by habitat composition at the local-level, and then patch size and shape at the patch-level.

This research highlights the need for a multi-species, multi-scaled approach to research and urban conservation planning and management. The major findings of this project are synthesised into a set of guidelines and a decision-support tree that will enable urban decision-makers to target priority habitat and landscape attributes for the conservation of native reptile and small mammal communities in urban landscapes.

Dr Jenni Garden, Ecologist
Natural Solutions,
Suite 16 Level 2, Central Brunswick
PO Box 1156, Fortitude Valley
QLD 4006

Thesis Abstract: Investigations into the Fabrication, Modification and Characterisation of Electrodes for the Development of a Novel Voltammetric Ion Selective Electrode

ALEX HARRIS

Abstract of a Thesis submitted for the Degree of
Doctor of Philosophy, Monash University

Investigations into surface fabrication, modification and characterisation and the development of a voltammetric ion selective electrode have been undertaken. An atomic force microscope (AFM) capable of measuring force curves and capturing deflection, topography and torsion images has been developed. Optimisation and characterisation of the AFM provides the potential for future development of high speed imaging coupled to other techniques. The bandwidth of tapping mode probes was found to depend on the probes design, free amplitude and setpoint and the sample topography and environment.

Electrocrystallization of phase I CuTCNQ, $Co[TCNQ]_2(H_2O)_2$ and red and blue coloured AgTCNQ (TCNQ = 7,7,8,8-tetracyanoquinodimethane) from acetonitrile at concentrations exceeding their solubility product have been studied by multiple techniques. Two routes were found for crystal formation. The first route involves the reduction of $TCNQ_{(MeCN)}$ to $TCNQ^{\bullet-}_{(MeCN)}$ in the presence of the metal cation. When the solubility product of the MTCNQ salt was exceeded, it precipitated onto the electrode surface at defect sites. At more negative potentials and longer time periods, reduction of a metal cation stabilised $(TCNQ^{\bullet-})(TCNQ)$ anion dimer produced crystals of the same phase as the first route but they were smaller and coated the entire electrode surface. The oxidative stripping potential of the crystals was affected by their morphology, phase, strength of adhesion and conductivity.

Screen printed planar and well electrodes produced by Oxford Biosensors have been characterised. Microscopic examination revealed the electrode surface was rough. DC cyclic voltammetry, Fourier Transform ac voltammetry and simulations have indicated resistance and area of mechanically punched well electrodes are highly variable. Fourier Transform ac voltammetry was investigated as a possible quality control technique.

Reduction of $TCNQ_{(s)}$ and oxidation of $TTF_{(s)}$ (tetrathiafulvalene) modified electrodes is capable of determining the concentrations of $Na^+_{(aq)}$ and $Cl^-_{(aq)}$ respectively. The sensor was improved by the addition of a 50 mM TRIS, 50 mM HEPES 'innocent' supporting electrolyte (buffer) and coating the electrode by a polymer permeable to the analyte ion. Grinding up of the crystals enabled application of the sensor to screen printed electrodes without damaging them. However, shifting of the reference electrode potential by exposure to the solution requires the use of a calibration redox compound. The TCNQ and TTF crystal voltammetric ion selective electrodes (ISE) were used to obtain Na^+ and Cl^- concentrations respectively from seawater, where the primary analyte ion was in great excess over any interfering ions. Comparison with potentiometric and spectrophotometric methods indicated the sensor could obtain approximate Na^+ and Cl^- concentrations. However, standard addition or dilution may need to be introduced to improve the accuracy.

A more selective voltammetric ion sensor was created by modifying an electrode with a poly(vinyl chloride) (PVC) supported 2-nitrophenyloctylether (NPOE) membrane containing TCNQ or decamethylferrocene as a

redox active species, a supporting electrolyte such as tetraheptylammonium tetraphenylborate and various ionophores for Na^+, K^+, Ca^{2+} and Cl^-. The components were dissolved in tetrahydrofuran (THF) and drop cast onto the electrode, then allowing the THF to evaporate. Reduction of TCNQ or oxidation of decamethylferrocene resulted in selective transfer of a counter ion into the film with Nernstian sensitivity. Beverages, seawater, blood plasma and whole blood were tested for Na^+, K^+ and Ca^{2+} content and results were in excellent agreement with potentiometric and spectrophotometric techniques. Application of the thin film ISE to screen printed electrodes was achieved by replacing the THF and PVC with dielectric ink.

Dr Alex Harris
email: alexrharris@gmail.com

Thesis Abstract: Effects of Pneumococcal Vaccination on Otitis Media and Bacterial Carriage in Remote Australian Aboriginal Communities

GRANT A. MACKENZIE

Abstract of a Thesis submitted for the Degree of
Doctor of Philosophy, Flinders University, South Australia

Background

Populations living in poor socio-economic conditions experience high mortality due to *Streptococcus pneumoniae* infection. Australian Aboriginal people of all ages experience some of the highest recorded rates of pneumococcal infection. Pneumococcal vaccination may prevent pneumococcal infection. However, pneumococcal vaccination programs have had limited introduction and effectiveness, particularly in populations at high risk of disease.

Areas of research addressed by this thesis

The focus of this thesis is the effects of pneumococcal vaccines on otitis media (OM) and upper respiratory tract carriage of *S. pneumoniae*. All the studies were undertaken on the Tiwi Islands north of Darwin. Universal infant pneumococcal vaccination combining 3 doses of 7-valent pneumococcal conjugate vaccine (7PCV) and booster 23-valent pneumococcal polysaccharide vaccine (23PPV) began on the Tiwi Islands in late 2001. Using historic comparison data, the effect of this vaccination program for preventing OM was evaluated. Likewise, the effects of vaccination on carriage of *S. pneumoniae*, non- typeable *Haemophilus influenzae*, and *Moraxella catarrhalis* in infants were documented. Studies among Tiwi adults and older children established the prevalence of and risk factors for pneumococcal carriage. The effects of adult pneumococcal polysaccharide vaccination on carriage were studied. Finally, indirect effects of infant pneumococcal vaccination on pneumococcal serotypes carried in older age groups were also explored.

Contributions to the field of study

The introduction of universal infant pneumococcal vaccination was associated with small reductions in the rate of severe OM. The clinical significance of these reductions is unclear. By age 12 months, 35% of comparison and 34% of vaccinated participants had experienced tympanic membrane perforation (TMP). Infant pneumococcal vaccination was associated with a non-significant 44% (95% confidence interval [95% CI] -5, 69) reduction in the risk of new episodes of TMP. Vaccinees were significantly less likely to experience perforation of both ears during follow-up compared to comparison participants (Odds ratio [OR]=0.40, 95% CI 0.17, 0.91) and significantly less likely to experience multiple episodes of perforation (OR=0.38,

95% CI 0.17, 0.84). Despite reduced risk of bilateral and recurrent perforation, similar proportions of comparison and vaccinated participants remained free of perforation. By 12 months of age, 88% of comparison and 89% of vaccinees had experienced acute otitis media. Vaccination was associated with a non-significant 16% (95% CI -17, 42) reduced risk of acute otitis media episodes. Vaccination had no effect on the prevalence of middle ear effusion but was associated with a non-significant 15% (95% CI -20, 40) increase in the time to first middle ear effusion.

Small numbers of perforations from which pathogens were isolated limited statistical comparisons. Among vaccinees, odds of new perforation associated with pneumococcal serotypes included in the 7-valent conjugate vaccine (VT) were non-significantly reduced compared to the comparison group (OR=0.39; 95% CI 0.09, 1.66). Relative to the comparison group, odds of new perforation associated with vaccine-related serotypes (VR) were non-significantly increased in vaccinees (OR=2.65; 95% CI 0.41, 28.9). The proportion of new perforations with serotype 6B was non-significantly reduced in vaccinees compared to the comparison group (OR=0.27; 95% CI 0.02, 1.87).

In the first 18 months of life, vaccinees had reduced carriage of pneumococcal serotypes included in the conjugate vaccine; age 1–3 months (12% versus 33%), age 7–10 months (9% versus 47%), and age 12–17 months (25% versus 56%). The vaccination program was associated with a significant indirect effect of reduced carriage of serotypes included in the 7PCV at 1–3 months of age. Carriage of serotypes unrelated to those in the 7PCV was generally increased in vaccinees. This was not the case among those aged 18–24 months. Increased carriage at less than 17 months of age of serotypes included in the 23PPV but unrelated to 7PCV serotypes was not evident among those aged 18–24 months. Serotype 16F, followed by 19A, emerged as the dominant carriage serotypes. The vaccination program was associated with an indirect effect delaying first acquisition of pneumococcal carriage; median survival time to pneumococcal acquisition was 68 (95% CI

49, 75) days in vaccinated and 52 (95% CI 40, 54) days in comparison participants, the 75% survival time was 90 (95% CI 75, 97) days in vaccinated and 59 (95% CI 53, ∞) days in comparison participants. However, after 12 months of age the prevalence of pneumococcal carriage was unaffected. Significant indirect effects of vaccination delaying acquisition of carriage were not associated with delay in onset of OM in vaccinees (Hazard Ratio=0.85; 95% CI 0.60, 1.20).

Around 25% of Tiwi adults and 68% of those aged 2 to 15 years were carriers of *S. pneumoniae*. Independent risk factors for carriage among children were young age, a recent runny nose, no recent prescription of antibiotics, the presence of an outside fire at the household, and whether children slept in a room with only other children (rather than a room with adults also). Independent risk factors for carriage among adults were older age, male gender, a recent chest infection, frequently sitting at outside fires, and unemployment. Recent vaccination with 23PPV in Tiwi adults did not appear to reduce carriage of pneumococcal serotypes included in this vaccine. Following introduction of infant pneumococcal vaccination in late 2001, with high coverage and a catch-up program, VT carriage in the unimmunised was unchanged between late 2002 (10%) and early 2004 (10%). Among unimmunised children 2–15 years of age, universal infant pneumococcal vaccination was associated with an indirect effect of reduced carriage of serotypes included in the 7-valent vaccine (comparison versus vaccinated group OR=2.11 (95% CI 1.29, 3.47). Among children 2–15 years of age, a similar proportion of nasal (73%) and nasopharyngeal (61%) swabs detected *S. pneumoniae*.

Conclusions

These studies suggest that among Tiwi infants receiving regular clinical review, the introduction of universal pneumococcal vaccination was associated with reduced risk of recurrent TMP. The clinical benefit of reduced perforation episodes is uncertain though as reductions were limited to recurrent perforation only. There was no change in the cumulative proportion of infants experiencing perforation or acute

otitis media by 12 months of age. Vaccination may have resulted in reduced new perforations associated with VT although the evidence is not strong due to small numbers. Vaccine immunogenicity has resulted in reduced carriage of VT and increased carriage of NVT. As other studies have correlated conjugate vaccination with reduced VT carriage and disease, it seems that appropriate carriage studies may be used to establish vaccine efficacy against VT disease. Temporal changes and participant selection may have biased these results.

Due to continuing high prevalence of severe OM among Aboriginal infants it is recommended that conjugate vaccines of greater valency be introduced as soon as possible. Administration of booster 23PPV at 9 or 12 months of age should also be evaluated. Other interventions aimed at reducing bacterial transmission are needed.

Vaccination was associated with increased carriage of serotypes not included in the 7PCV. Increased carriage of these serotypes was associated with a small non-significant increase in perforation associated with these types relative to the decrease in perforation associated with vaccine serotypes. Replacement carriage and OM does occur, but at present it only partially offsets reduction in perforation associated with vaccine-types.

There is evidence of relatively high pneumococcal carriage prevalence among older age groups of the Tiwi population. Increasing adult age was associated with increased risk of pneumococcal carriage and is also associated with increased rates of invasive disease. Therefore, intervention studies among adults should consider carriage as an outcome measure. Carriage studies among older children in remote Aboriginal communities, and similar populations, may use nasal rather than nasopharyngeal specimens with similar rates of detection of pneumococcal carriage. Vaccination of Tiwi adults with 23PPV did not reduce carriage of serotypes included in the vaccine. Other studies suggesting poor efficacy in certain populations suggest that 23PPV should be formally evaluated in Aboriginal adults. Finally, universal infant pneumococcal vaccination had an indirect effect among older Tiwi children whereby carriage of serotypes included in the 7PCV was reduced. With introduction of infant pneumococcal vaccination where high coverage is achieved and where catch-up vaccination is performed, immediate and indirect effects on carriage in the unimmunised population need only be assessed with a single post- introduction survey. Potentially increased indirect beneficial effects of greater valency conjugate vaccines and common pneumococcal antigen vaccines should stimulate clinicians, public health organisations, and researchers to advocate for their further development and licensure.

Dr Grant Mackenzie,
MBBS, BMedSci, FRACP
Menzies School of Health Research
PO Box 41096, Casuarina, 0811
Northern Territory, Australia
email: drbobcat@hotmail.com

Thesis Abstract: 'Through the Looking Glass . . . ' From Comfort and Conformity to Challenge and Collaboration.

The changing role of parents in the Catholic education of their children through the twentieth century in New South Wales.

NANCE MILLAR

The sociological investigation examined the changing role of parents in the education of their children in Catholic schools in New South Wales over the twentieth century. The argument was centred on the premise that Catholic Church documents over centuries (and secular documents in more recent times), have specifically stated that parents are the first and foremost educators of their children and have the primary responsibility for their children's religious education. Catholic schools were established to inculcate faith, and assist the parents in their role. The thesis addressed the questions: to what extent has that role been realised? What recognition or assistance has been given to this principle at the school level?

It unravelled the processes that determined and defined the changing role of Catholic parents during the period. Additionally it identified significant shifts in institutional thinking and practices related to parents and resultant shifts in cultural and social perceptions. After half a century of conformity and comfort, a significant era followed as the Australian Church responded to challenges, including financial crisis for Catholic schools, reform in the Australian education system and the impact of the Second Vatican Council.

Cohorts from three generations of parents and religious teachers were selected, representing three distinct periods of the twentieth century, 1900–1950, 1950–1975-, 1975–2000. Individual interviews and focus groups elicited memories and perceptions of the sixty participants, which were recorded and analysed, in terms of the integral questions; the role and involvement of parents in Catholic schools. Their perceptions of the parent role, were collected in two ways, i.e. as childhood memories and then, in their adult roles, as either parents or teachers. The analysis was theoretically informed by the work of Durkheim, Greeley, Coleman and Bourdieu. A review of Church documents, related to the education of children, showed the official Church position.

Despite numerous rhetorical statements issued by Catholic authorities, emphasising the role of parents as 'primary educators', the practical responses ranged form active encouragement to dismissal. Teachers in Catholic schools and related bureaucracies were, seemingly, reluctant to initiate a more inclusive partnership. Gradually, and in a piecemeal fashion, the Catholic Church and its schools have been responding to growing parental consciousness of their authority and responsibilities.

A significant shift was signalled by the New South Wales Bishops in establishing the Council of Catholic School Parents, to be supported by a full-time, salaried Executive Officer, in 2003. But any accommodation to new understandings of parent/teacher, or family/school relation is complex and not to be oversimplified as a simple sharing, or ceding of authority.

The research demonstrates that parents were effectively marginalised in the first fifty years and adopted a submissive role. However, due to factors of social change, both in society and the Catholic Church, parents now better-educated, are voicing their expectations of participation. This, however, does not apply to all parents who for various reasons are still on the periphery.

Three significant issues have emerged from the research: introduction of the principle of 'parents as the primary educators' at the pre-service level, i.e. the Batchelor of Education degree; secondly, recognition by teachers and parents that they are the 'significant others' in the socialisation and education of children and thirdly, the need for an approach regarding 'the parents on the fringe of the school community'.

During the applicable years of under-graduate teacher training an integrated, sequential module in each year could be instituted and subsequently continued and expanded in Post-Graduate education. The modules would be based on the premise of 'parents as the primary educators of their children' – as stated in the Code of Canon Law, other official documents and Vision and Mission Statements issued from the Catholic Education Offices and Catholic schools. As a result, teachers coming into a school would have been given some exposure to the principle of parents and teachers sharing complementary roles in the education and socialisation of the child as the 'significant others'. It is crucial that such a relationship is established as it incurs and implies a shared responsibility in equipping children in the life-long education process, of becoming self-sufficient, motivated members of society.

It is essential that knowledge and communication skills related to strategies aimed at the involvement/participation of all parents be part of pre-service and post-graduate teacher-education; the aim being to include, not only parents who are supportive, but also those who are difficult, indifferent or those who are merely surviving. Parents in special circumstance such as indigenous or others, who are experiencing language difficulties emanating from cultural differences, would require a sensitive focus. Thus additionally, a pastoral care approach would be incorporated within the school community and the role of parents would be given constructive recognition as decreed in the Catholic Church documents over centuries.

Dr Nance Millar
email: nmillar@myisp.net.au

Thesis Abstract: Monitoring and Modelling Threats to Koala Populations in Rapidly Urbanising Landscapes: Koala Coast, South East Queensland, Australia.

HARRIET J. PREECE

Abstract of a Thesis submitted for the Degree of
Doctor of Philosophy, University of Queensland

The aim of this study was to develop tools for monitoring and modelling threats to wildlife and apply these approaches to koala populations in a rapidly urbanising landscape. The study addressed problems in establishing the conservation status of a population through the examination of the direct and indirect threats to species' persistence at the landscape scale (10000s ha).

Wildlife populations are increasingly under pressure as human activities expand into natural ecosystems. In Australia, rapid population growth along the eastern seaboard is impacting heavily on regional biodiversity and threatening the persistence of many species, including the koala (*Phascolarctos cinereus*). Land clearing for residential developments and associated infrastructure such as roads, results in direct threats to habitat amount and species abundance; and introduces new threats associated with habitat fragmentation, vehicles, dogs and disease. Effective management of wildlife pop-

ulations in these rapidly urbanising landscapes requires detailed regional information and monitoring tools to assess the current conservation status and trends in the population, habitat and threatening processes.

This study integrated traditional ecological survey techniques with remote sensing, geographical information systems and landscape fragmentation analysis, to monitor the direct threats of habitat loss; decline in abundance; and contraction in extent of a regional koala population. The associated threats of increased mortality caused by vehicles, dogs and disease were monitored using statistical techniques applied to a long-term data set of incidental koala mortality. Spatial modelling underpinned much of this research and was integrated with satellite image processing to assess changes in koala habitat and abundance. Spatial modelling was also applied to examine the major causes of mortality and estimate the impacts on koala persistence. The inter-relationship between landscape configuration, forest fragmentation and the causes of koala mortality were also tested using geostatistical techniques.

The study was conducted in an area of $375\,\mathrm{km}^2$ known as the Koala Coast, located $20\,\mathrm{km}$ south-east of Brisbane, South East Queensland, Australia. Tools were developed to provide: an assessment of the conservation status of a population based on habitat; an estimate of a regional koala population size using direct counts; an assessment the anthropogenic

mortality rate; the first comprehensive evaluation of road kill blackspots for an entire regional road network; and the first enumeration of the association between traffic volume and koala mortality.

The study found that koala populations on the urban footprint will not be able to withstand the high rates of anthropogenic mortality and that this will result in localised extinctions. The landscape configuration of the remaining non-urban area was found to be too small to maintain a viable population of 5000 koalas and indicates that the Koala Coast population may be reaching a point where extinction of the population becomes inevitable.

Long-term persistence of wildlife in rapidly urbanising landscapes is dependent on the ability to address local threats and implement conservation plans. This study provides some of the tools and approaches to better manage wildlife populations such as the koala. Land managers and planners now need to prevent the loss of koalas and koala populations; mitigate the threats affecting koala survival; reverse the declines in habitat and abundance; and monitor the success of management actions.

Dr Harriet Preece
Conservation Services
Queensland Parks and Wildlife Service
Southern Region
PO Box 64, Bellbowrie, QLD 4070
email: Harriet.Preece@epa.qld.gov.au

Thesis Abstract: Variation in Great-Call Structure of Hybrid Gibbons in Central Borneo

SUNNY SANDERSON

Abstract of a Thesis submitted for the Degree of
Master of Philosophy, University of Queensland in 2006

A study on the variation in great-call structure of hybrid gibbons (*Hylobates agilis* x *H. muelleri*) was conducted throughout the headwaters of the Barito River in Central Kalimantan, Indonesia. A total of 88 females from 22 sites were recorded between September–November, 2004 and May–August, 2005. A detailed spectrographic analysis was made on 469 great-calls, which revealed that six of the 45 variables measured could accurately differentiate between agile and Müller's gibbons: (1) Number of great-call notes, (2) Great-call rate of emission, (3) Number of climax notes, (4) Climax rate of emission, (5) Mid-climax note duration, and (6) Inter-climax note interval. Of these, only the variable 'climax rate of emission' could reliably distinguish between the calls of agile (n = 23 females), Müller's (n = 14 females) and hybrid gibbons (n = 51 females).

A coefficient of variation indicated that intra-individual variation in great-call structure was low for each of the six variables. Nonparametric tests revealed that intra-population variation in great-call structure varied significantly ($P < 0.05$). A discriminant function analysis found that great-calls could be correctly assigned to the individual that produced them at a rate higher than would be expected by chance (cross-validated classification rate: hybrid = 81.9%; agile = 54.4%; Müller's = 52.4%).

There was a significant ($P < 0.05$) level of inter-population variation in great-call structure. The cross-validated correct assignment rate was 94%, indicating that the agile, Müller's, and hybrid populations could be reliably distinguished by the two functions of the discriminant function analysis. One of the main variables in each of the two functions was 'climax rate of emission'.

Within the hybrid population, females located on the western side of the hybrid zone had a slower climax rate of emission (mean = 2.07 notes/s) than those located on the eastern side (mean = 4.55 notes/s). This finding is likely due to a larger proportion of agile genes on the western side of the hybrid zone, and a larger proportion of Müller's genes on the eastern side. It appears that the average climax rates of emission on both sides of the hybrid zone have increased since last surveyed by Mather (1992), indicating that the rate of emission of hybrid great-calls is accelerating.

There was a significant level of variation between mother-daughter pairs, one generally having a faster climax rate of emission than the other. It appeared that the regular participation of daughters in song bouts was to practice their own song, rather than learn that of their mother. Female neighbours also varied significantly in their call structure. The wide range of inter-individual variation indicates that great-call structure is inherited and not learnt.

The hybrid zone appears to have increased in size since it was last surveyed (Mather, 1992). Fifteen of the 29 females recorded between the western side of the Busang River and the northern side of the Joloi River were hybrids. These females were sparsely distributed from the village of Parahau down to the northern banks of the Joloi River. They had a faster climax rate of emission (range = 0.67–4.89 notes/s) than the agile gibbons in the same region (range = 0.37–0.65 notes/s). It is likely that limited hybridisation has long been present in this region, but that hybrids have become more abundant than when last surveyed.

Dr Sunny Sanderson B.Sc., B.A.
The School of Integrative Biology
The University of Queensland
St Lucia, QLD 4072
email: s.sanderson@uq.edu.au

Thesis Abstract: An Analysis of the Underlying Biochemical and Genetic Mechanisms that Control Gender and Fertility in the Kuruma Shrimp, Marsupenaeus japonicus (Bate)

M.J. SELLARS

Abstract of a Thesis submitted for
Doctor of Philosophy, University of Queensland

The development of techniques to control gender and fertility in the Kuruma shrimp *Marsupenaeus japonicus* (Bate) is of commercial interest for two reasons. First, *M. japonicus* are sexually dimorphic with females growing 30% larger than males and second, recent success in the genetic improvement of *M. japonicus* has prompted farmers to seek ways to protect superior genetic stocks from unlicensed breeding and to prevent escapees from genetically contributing to natural fishery populations.

To-date there is a lack of understanding of how gender and fertility are determined in penaeid shrimp. Accordingly, this research project investigated three methodolgies to achieve gender and/or fertility control in *M. japonicus*; (1) the potential of ploidy manipulation to control gender and fertility; (2) the effect of ionizing radiation on fertility; (3) the potential of genetic engineering to control gender determination and germ cell specification.

Ploidy manipulation

Previous research on *M. japonicus* has shown that triploids produced by preventing polar body (PB) II extrusion are always female and sterile, however, induction rates never result in 100% triploid progeny. Therefore, experiments in the present study focused on developing a technique to produce triploids with a 100% induction rate. As mating of tetraploids and diploids is the only documented technique that has achieved 100% triploids in other cultured species, the present study investigated methods to induce tetraploidy in *M. japonicus*.

Tetraploid *M. japonicus* embryos were produced by stopping the first division in mitosis using a 36°C heat shock, however, they were not viable and did not hatch. Preventing the extrusion of PBI and both PBI and II using 150 μM 6-dimethylaminopurine consistently resulted in the production of viable triploid *M. japonicus* embryos, which hatched into nauplii. No tetraploids were produced by preventing the extrusion of PBI or both PBI and II. This is the first report of successful PBI, and PBI and II prevention in shrimp, and production of triploids using the reported treatment regimes.

Ionizing radiation (IR)

IR was found to impair the reproductive performance of *M. japonicus* when treated at harvest age and when treated as postlarvae and reared to reproductive maturity. Harvest age male shrimp were reproductively impaired at 10 Gy as compared to 20 Gy for harvest age females. PL15 females treated with 0 Gy of IR matured and spawned more frequently than PL15 females treated with 10, 15 and 20 Gy of IR. IR doses higher than 35 Gy resulted in 100% mortality (i.e. lethal dose rate) of PL15 *M. japonicus* within 30 days after treatment, whilst doses of 25 and 30 Gy significantly reduced postlarval survival compared to controls. Dose rates of 25 Gy or more resulted in 100% mortality of harvest age females, whilst 20 Gy significantly reduced harvest age male survival. These findings indicate that IR doses that do not result in 100% mortality of harvest age and postlarval *M. japonicus* can reduce their reproductive capacity, however, these doses of IR can not confer 100% sterility.

Genetic engineering

In the present study a partial coding sequence for a *dsx*-like gene homologue, *DMRT2*,

and a complete coding sequence for a PL10 *vasa*-like gene (named *Mjpl*10) were isolated from *M. japonicus*. Both genes were differentially expressed during embryonic, larval and postlarval development, and in female and male gonad as demonstrated through real-time PCR. Future studies aim to utilize RNAi to produce loss-of-function genotypes to determine if these genes are involved in shrimp gender and fertility determination.

Dr M.J. Sellars
School of Integrative Biology,
The University of Queensland
CSIRO Food Futures National Research
Flagship & CSIRO Marine and Atmospheric
Research
email: Melony.Sellars@csiro.au

Thesis Abstract: Chinese EFL Learners' Pragmatic Competence in Requests

VINCENT XIAN WANG

Abstract of a Thesis submitted for the Degree of
Doctor of Philosophy, University of Queensland

This study examines the development of pragmatic competence in requests in two groups of Chinese EFL learners (advanced and intermediate) in a tertiary institute in Macau, China. The learners answer a written discourse completion test that contains ten scenarios where they request common services or ask for favours. The request behaviours are examined in terms of utterance length, strategy types, formulaic expressions, and modifications (internal and external). It is found that, compared with a group of native speakers of English, the learners have not developed native-like pragmatic behaviours. Although the advanced and the intermediate learner groups reach native-like distribution in STRATEGY TYPE for the scenarios taken together, statistically significant differences from the native group are observed in several individual scenarios (particularly with the intermediate learners). In addition, the two groups of learners employ formulaic expressions sharply differently from the native group in types and according to scenario. The learners do not use internal modifiers as frequently or situation-differentially as the native group: they do not show a strong preference for bi-clausal structures and conditionals in the scenarios of substantial favour asking. The learners employ elaborated external modifications and are verbose in requests. According to Bialystok (1993, 1994) two-dimensional model of pragmatic competence, the learners are missing analytical knowledge of the scenario-specific behaviours, and their control ability is not fully developed. This study examines adult Chinese learners of English in a foreign language environment, and extends our knowledge of the development of request behaviours in children in second language environments (Achiba, 2003; Ellis, 1992). It also relates to the research on formulae in SLA (Wray, 2000, 2002; Kecskes, 2002) by providing empirical data on formulaic expressions in learners' requests. It is further argued that examination of interlanguage pragmatics should be (a) scenario-based, and (b) formulae-based.

Dr Vincent Xian Wang
Department of English, FSH,
The University of Macau
email: vincentxwang@yahoo.com

NOTICE TO AUTHORS

Manuscripts should be addressed to The Honorary Secretary, Royal Society of New South Wales, Building H47 University of Sydney NSW 2006.

Manuscripts will be reviewed by the Hon. Editor, in consultation with the Editorial Board, to decide whether the paper will be considered for publication in the Journal. Manuscripts are subjected to peer review by an independant referee. In the event of initial rejection, manuscripts may be sent to two other referees.

Papers, other than those specially invited by the Editorial Board on behalf of Council, will only be considered if the content is substantially new material which has not been published previously, has not been submitted concurrently elsewhere nor is likely to be published substantially in the same form elsewhere. Letters to the Editor and short notes may also be submitted for publication.

Three, single sided, typed copies of the manuscript (double spacing) should be submitted on A4 paper.

Spelling should conform with 'The Concise Oxford Dictionary' or 'The Macquarie Dictionary'. The Systéme International d'Unites (SI) is to be used, with the abbreviations and symbols set out in Australian Standard AS1000.

All stratigraphic names must conform with the International Stratigraphic Guide and new names must first be cleared with the Central Register of Australian Stratigraphic Names, Australian Geological Survey Organisation, Canberra, ACT 2601, Australia. The codes of Botanical and Zoological Nomenclature must also be adhered to as neccessary.

The Abstract should be brief and informative.

Tables and Illustrations should be in the form and size intended for insertion in the master manuscript – 150 mm x 200 mm.

If this is not readily possible then an indication of the required reduction (such as 'reduce to 1/2 size') must be clearly stated. Tables and illustrations should be numbered consecutively with Arabic numerals in a single sequence and each must have a caption.

Half-tone illustrations (photographs) should be included only when essential and should be presented on glossy paper.

Maps, diagrams and graphs should generally not be larger than a single page. However, larger figures may be split and printed across two opposite pages. The scale of maps or diagrams must be given in bar form.

References are to be cited in the text by giving the author's name and year of publication. References in the Reference List should be listed alphabetically by author and then chronologically by date. Titles of journals should be cited in full – not abbreviated.

Details of submission guidelines can be found in the on-line Style Guide for Authors at http://nsw.royalsoc.org.au

MASTER MANUSCRIPT FOR PRINTING

The journal is printed from master pages prepared by the LaTeX 2$_\varepsilon$ typesetting program. When a paper has been accepted for publication, the author(s) will be required to submit the paper in a suitable electronic format. Details can be found in the on-line Style Guide. Galley proofs will be provided to authors for final checking prior to publication.

REPRINTS

An author who is a member of the Society will receive a number of reprints of their paper free. Authors who are not a members of the Society may purchase reprints.

CONTENTS Continued

Vol. 140 Parts 3 and 4

CONTENTS

Vol. 140 Parts 3 and 4